

Electronic Supplementary Information

New Journal of Chemistry

Glycine betaine-based ionic liquids and their influence on bacteria, fungi, insects and plants

Damian Krystian Kaczmarek,^{*a} Daniela Gwiazdowska,^b Krzysztof Juś,^b Tomasz Klejdysz,^c Marta Wojcieszak,^a Katarzyna Materna^a and Juliusz Pernak^a

^aDepartment of Chemical Technology, Poznan University of Technology, ul. Berdychowo 4, Poznan 60-965, Poland

^bDepartment of Natural Science and Quality Assurance, Poznan University of Economics and Business, Al. Niepodległości 10, Poznan 61-875, Poland

^cInstitute of Plant Protection – National Research Institute, ul. W. Węgorka 20, Poznan 60-318, Poland

*E-mail: damian.rom.kaczmarek@doctorate.put.poznan.pl

Experimental

Materials

N,N-Dodecyldimethylamine (97%, CAS Number 112-18-5), *N,N*-butyldimethylamine (99%, CAS Number 927-62-8), betaine hydrochloride ($\geq 99\%$, CAS Number 590-46-5), chloroacetic acid (99%, CAS Number 79-11-8), docusate sodium salt ($\geq 97\%$, CAS Number 577-11-7), *D*-gluconic acid solution (49-53 wt. % in H₂O, CAS Number 526-95-4), α -ketoglutaric acid ($\geq 98.5\%$, CAS Number 328-50-7), *L*-pyroglutamic acid ($\geq 99.0\%$, CAS Number 98-79-3), cholic acid ($\geq 98\%$, CAS Number 81-25-4), and bis(2-ethylhexyl)phosphate (97%, CAS Number 298-07-7) were purchased from Sigma-Aldrich. Sodium glycolate (97%, CAS Number 2836-32-0) and potassium hydroxide (85%, CAS Number 1310-58-3) was purchased from Alfa Aesar. All solvents (water, methanol, dimethyl sulfoxide (DMSO), acetonitrile, acetone, 2-propanol, ethyl acetate, chloroform, toluene, hexane) were also provided by Sigma-Aldrich. Water for solubility and surface-activity measurements was deionized, with the conductivity below 0.1 $\mu\text{S cm}^{-1}$, from demineralizer HLP Smart 1000 (Hydrolab).

Synthesis

Salts with dioctyl sulfosuccinate or glycolate anions. Sodium salts of dioctyl sulfosuccinate or glycolate (0.05 mol) were placed in a reaction vessel and dissolved in 30 mL of ethanol. Then, alkylbetainium chloride (obtained in accordance with the methodology described in the literature¹) was added at a stoichiometric ratio. The reaction mixture was stirred at 25 °C until inorganic salts precipitated. Then, the mixture was cooled to 5 °C, and the inorganic salt was filtered off. In the next step, ethanol was evaporated from the filtrate. To remove inorganic salt residues, the product was dissolved in a mixture of anhydrous acetone and methanol (ratio 10:1 v/v) and the mixture was cooled to 5 °C. The precipitated residue was filtered off, and the solvent was evaporated. Finally, the product was dried in a laboratory dryer under reduced pressure at 70 °C for 24 h. All synthesized salts were stored under vacuum over P₄O₁₀.

Salts with *D*-gluconate, α -ketoglutarate, *L*-pyroglutamate, cholate or bis(2-ethylhexyl)phosphate anions. Alkylbetaine (obtained in accordance with the methodology described in the literature²) (0.05 mol) was placed into a reaction vessel and subsequently dissolved in 30 mL of ethanol. Then, *D*-gluconic, α -ketoglutaric, *L*-pyroglutamic, cholic or bis(2-ethylhexyl)-phosphate acid was added at a stoichiometric ratio. The reaction mixture was stirred at 25 °C for 30 min. Then, the solvent was evaporated using a rotary vacuum evaporator. Finally, the product was dried in a laboratory dryer under reduced pressure at 70 °C for 24 h. All synthesized salts were stored under vacuum over P₄O₁₀.

General

The methodology was carried out in accordance with the method previously described.¹ The ¹H and ¹³C NMR spectra were collected by using a Varian VNMR-S 400 spectrometer operating at 400 and 100 MHz, respectively. Tetramethylsilane (TMS) was used as internal standard and deuterated methanol (CD₃OD) was used as the solvent in the analysis. Elemental analyses (CHN) were performed at the Adam Mickiewicz University, Poznan (Poland). The water content in the obtained products was assayed by Karl Fischer titration using a TitroLine KF Trace coulometric titrator (SI Analytics). The IR spectra were collected by using semi-automated system EasyMax 102 (Mettler Toledo) connected with ReactIR iC15 (Mettler Toledo) probe equipped with an MCT detector and a 9.5-mm AgX probe with a diamond tip. The data were sampled from 3000 to 650 cm⁻¹ with 8 cm⁻¹ resolution and processed by iCIR 4.3 software.

Thermal analysis

Thermal analysis was performed based on the method described in the literature.³ Thermal gravimetric analysis (TGA) was performed using a Mettler Toledo Star^e TGA/DSC1 unit (Leicester, UK) under nitrogen. Samples (2–10 mg) were placed in aluminium pans and heated from 30 to 450 °C at a heating rate of 10 °C min⁻¹. Phase transition temperatures were determined by differential scanning calorimetry (DSC), with a Mettler Toledo Star^e DSC1 (Leicester, UK) unit under nitrogen. Samples (5–15 mg) were placed in aluminium pans and heated from 25 to 100 °C at a heating rate of 10 °C min⁻¹ and cooled with an intracooler at a cooling rate of 10 °C min⁻¹ to -100 °C and then heated again to 100 °C.

Solubility

The solubility of the obtained ILs was determined following the methodology described in Vogel's Textbook of Practical Organic Chemistry.⁴ On the basis of their usefulness in synthesis and agrochemistry, five solvents (water, ethanol, DMSO, acetone, and 2-propanol) were selected for the solubility test. In compliance with the methodology, a sample of the compound (0.1 ± 0.0001 g) was introduced into three volumes of each solvent, and the behavior of the sample was recorded. The term "good solubility" refers to compounds that dissolved in 1 mL of the solvent; "limited solubility" applies to the ILs that dissolved in 3 mL of the solvent; and "poor solubility" refers to the compounds that were insoluble in 3 mL of the solvent. All the analyses were conducted at 25 °C.

Surface activity

Measurements of the surface tension and contact angle were carried out using a DSA 100E analyzer (Krüss, Germany, accuracy ± 0.01 mN m⁻¹) at 25 °C, following a methodology described recently.⁵ The surface tension was determined by the drop shape method. The method depends on forming an axisymmetric drop at the tip of a

needle of a syringe, after which the image of the drop is acquired with a USB 3 uEye CP camera (IDS Imaging Development Systems GmbH, Obersulm, Germany) and digitized. The surface tension (γ in mN m^{-1}) was calculated based on an automatic analysis of the drop profile according to the Laplace equation. Determination of the contact angle was based on the sessile drop method. The principle of this method is to deposit drops of liquid on a solid hydrophobic surface (paraffin, the hydrophobic surface serving as the model surface of leaves).

Greenhouse experiment

The experiment was conducted as a double-blind randomized design in four replications under greenhouse conditions (temperature: 25 ± 2 °C, humidity: 60%). Seeds of cornflower (*Centaurea cyanus*) were planted in 0.5-L plastic pots filled with soil (67 mg P/kg soil, 55 mg K/kg soil, 54 mg Mg/kg soil, 100 mg Fe/kg soil, pH of 5.75 (in CaCl_2), and C organic content of 1.90% (19.00 g/kg soil)). The plants were thinned to five per pot within 10 days after emergence and watered as needed. Next, the plants were sprayed at the 4-leaf stage. The herbicide iodosulfuron-methyl sodium and appropriate ILs or the commercial adjuvant Biopower (Bayer Crop Science, Cambridge, United Kingdom; 27.8% alkyl ether sulfate sodium) were dispersed in water and applied at doses corresponding to 7.5 g of active ingredient per 1 ha for the herbicide and 0.1% for all the adjuvants. The fresh weight of the plants was measured three weeks after treatment using a technical balance with 0.01 g precision (Analytical Balance ME204E, Mettler Toledo, Switzerland). The results of the biological activity are presented as the mean values (\bar{X}) of fresh weight reduction with the standard error (SE).

Feeding deterrent experiment

Deterrent activity studies of the obtained salts were carried out on two species of essential storage grain pests: the granary weevil (*Sitophilus granarius* Linnaeus, 1758) and the khapra beetle (*Trogoderma granarium* Everts, 1898). The above insects were reared in the laboratory in an incubator at 26 ± 10 °C and a relative humidity of $60 \pm 5\%$ on uncrushed wheat grain (granary weevil) and crushed wheat grain products: flour, bran and others (khapra beetle). Azadirachtin was used as a reference substance in the experiment. Choice and no-choice tests were conducted according to a methodology described in the literature.³ Wafer disks 1 cm in diameter and 1 mm in thickness (average weight of approximately 15 mg) were made of wheat flour. The prepared wafers were saturated by dipping in methanol (control) or a 1% solution of salt in methanol and then left to air-dry for 30 min. After evaporation of the solvent, the wafers were weighed and offered to the insects in plastic boxes as the sole food source for five days. The wafers were placed in the petri dish following the type of test:

- two disks treated with solvent (control for an experiment in a test variant without choice),

- one disk previously dipped in solvent and one disk dipped in a 1% solution of the test compound (choice test),
- two disks previously dipped in a 1% solution of the test compound (no-choice test).

Both variants of the experiment and control were carried out in 5 repeats, where 3 adults of the granary weevil or 10 larvae of the khapra beetle were placed in each of them. The number of insects used in the experiments depended on the feeding intensity. After the 5th day, the wafers were weighed again, and the average weight of the food consumed was calculated. The values of coefficients A (absolute coefficient of deterrence) and R (relative coefficient of deterrence) were calculated as follows:

$$R = \frac{(C-E)}{(C+E)} \times 100 \text{ (choice test)}$$

$$A = \frac{(CC-EE)}{(CC+EE)} \times 100 \text{ (no-choice test)}$$

where C and CC correspond to the amount of consumed food from the control disks, and E and EE correspond to the amount of consumed food treated with the tested compound.

The total coefficient of deterrence (T) was the sum of the relative and absolute coefficients.

The deterrent activity was defined according to a predetermined scale, where the total coefficient of deterrence was used. Biological activities with T values between 151 and 200 indicate very good deterrents, those with values between 101 and 150 indicate good deterrents, those with values between 51 and 100 indicate moderate deterrents, and those with values below 50 indicate weak deterrents. The coefficients of deterrence of the group of compounds were analyzed through one-way ANOVA followed by Tukey's post hoc test with homogenous subsets.

Phytotoxicity

Effect on the germination and early development of plants. The analysis of the impact of ILs involved studies regarding the germination and early development of white mustard (*Sinapis alba*). The culture was carried out in a vertical plastic Phytotoxkit (Phytotoxkit, Tigret, Belgium). The plates were filled with 100 g of soil, and then containers containing a quantity of the analyzed substance dissolved in water (25 mL) were added to achieve effective concentrations of 1 g/kg of soil dry weight. The solutions consisting of commercial adjuvant (Biopower, Bayer CropScience, Cambridge, United Kingdom) were used as reference samples. Thus, prepared soil was used to plate 10 seeds of white mustard separately. Phytotoxkit plastic containers were placed in the dark and maintained at a temperature of 25 ± 1 °C. After the end of the experiment, the number of germinated seeds was counted, and measurements were taken of the root length, shoot height and mass.

Soil with the following elemental composition was used for the experiment: 67 mg P/kg soil, 55 mg K/kg soil, 54 mg Mg/kg soil, 100 mg Fe/kg soil, pH of 5.75 (in CaCl₂), and a C organic content of 1.90% (19.00 g/kg soil). The influence of ILs was investigated using the phytotoxicity test based on the ISO-11269-2:2003 international standard.

After termination of the germination tests, the impact of herbicides on the root growth inhibition of plants was assessed. Based on the obtained data, the germination capacity was calculated according to the following equation:

$$G = \left(\frac{Gs}{G} \right) \times 100\%$$

where *G_s* is the number of germinated seeds and *G* is the total number of examined seeds.

All experiments were conducted in triplicate, and all error bars presented in the figures represent standard errors of the mean (with respect to the number of replicates).

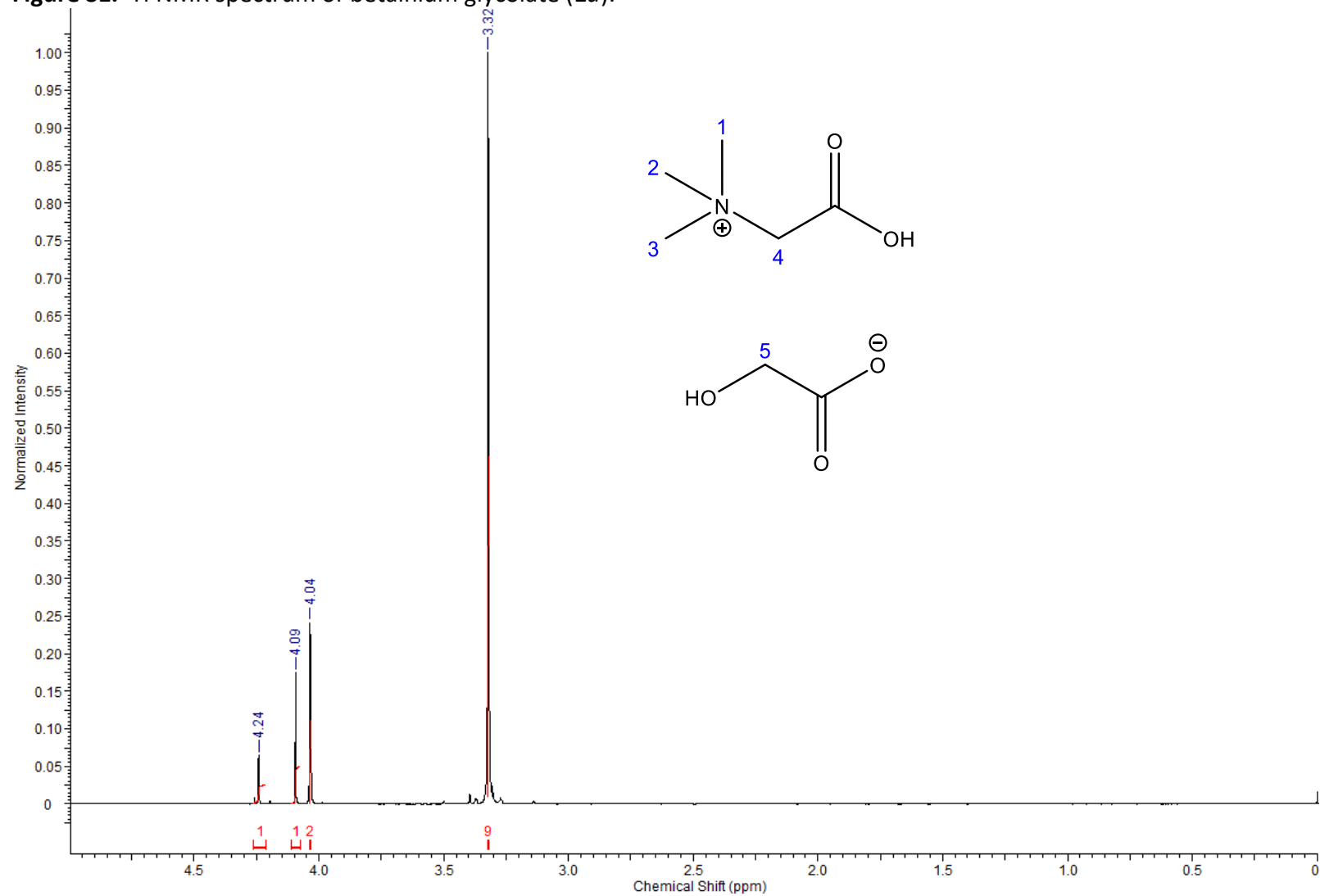
Microbial toxicity assay

Antimicrobial activity was determined via broth microdilution method. The tested microorganisms included gam-positive bacteria: *Staphylococcus aureus* ATCC 33862, *Staphylococcus epidermidis* ATCC 12228, *Enterococcus faecalis* ATCC 19433, *Bacillus subtilis* ATCC 11774, *Micrococcus luteus* ATCC 4698, gram-negative bacteria: *Escherichia coli* ATCC 8739, *Pseudomonas aeruginosa* ATCC 9027, *Serratia marcescens* ATCC 8100, *Proteus vulgaris* ATCC 49132, *Moraxella catarrhalis* ATCC 25238 and yeasts *Candida albicans* ATCC 10231 and *Rhodotorula rubra* (PUEB collection). The bacterial suspensions in Mueller-Hinton broth (Oxoid, Canada) and yeasts solution in Sabouraud broth (Oxoid, Canada) from 24 h cultures were standardized to obtain density 0.5 McFarland's standard. Twofold serial dilutions of tested ILs in the concentration ranging 0.5 to 1000 µg mL⁻¹ were prepared in 96-well microtiter plates in sterile Mueller-Hinton broth or Sabouraud broth. Next, 100 µL of strains suspensions were introduced into the wells containing 100 µL of ILs in dilution series to achieve a final density 5 × 10⁵ CFU mL⁻¹. The plates were incubated at temperature 30–37 °C for 24 h, depending on the indicator organism. Medium with ILs was used as a negative control, while bacterial or fungal culture without an inhibitory agent was used as the positive control. After incubation, the optical density of microorganisms growth was determined at 600 nm using BioTek Epoch 2 microplate reader. The results are expressed as the average of three replicates. The MIC value was defined as the concentration of ILs, inhibiting the growth of the microorganism by at least 90%. Minimum Bactericidal/Fungicidal Concentration was determined by spot inoculation of 10 µL of cultures from wells with no growth observed in the MIC assay on an agar medium and incubation for 24–48 h at 30 or 37 °C. The lowest concentration of the tested ILs supporting no microorganisms growth was defined as the MBC/MFC.

Table S1. Elemental analysis of the obtained salts.

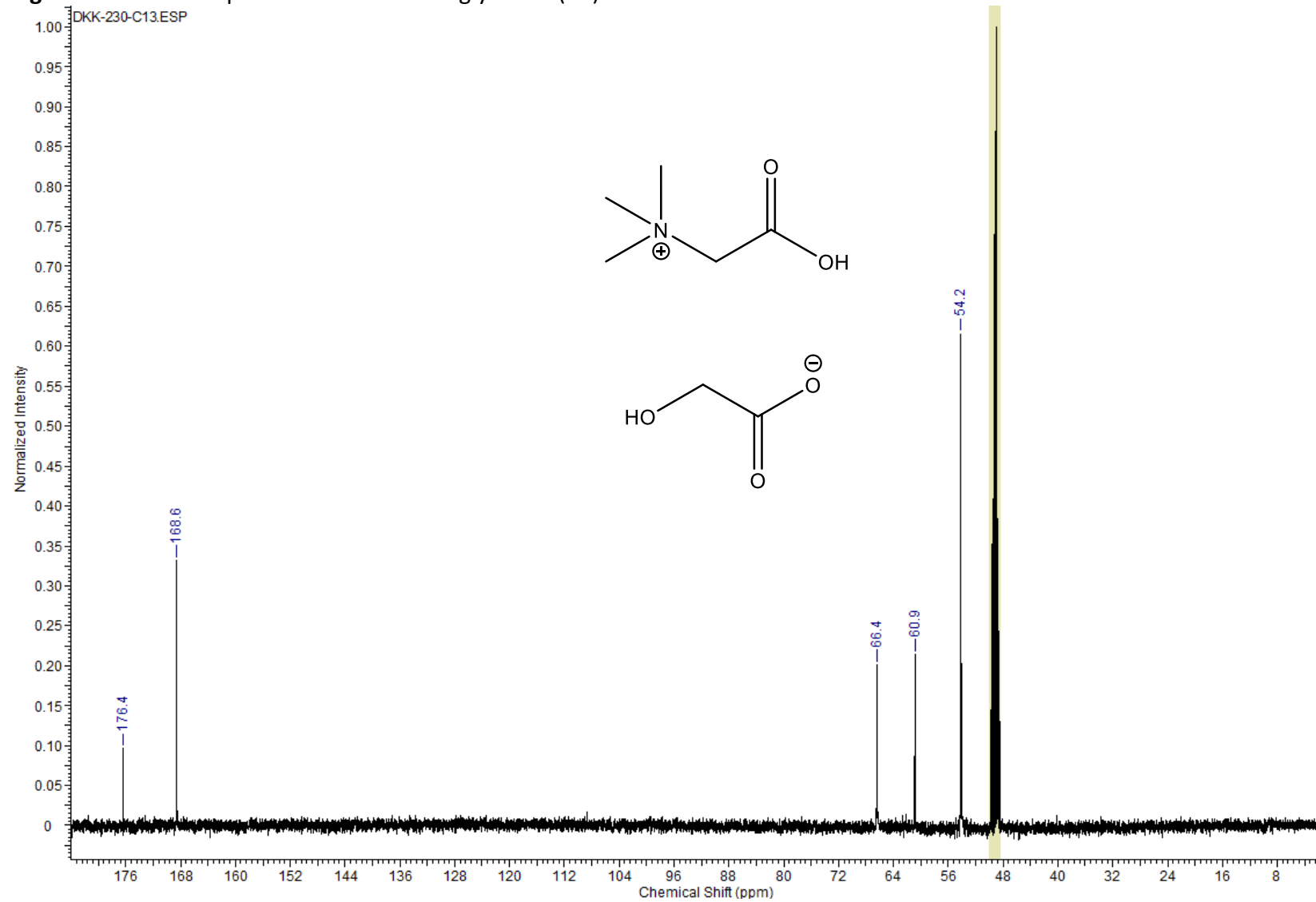
No.	Chemical formula	Molecular weight [g mol ⁻¹]	Calculated values			Obtained values		
			[%]			[%]		
			C	H	N	C	H	N
1a	C ₇ H ₁₅ NO ₅	193.20	43.52	7.83	7.25	43.69	7.57	7.40
2a	C ₁₀ H ₂₁ NO ₅	235.28	51.05	9.00	5.95	51.15	8.79	5.79
3a	C ₁₈ H ₃₇ NO ₅	347.50	62.22	10.73	4.03	61.80	10.47	3.94
1b	C ₁₁ H ₂₃ NO ₉	313.30	42.17	7.40	4.47	41.94	7.58	4.72
2b	C ₁₄ H ₂₉ NO ₉	355.38	47.32	8.23	3.94	47.54	8.45	3.85
3b	C ₂₂ H ₄₅ NO ₉	467.60	56.51	9.70	3.00	56.59	9.49	2.90
1c	C ₁₅ H ₂₈ N ₂ O ₉	380.39	47.36	7.42	7.36	47.03	7.16	7.48
2c	C ₂₁ H ₄₀ N ₂ O ₉	464.56	54.30	8.68	6.03	54.19	8.46	6.28
3c	C ₃₇ H ₇₂ N ₂ O ₉	688.99	64.50	10.53	4.07	64.15	10.66	4.25
1d	C ₁₀ H ₁₈ N ₂ O ₅	246.26	48.77	7.37	11.38	49.01	7.68	11.51
2d	C ₁₃ H ₂₄ N ₂ O ₅	288.26	54.15	8.39	9.72	53.72	8.08	9.99
3d	C ₂₁ H ₄₀ N ₂ O ₅	400.56	62.97	10.07	6.99	63.08	10.40	6.77
1e	C ₂₉ H ₅₁ NO ₇	525.73	66.25	9.78	2.66	66.05	9.89	2.73
2e	C ₃₂ H ₅₇ NO ₇	567.81	67.69	10.12	2.47	67.31	10.33	2.27
3e	C ₄₀ H ₇₃ NO ₇	680.02	70.65	10.82	2.06	71.16	11.20	1.86
1f	C ₂₅ H ₄₉ NO ₉ S	539.73	55.63	9.15	2.60	55.43	9.04	2.80
2f	C ₂₈ H ₅₅ NO ₉ S	581.81	57.80	9.53	2.41	57.49	9.29	2.63
3f	C ₃₆ H ₇₁ NO ₉ S	694.02	62.30	10.31	2.02	62.09	10.18	2.14
1g	C ₂₁ H ₄₆ NO ₆ P	439.57	57.38	10.55	3.19	57.77	10.28	3.42
2g	C ₂₄ H ₅₂ NO ₆ P	481.65	59.85	10.88	2.91	60.10	10.94	2.80
3g	C ₃₂ H ₆₈ NO ₆ P	593.87	64.72	11.54	2.36	65.13	11.27	2.11

Figure S1. ^1H NMR spectrum of betainium glycolate (**1a**).



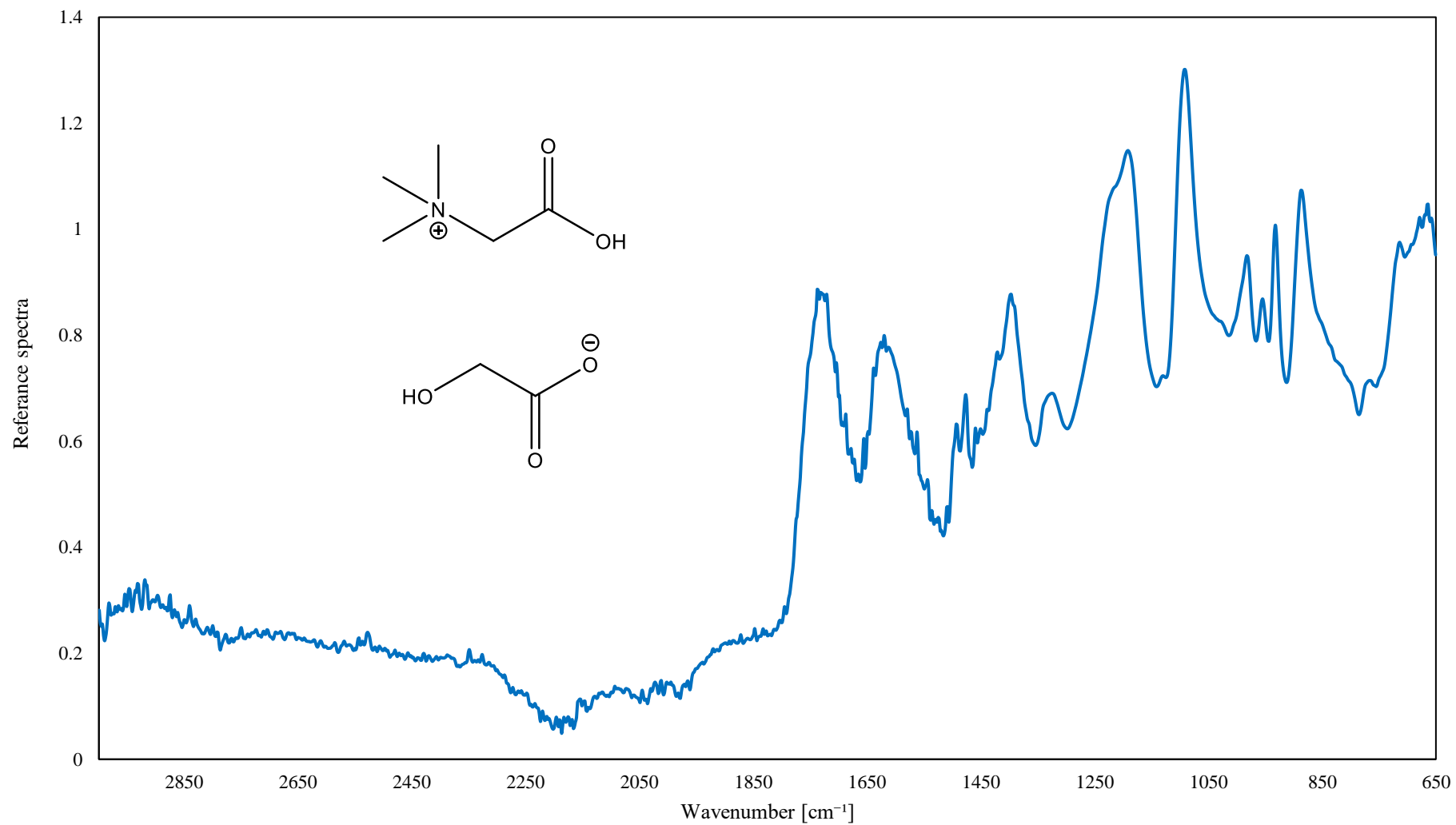
^1H NMR ($\text{CD}_3\text{OD}-d_4$, 298K, 400 MHz): δ_{H} [ppm] = 3.32 (s, 9H; H-1, H-2, H-3); 4.04 (s, 2H; H-4); 4.09 (s, 1H; H-5); 4.24 (s, 1H; H-5).

Figure S2. ^{13}C NMR spectrum of betainium glycolate (**1a**).



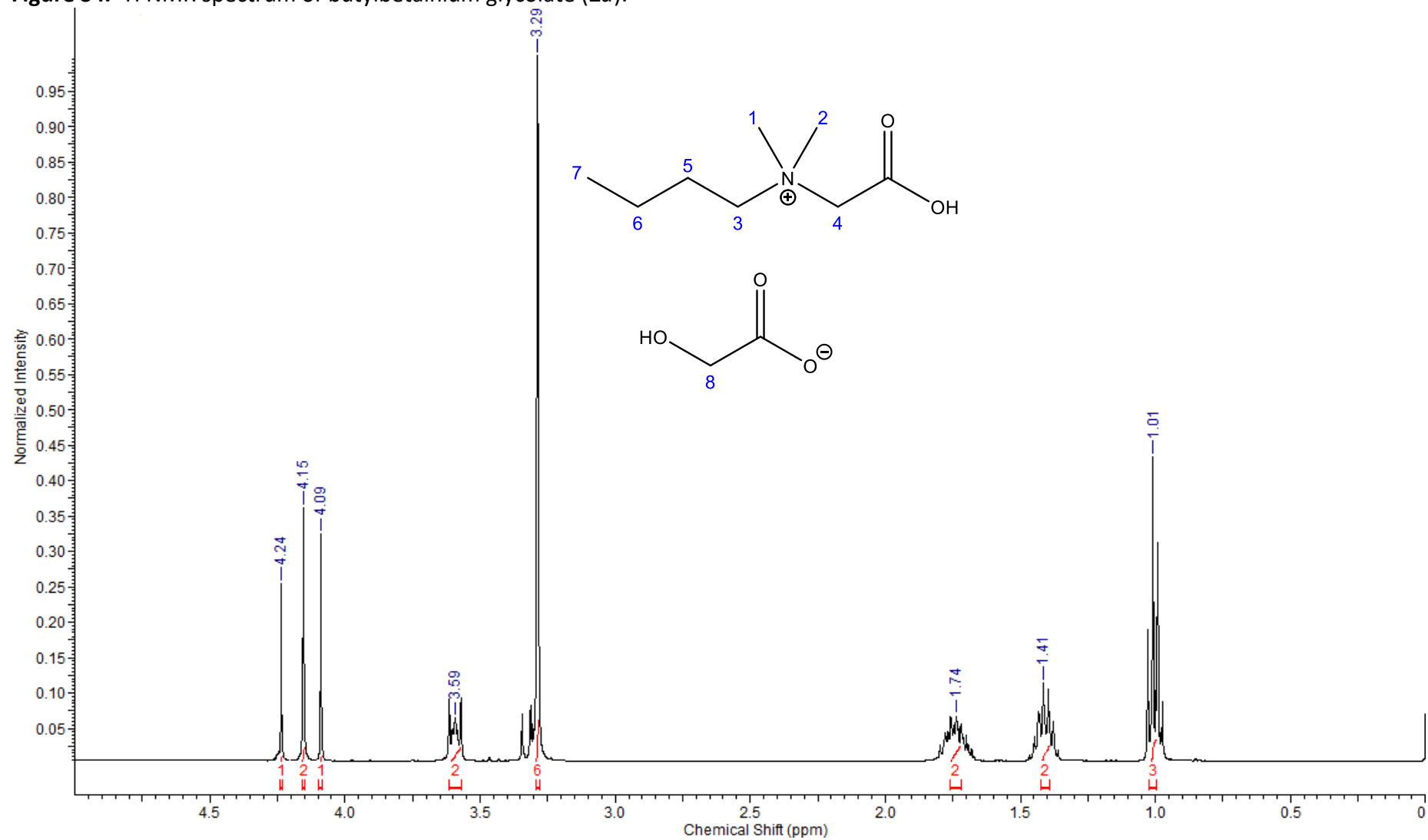
^{13}C NMR ($\text{CD}_3\text{OD}-d_4$, 298K, 100 MHz): δ_{C} [ppm] = 54.2 (3C), 60.9, 66.4, 168.6, 176.4.

Figure S3. IR spectrum of betainium glycolate (**1a**).



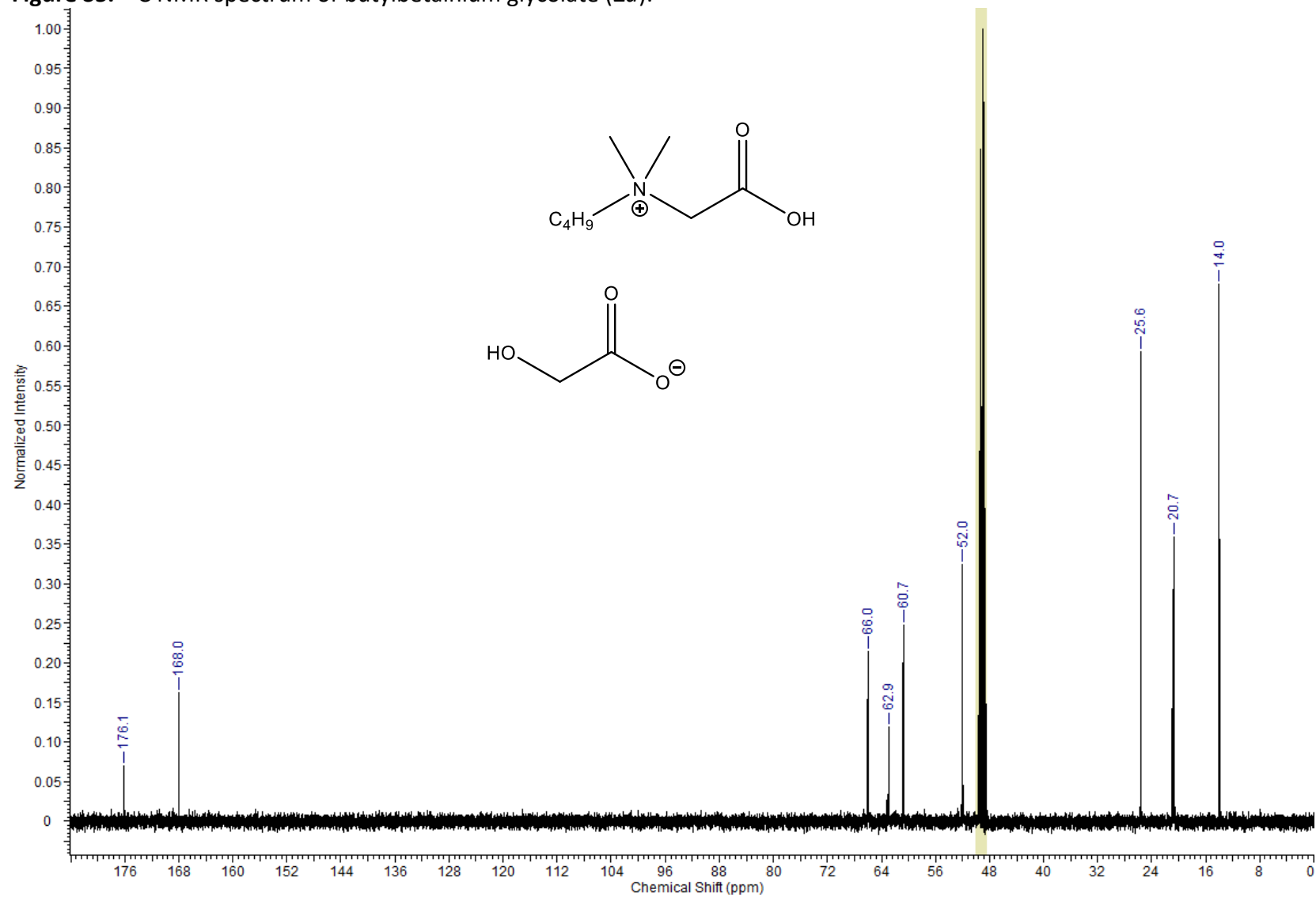
IR [cm^{-1}] = 665, 713, 766, 866, 932, 958, 982, 1029, 1191, 1325, 1397, 1477, 1620, 1736.

Figure S4. ^1H NMR spectrum of butylbetainium glycolate (**2a**).



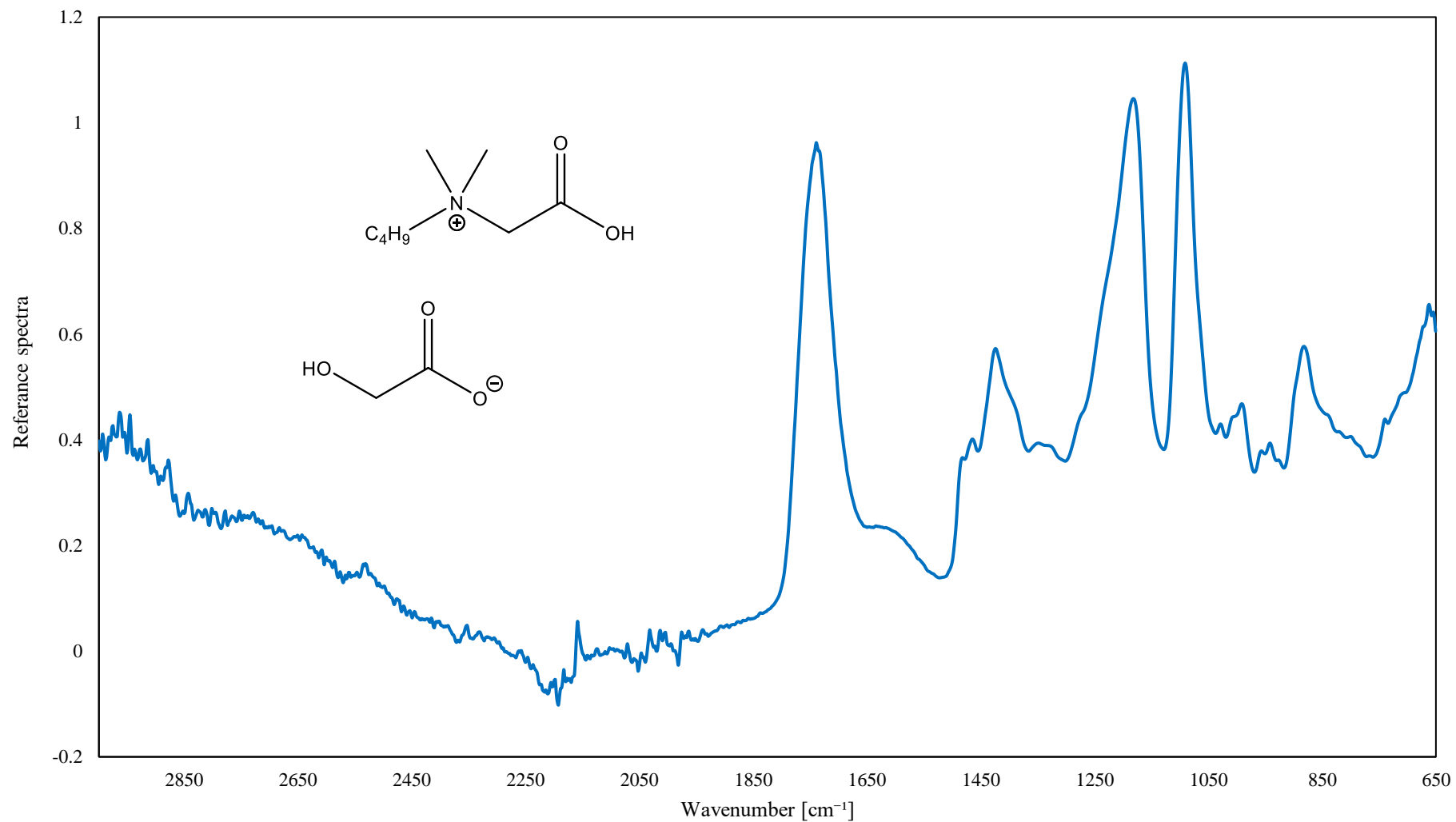
^1H NMR ($\text{CD}_3\text{OD}-d_4$, 298K, 400 MHz): δ_{H} [ppm] = 1.01 (t, 3H, $J = 7.16$ Hz; H-7); 1.41 (m, 2H; H-6); 1.74 (m, 2H; H-5); 3.29 (s, 6H; H-1, H-2); 3.59 (m, 2H; H-3); 4.09 (s, 1H; H-8); 4.15 (s, 2H; H-4); 4.24 (s, 1H; H-8).

Figure S5. ^{13}C NMR spectrum of butylbetainium glycolate (**2a**).



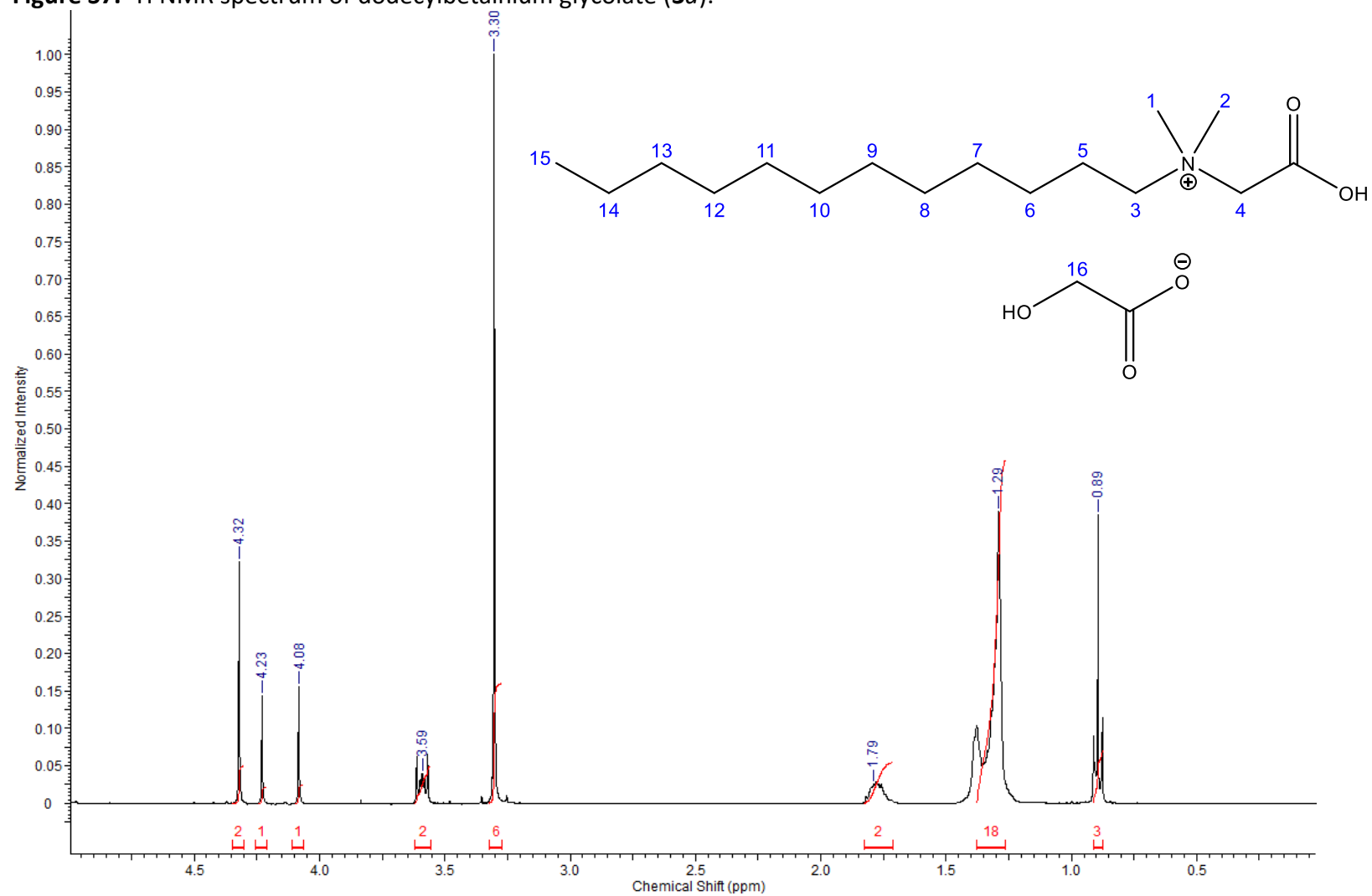
^{13}C NMR ($\text{CD}_3\text{OD}-d_4$, 298K, 100 MHz): δ_{C} [ppm] = 14.0, 20.7, 25.6, 52.0 (2C), 60.7, 62.9, 66.0, 168.0, 176.1.

Figure S6. IR spectrum of butylbetainium glycolate (**2a**).



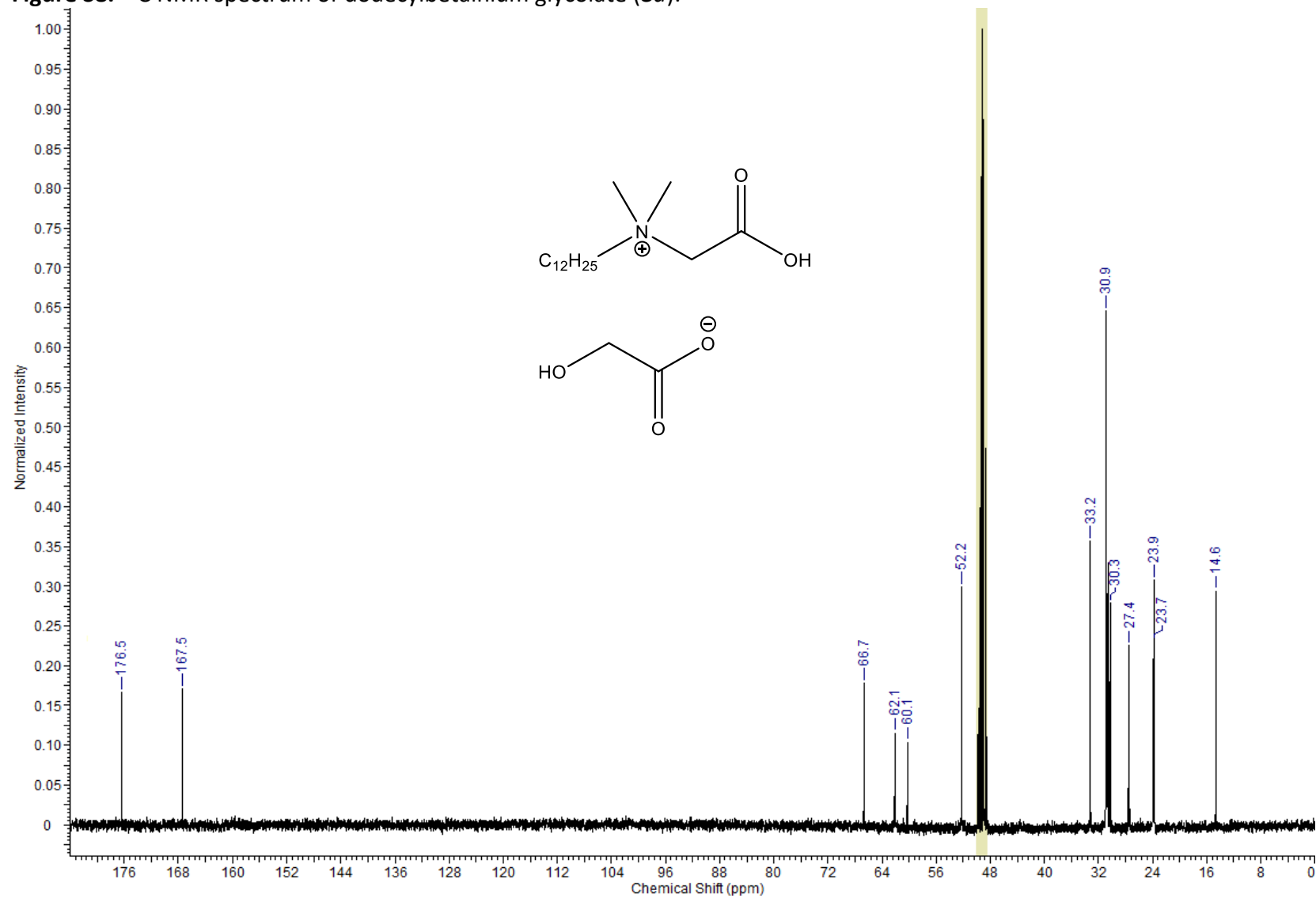
IR [cm⁻¹] = 662, 881, 942, 991, 1029, 1091, 1182, 1349, 1424, 1465, 1634, 1739, 2963.

Figure S7. ^1H NMR spectrum of dodecylbetainium glycolate (**3a**).



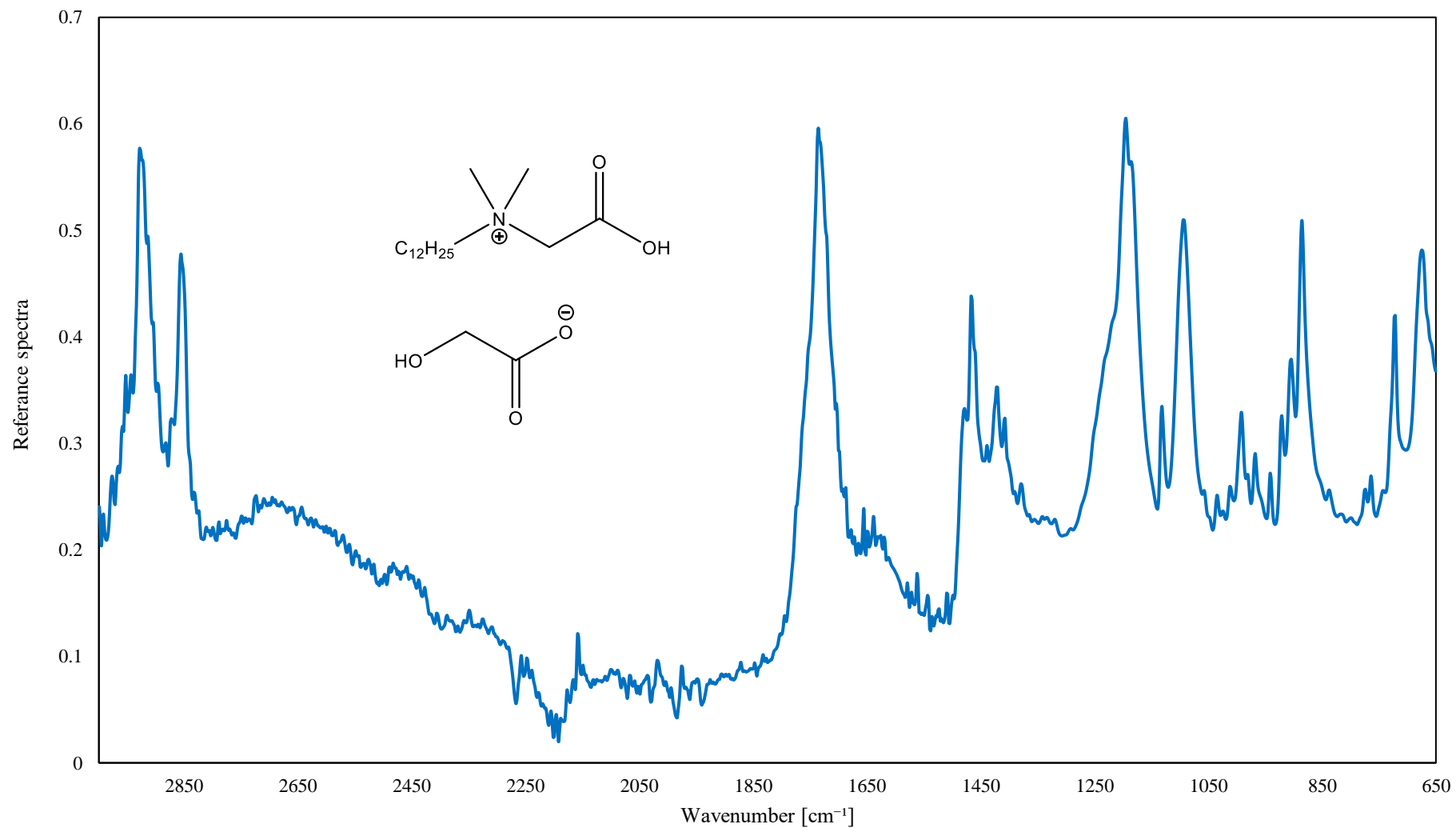
^1H NMR ($\text{CD}_3\text{OD}-d_4$, 298K, 400 MHz): δ_{H} [ppm] = 0.89 (t, 3H, J = 7.14 Hz; H-15); 1.29 (m, 18H; H-6–H-14); 1.79 (m, 2H; H-5); 3.30 (s, 6H; H-1, H-2); 3.59 (m, 2H; H-3); 4.08 (s, 1H; H-16); 4.23 (s, 1H; H-16); 4.32 (s, 2H; H-4).

Figure S8. ^{13}C NMR spectrum of dodecylbetainium glycolate (**3a**).



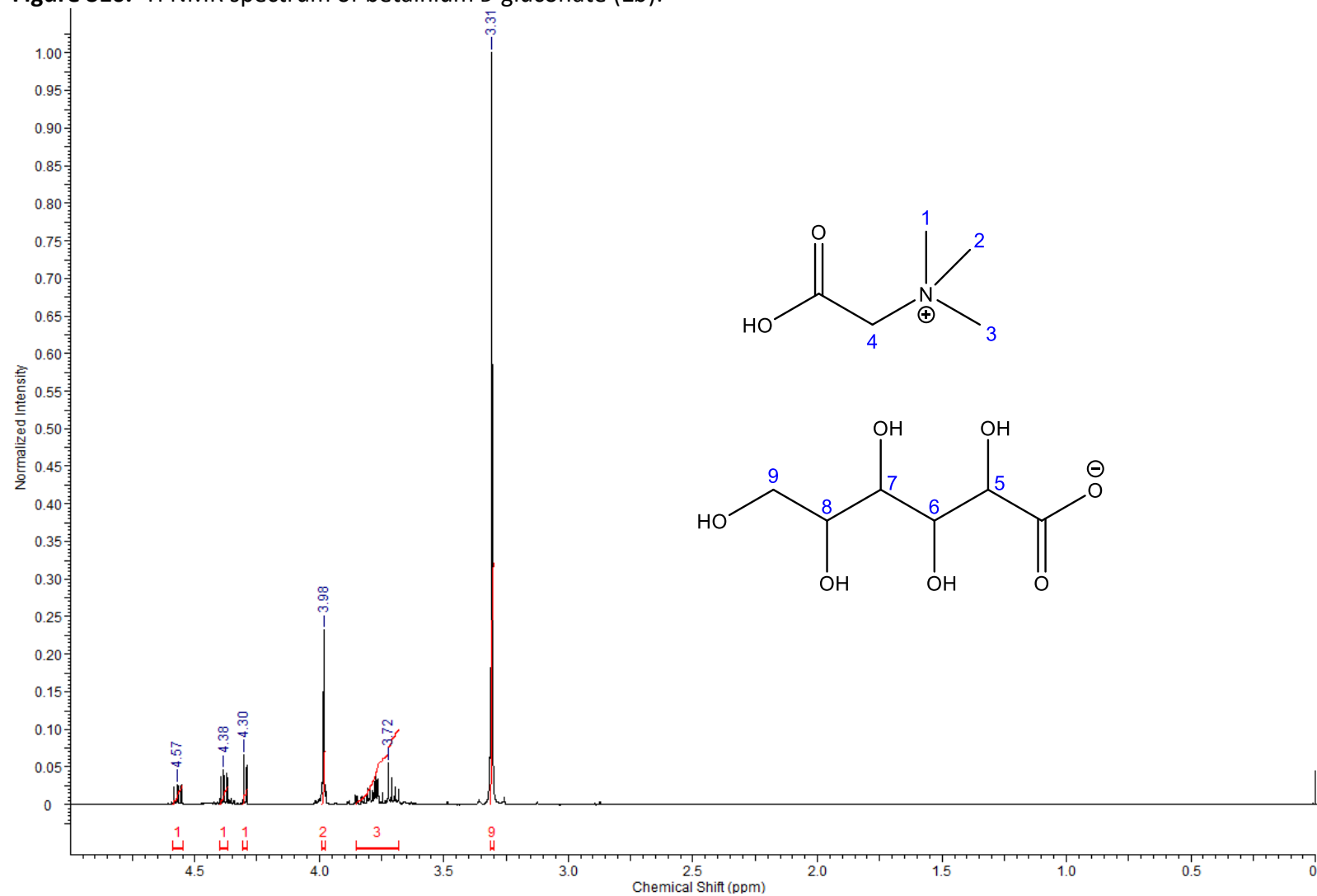
^{13}C NMR ($\text{CD}_3\text{OD}-d_4$, 298K, 100 MHz): δ_{C} [ppm] = 14.6, 23.7, 23.9, 27.4, 30.3 (2C), 30.9 (4C), 33.2, 52.2 (2C), 60.1, 62.1, 66.7, 167.5, 176.5.

Figure S9. IR spectrum of dodecylbetainium glycolate (**3a**).



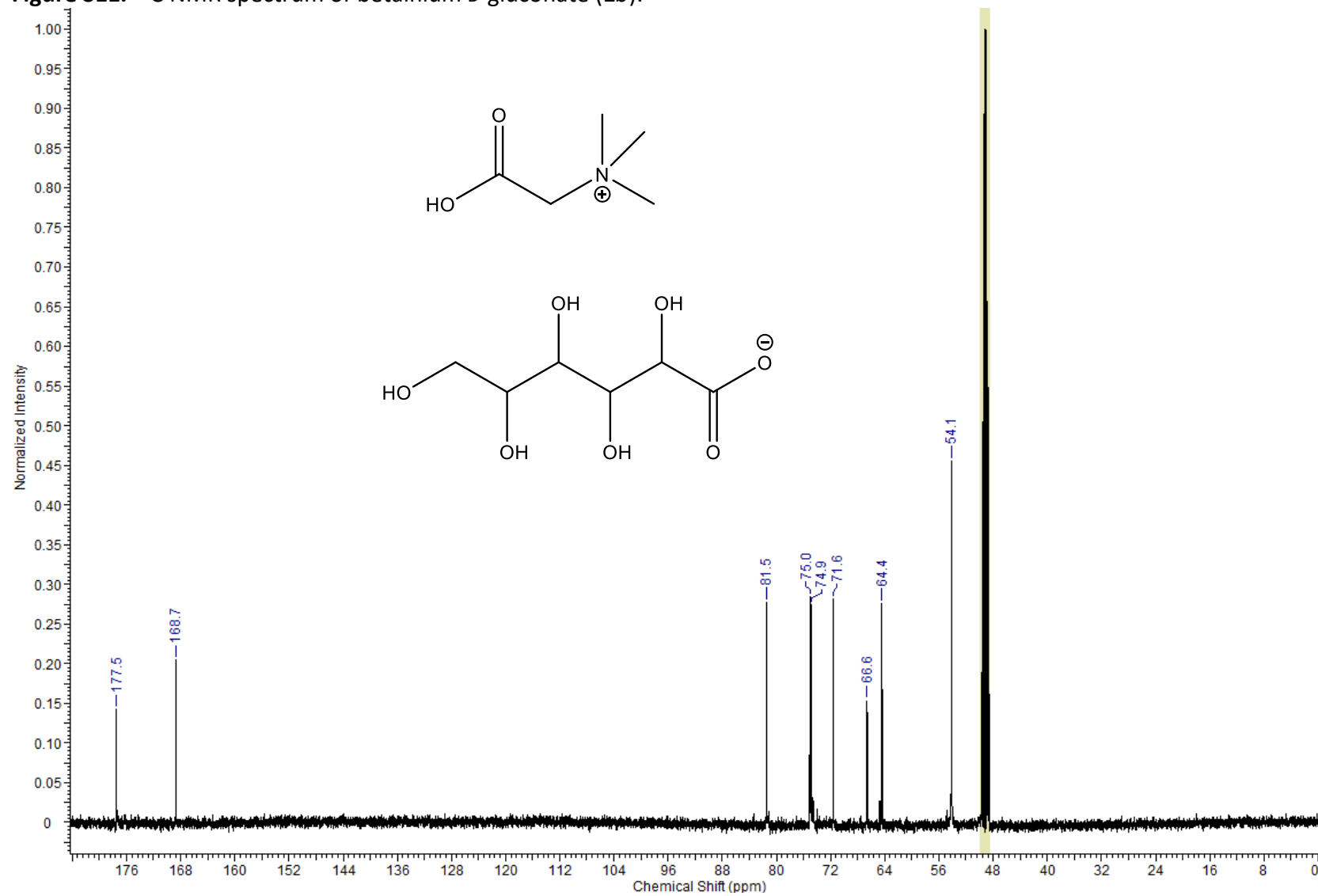
IR [cm^{-1}] = 675, 722, 763, 885, 991, 1093, 1131, 1195, 1422, 1466, 1639, 1735, 2695, 2855, 2927.

Figure S10. ^1H NMR spectrum of betainium D-gluconate (**1b**).



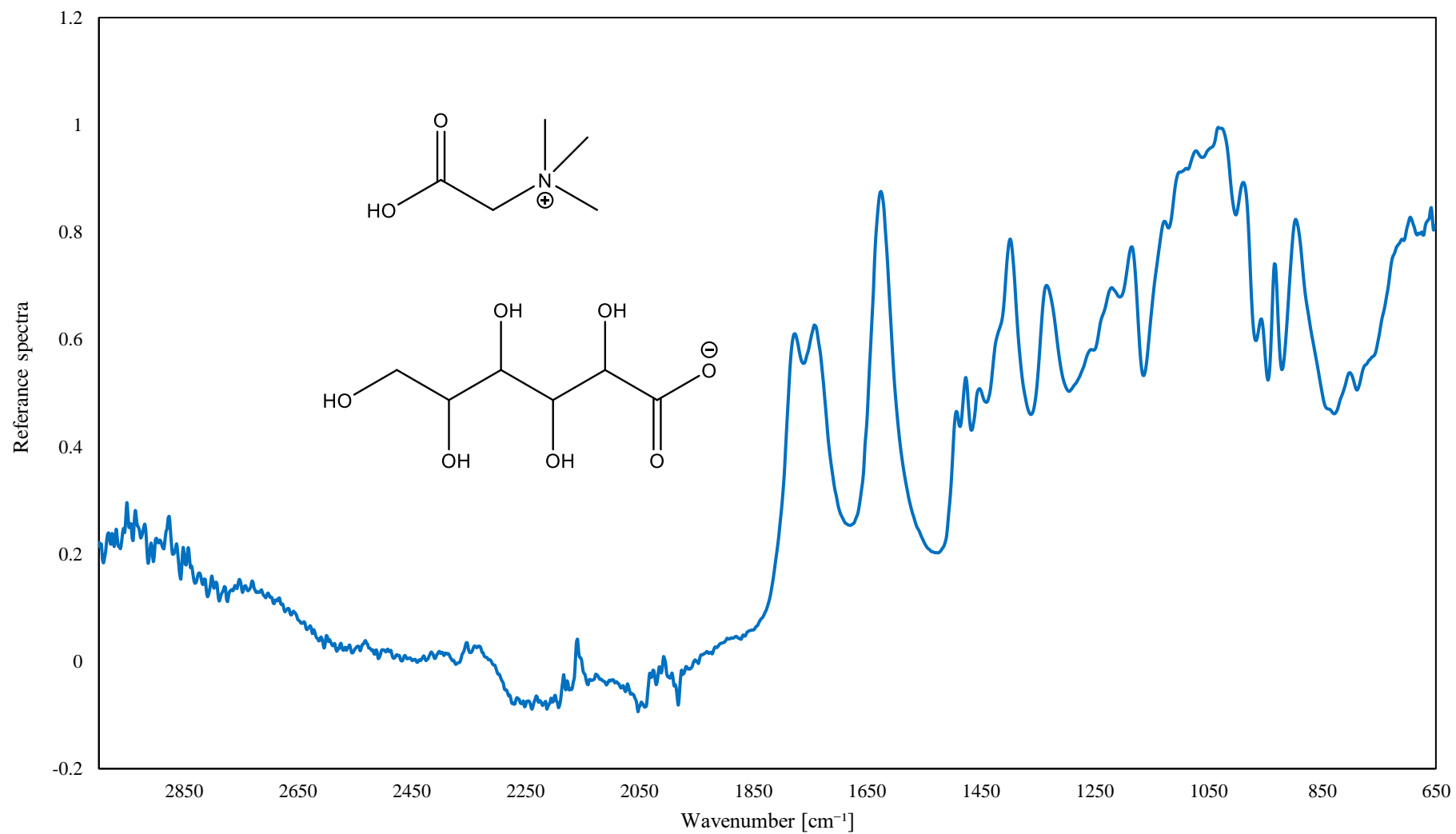
^1H NMR ($\text{CD}_3\text{OD}-d_4$, 298K, 400 MHz): δ_{H} [ppm] = 3.31 (s, 9H; H-1, H-2, H-3); 3.72 (m, 3H; H-8, H-9); 3.98 (s, 2H; H-4); 4.30 (d, 1H, $J = 4.6$ Hz; H-7); 4.38 (m, 1H; H-6); 4.57 (m, 1H; H-5).

Figure S11. ^{13}C NMR spectrum of betainium D-gluconate (**1b**).



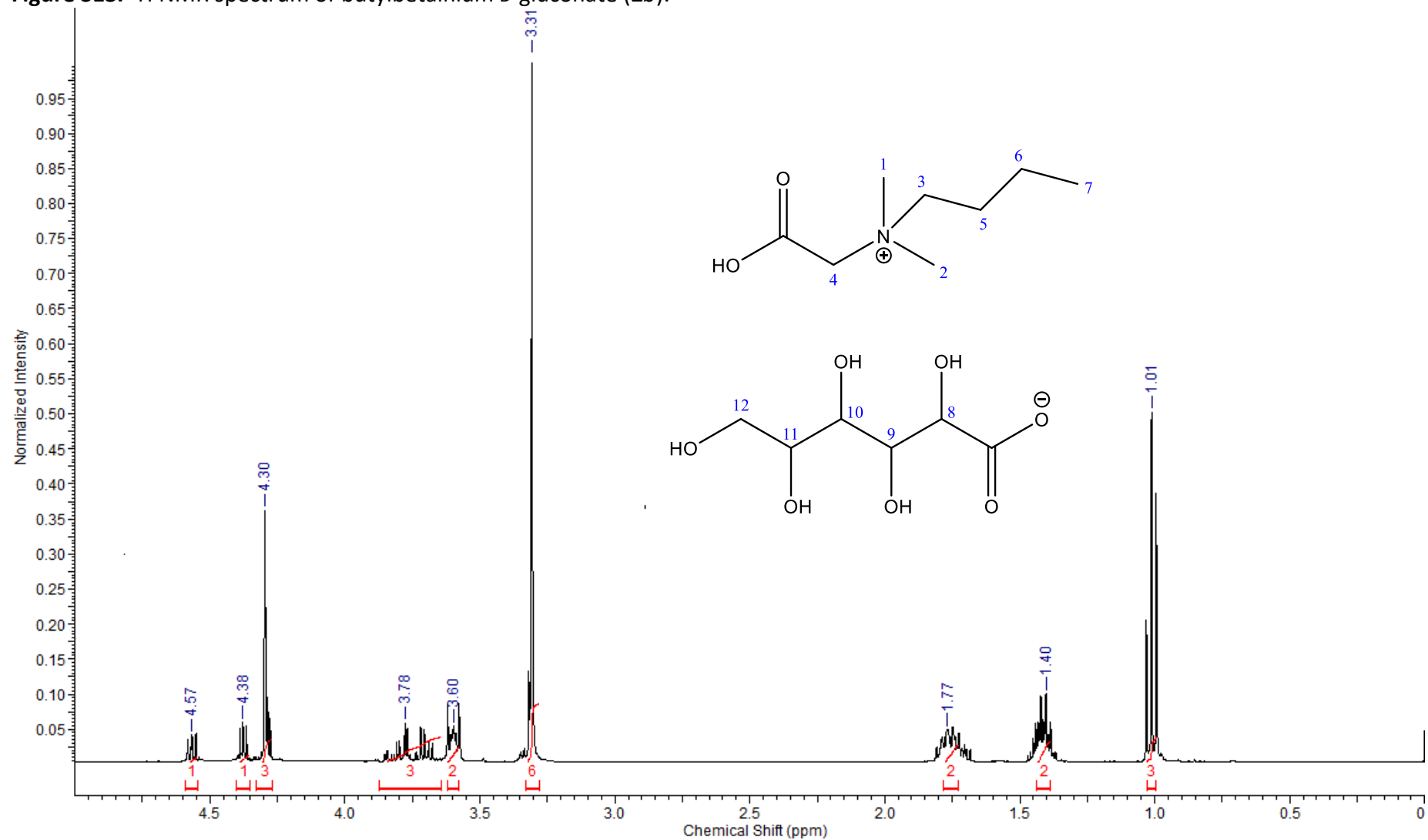
^{13}C NMR ($\text{CD}_3\text{OD}-d_4$, 298K, 100 MHz): δ_{C} [ppm] = 54.1 (3C), 64.4, 66.6, 71.6, 74.9, 75.0, 81.5, 168.7, 177.5.

Figure S12. IR spectrum of betainium D-gluconate (**1b**).



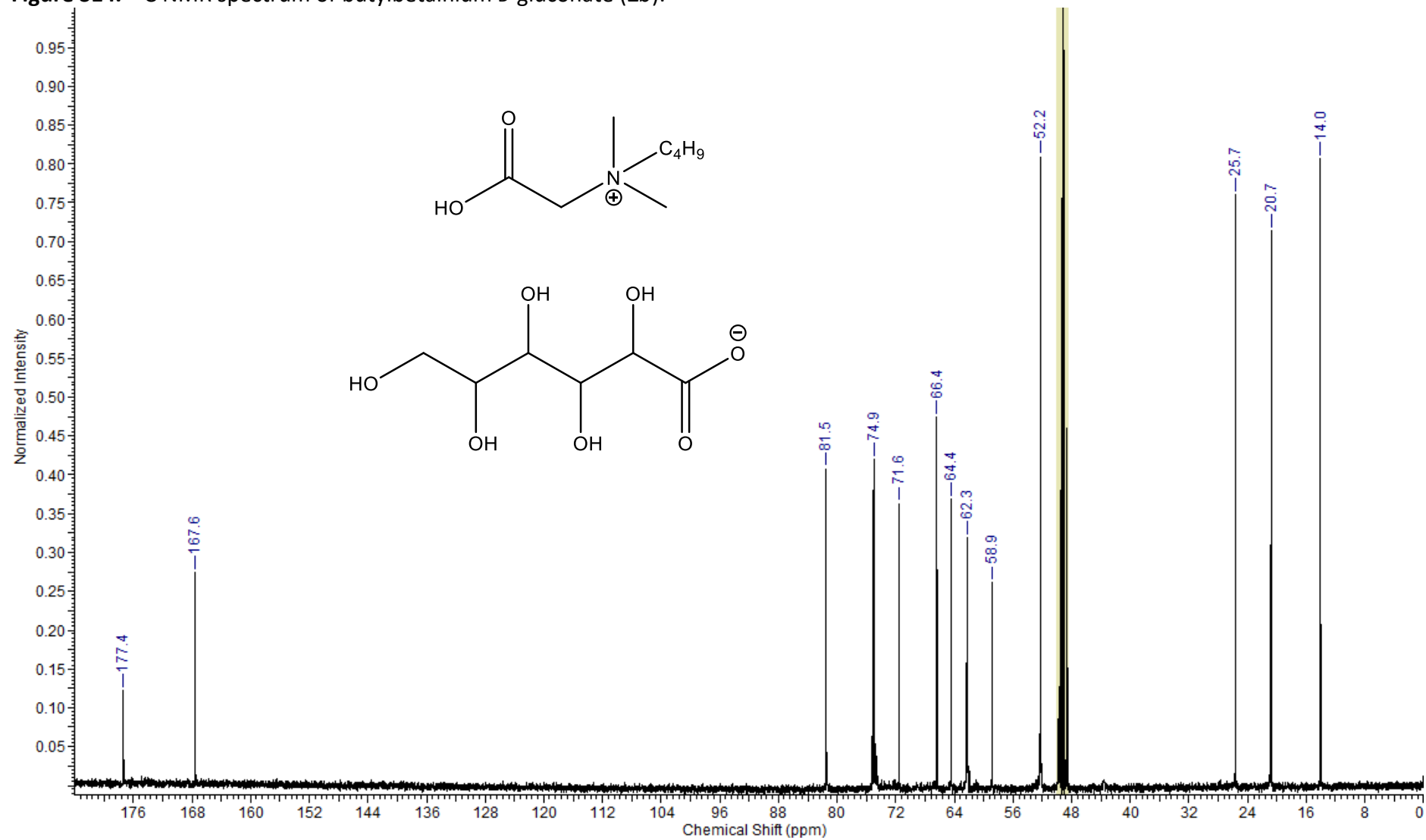
IR [cm⁻¹] = 659, 695, 801, 896, 933, 957, 989, 1031, 1185, 1219, 1334, 1398, 1452, 1476, 1625, 1742, 1777.

Figure S13. ^1H NMR spectrum of butylbetainium D-gluconate (**2b**).



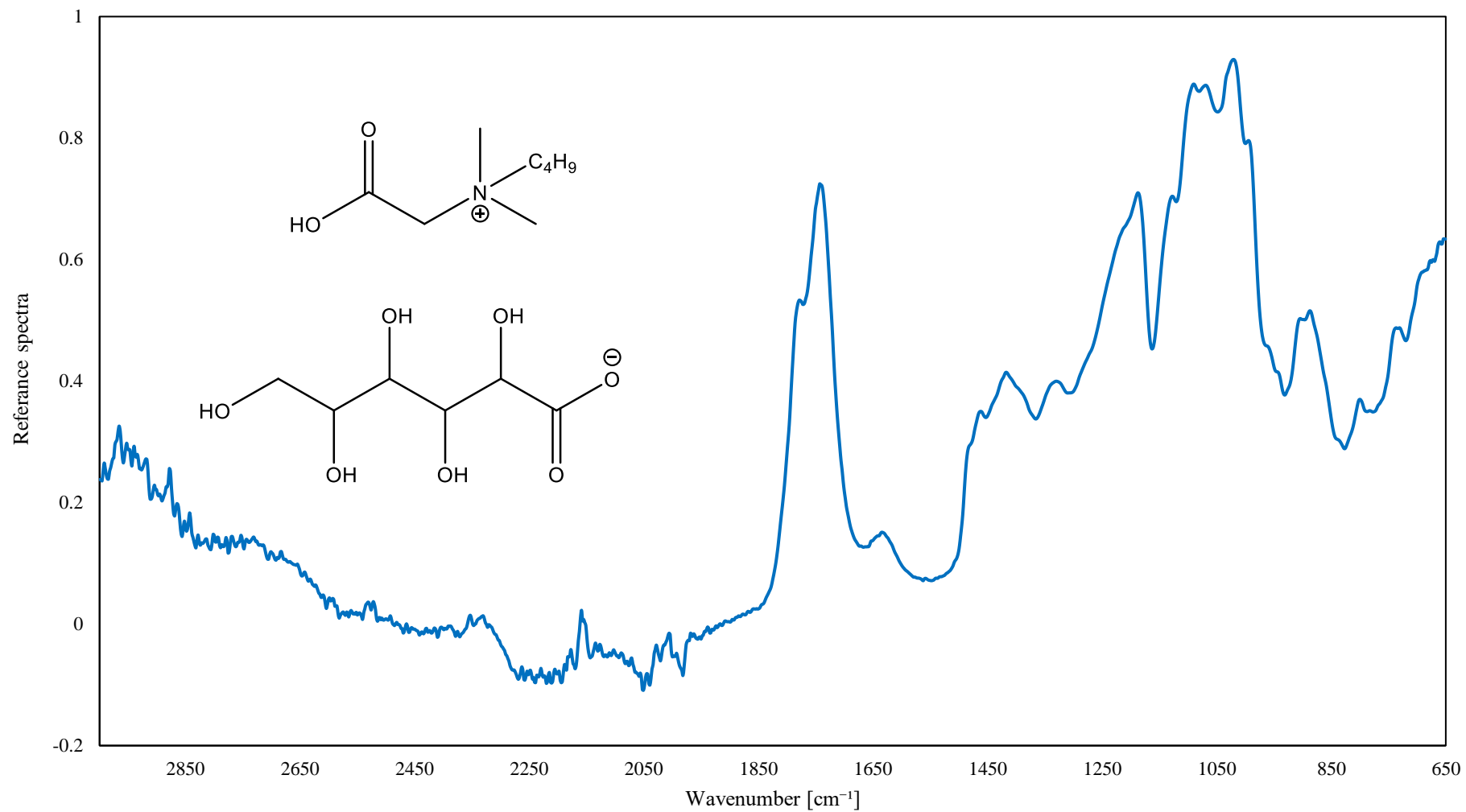
^1H NMR ($\text{CD}_3\text{OD}-d_4$, 298K, 400 MHz): δ_{H} [ppm] = 1.01 (t, $J = 7.36$ Hz, 3H; H-7); 1.40 (m, 2H; H-6); 1.77 (m, 2H; H-5); 3.31 (s, 6H; H-1, H-2); 3.60 (m, 2H; H-3); 3.78 (m, 3H; H-11, H-12); 4.30 (m, 3H; H-4, H-10); 4.38 (m, 1H; H-9); 4.57 (m, 1H; H-8).

Figure S14. ^{13}C NMR spectrum of butylbetainium D-gluconate (**2b**).



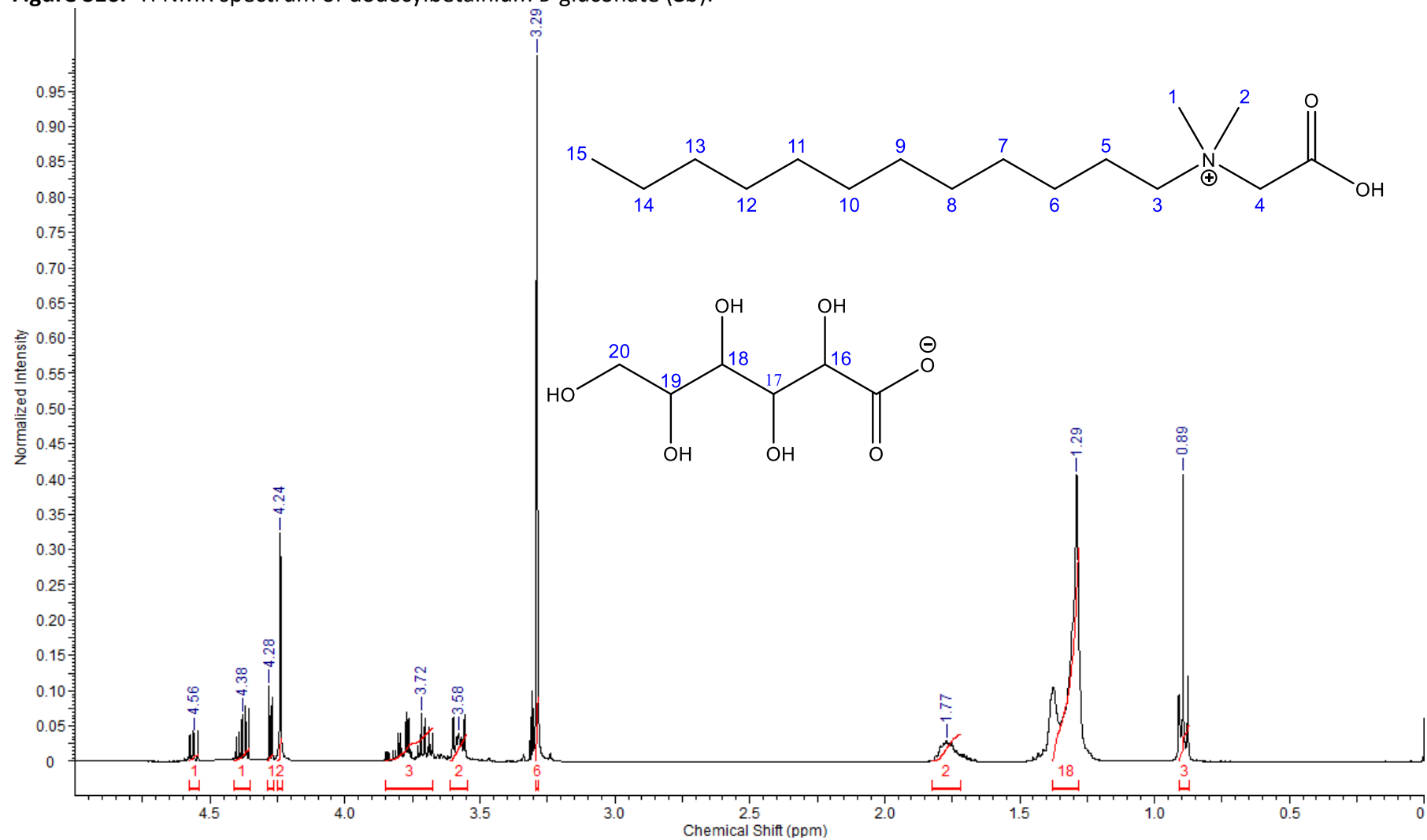
^{13}C NMR ($\text{CD}_3\text{OD}-d_4$, 298K, 100 MHz): δ_{C} [ppm] = 14.0, 20.7, 25.7, 52.2 (2C), 58.9, 62.3, 64.4, 66.4, 71.6, 74.9, 81.5, 167.6, 177.4.

Figure S15. IR spectrum of butylbetainium D-gluconate (**2b**).



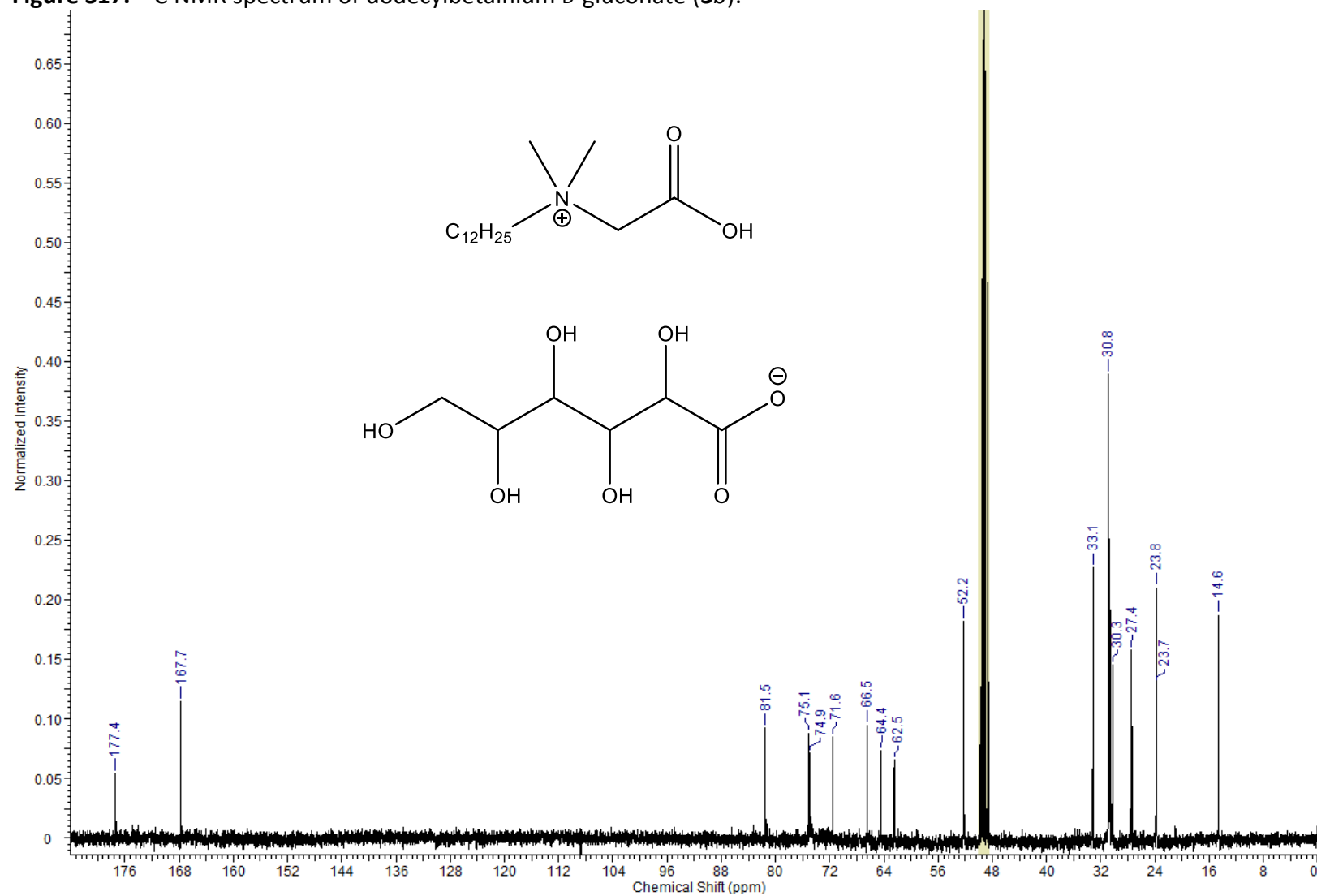
IR [cm⁻¹] = 653, 731, 800, 888, 1021, 1069, 1090 1187, 1330, 1417, 1462, 1634, 1741, 2966.

Figure S16. ¹H NMR spectrum of dodecylbetainium D-gluconate (**3b**).



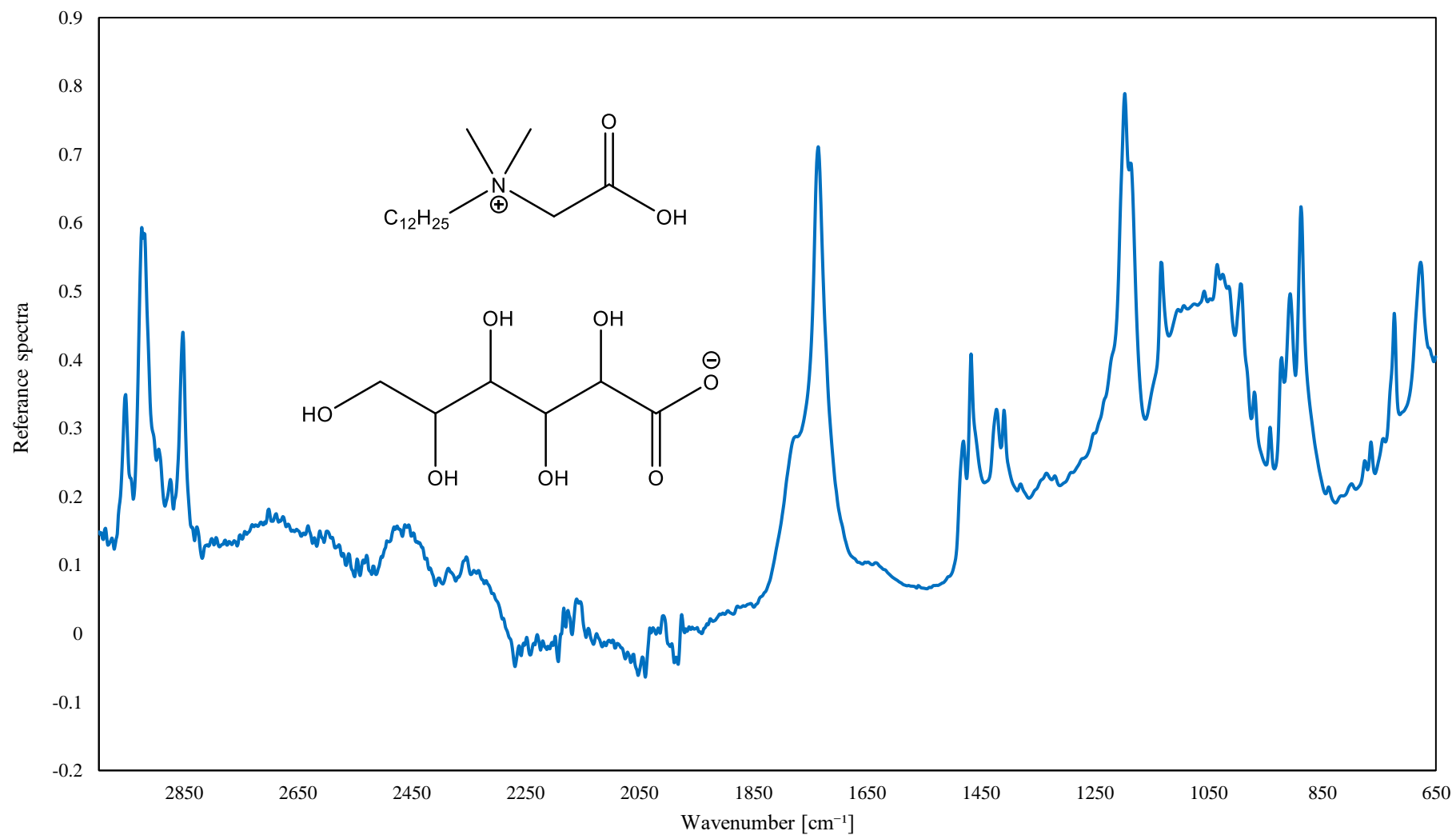
¹H NMR (CD₃OD-*d*₄, 298K, 400 MHz): δ_{H} [ppm] = 0.89 (t, 3H, $J = 7.14$ Hz; H-15); 1.29 (m, 18H; H-6-H-14); 1.77 (m, 2H; H-5); 3.29 (s, 6H; H-1, H-2); 3.58 (m, 2H; H-3); 3.72 (m, 3H; H-19, H-20); 4.24 (s, 2H; H-4); 4.28 (d, 1H, $J = 4.66$ Hz; H-18); 4.38 (m, 1H, H-17); 4.56 (m, 1H; H-16) .

Figure S17. ^{13}C NMR spectrum of dodecylbetainium D-gluconate (**3b**).



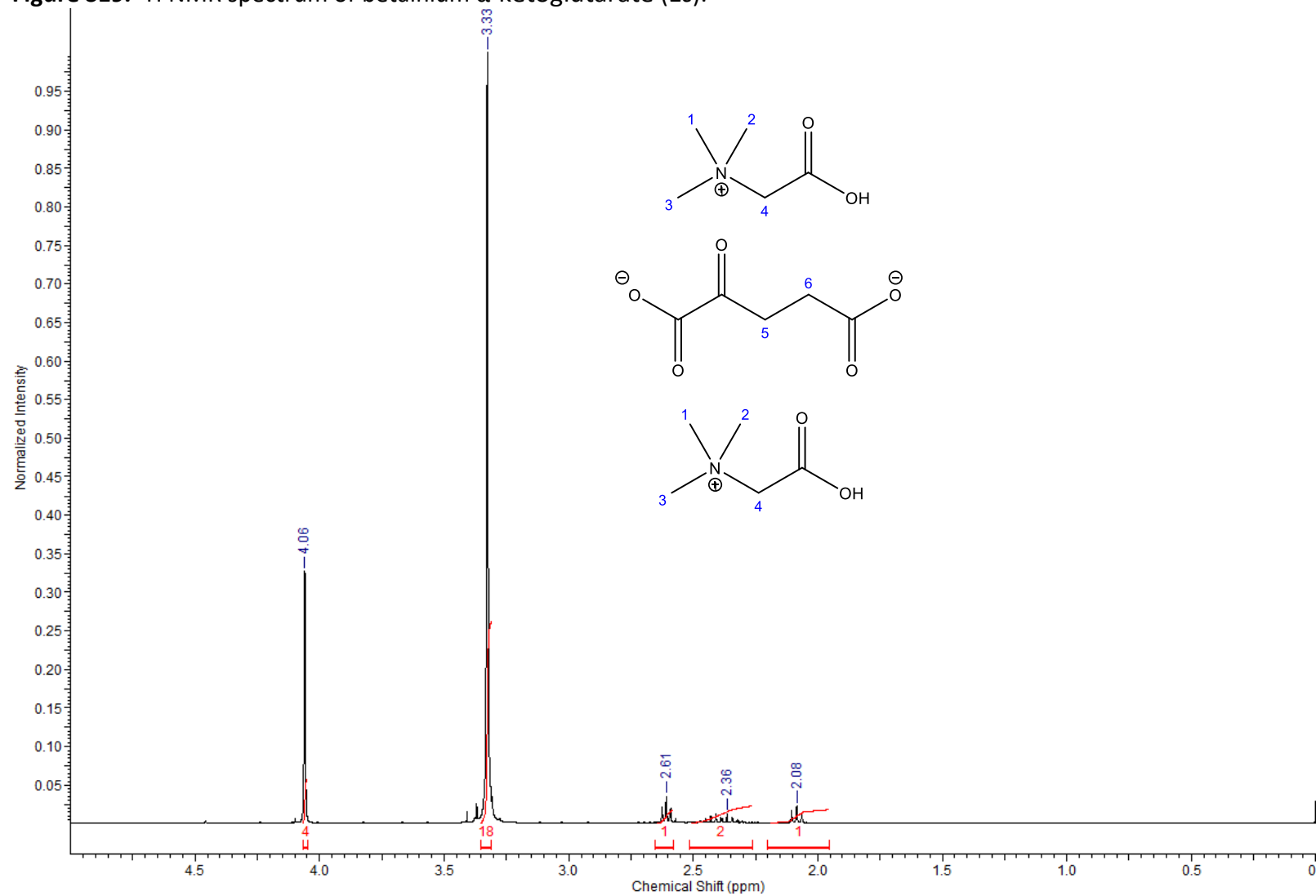
^{13}C NMR ($\text{CD}_3\text{OD}-d_4$, 298K, 100 MHz): δ_{C} [ppm] = 14.6, 23.7, 23.8, 27.4, 30.3 (2C), 30.8 (4C), 33.1, 52.2 (2C), 62.5, 64.4, 66.5, 71.6, 74.9, 75.1, 81.5, 167.7, 177.4.

Figure S18. IR spectrum of dodecylbetainium D-gluconate (**3b**).



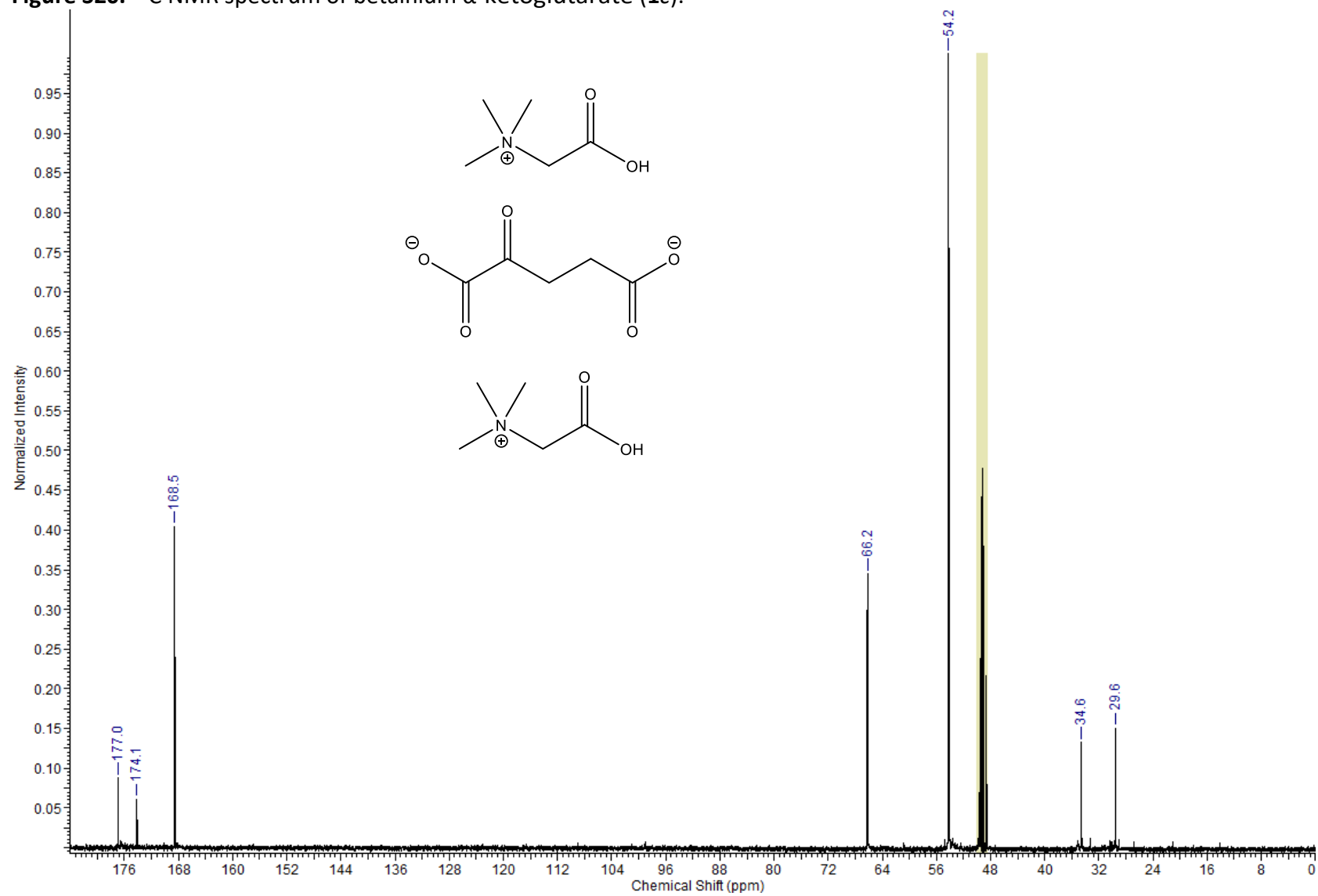
IR [cm^{-1}] = 677, 724, 764, 798, 887, 906, 993, 1034, 1057, 1132, 1197, 1334, 1423, 1467, 1649, 1736, 2853, 2923, 2953.

Figure S19. ¹H NMR spectrum of betainium α-ketoglutarate (1c).



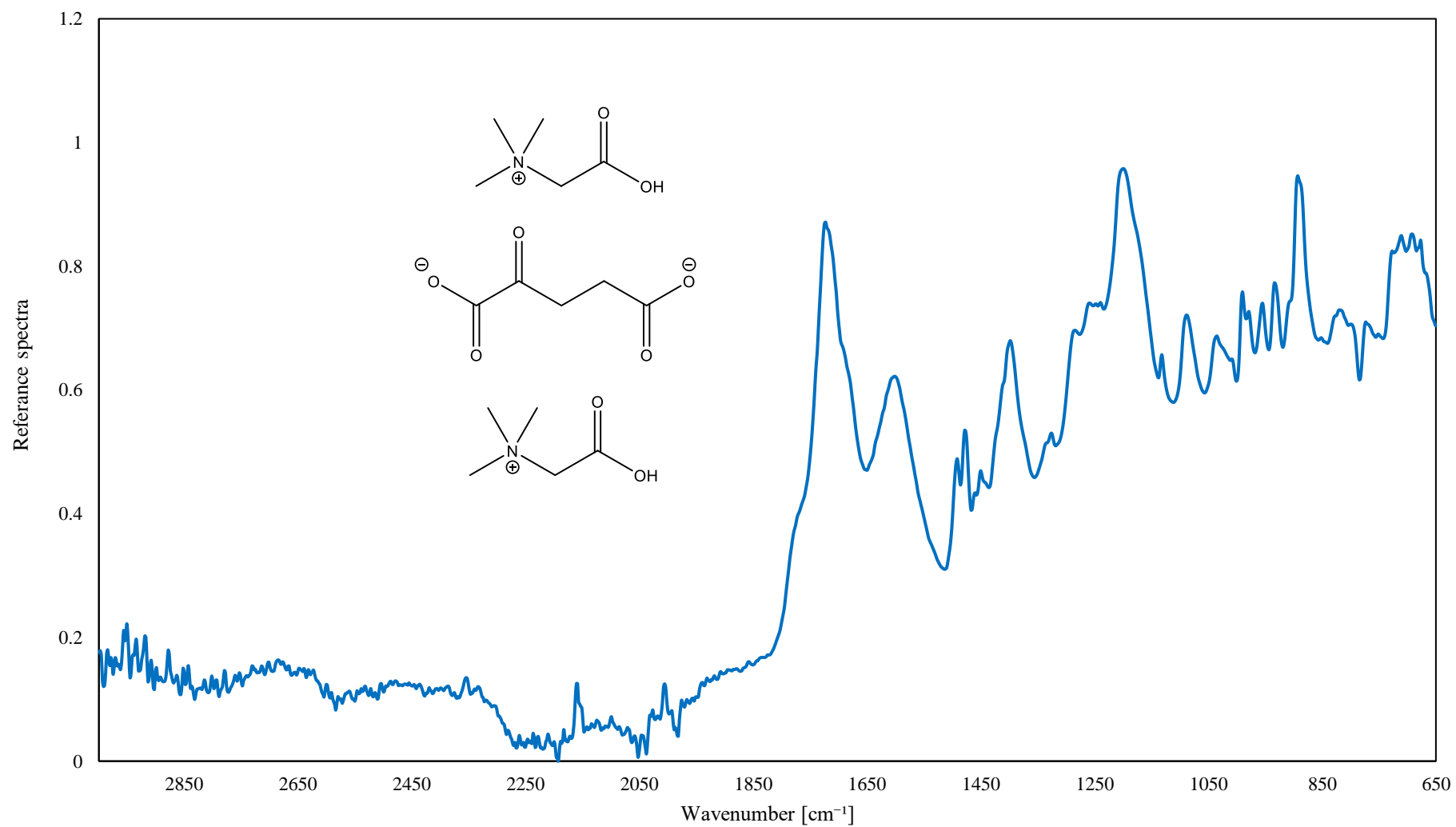
¹H NMR (CD₃OD-*d*₄, 298K, 400 MHz): δ_H [ppm] = 2.08 (t, 1H, *J* = 2.06 Hz; H-5); 2.38 (m, 2H, H-6); 2.61 (t, 1H, *J* = 2.61 Hz; H-5); 3.33 (s, 18H; H-1, H-2, H-3); 4.06 (s, 4H; H-4).

Figure S20. ^{13}C NMR spectrum of betainium α -ketoglutarate (**1c**).



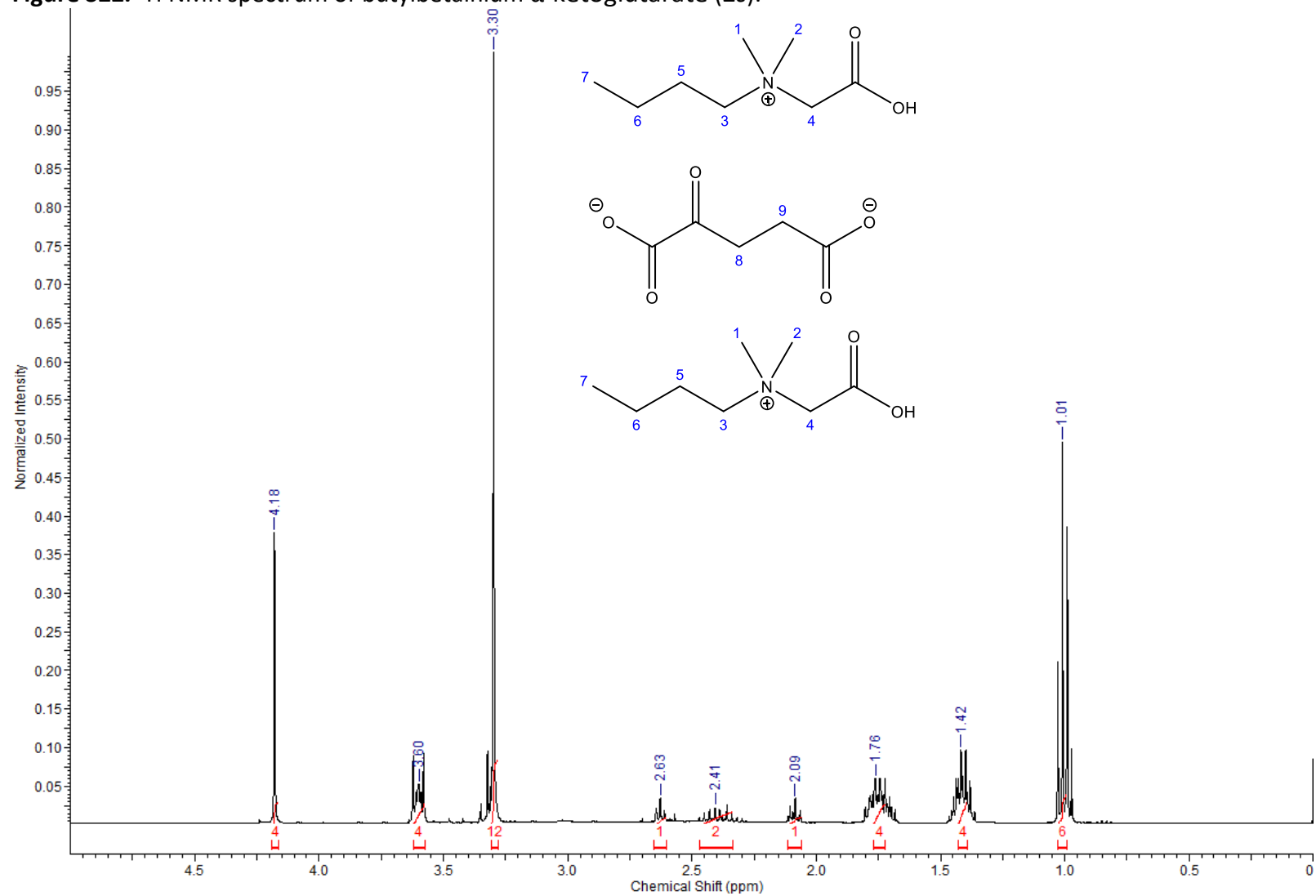
^{13}C NMR ($\text{CD}_3\text{OD}-d_4$, 298K, 100 MHz): δ_{C} [ppm] = 29.6, 34.6, 54.2 (6C), 66.2 (2C), 168.5 (3C), 174.1, 177.0.

Figure S21. IR spectrum of betainium α -ketoglutarate (**1c**).



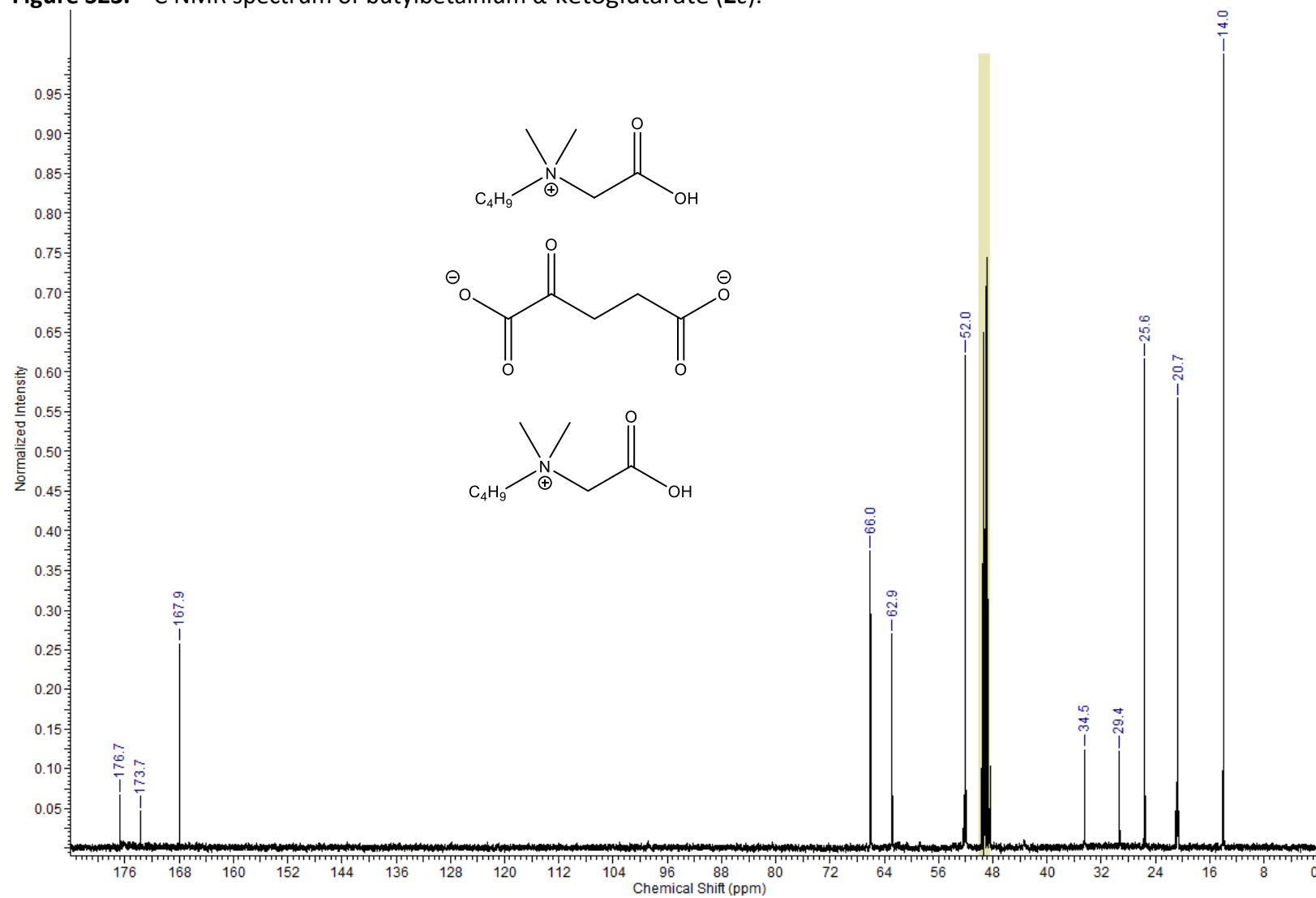
IR [cm^{-1}] = 692, 711, 772, 819, 892, 933, 955, 990, 1035, 1088, 1132, 1200, 1258, 1326, 1398, 1450, 1477, 1602, 1723.

Figure S22. ¹H NMR spectrum of butylbetainium α-ketoglutarate (2c).



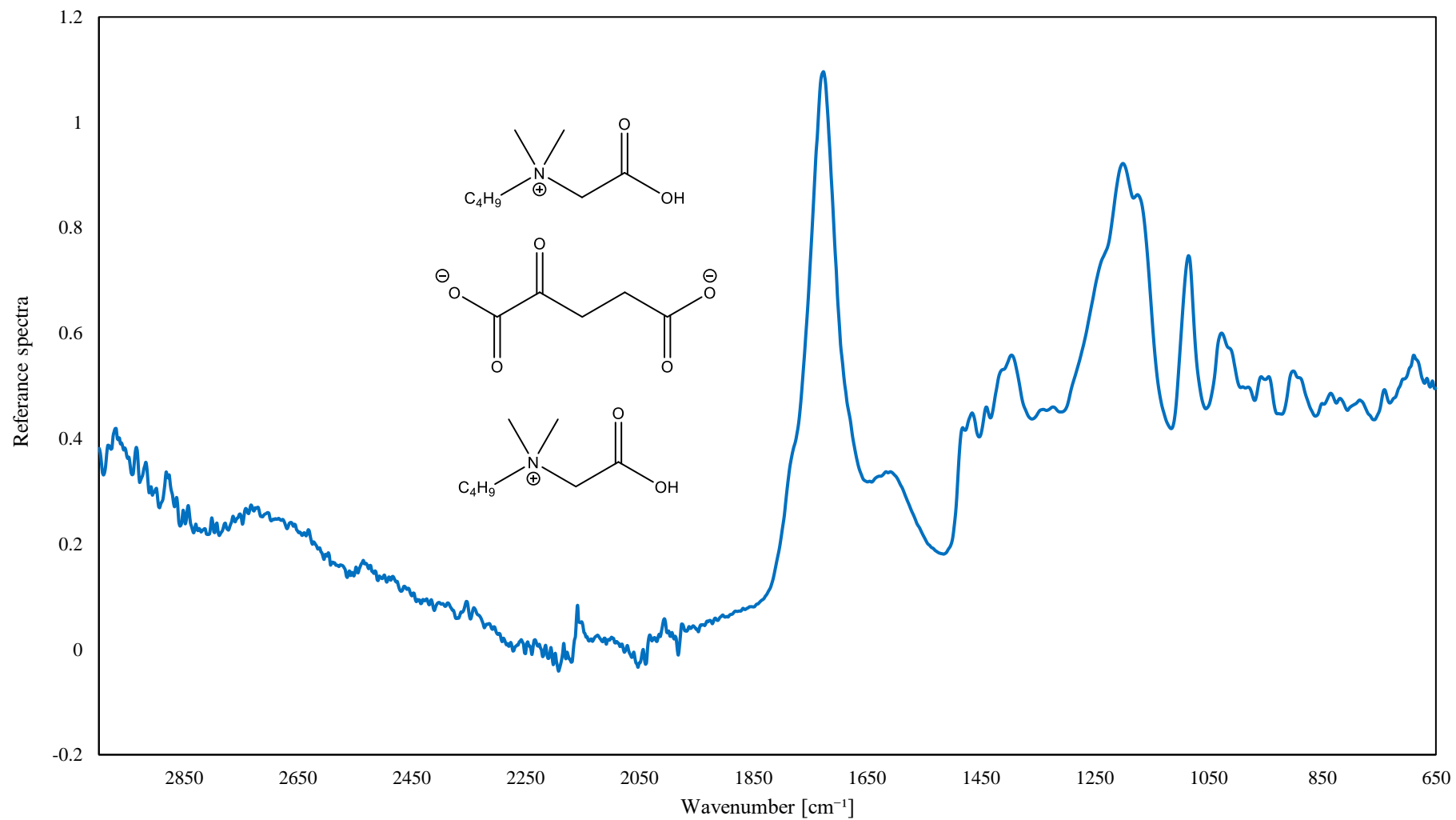
¹H NMR (CD₃OD-*d*₄, 298K, 400 MHz): δ_H [ppm] = 1.01 (m, 6H; H-7); 1.42 (m, 4H; H-6); 1.76 (m, 4H; H-5); 2.09 (m, 1H; H-8); 2.41 (m, 2H; H-9); 2.63 (m, 1H; H-8); 3.30 (s, 12H; H-1, H-2); 3.60 (m, 4H; H-3); 4.18 (s, 4H; H-4).

Figure S23. ^{13}C NMR spectrum of butylbetainium α -ketoglutarate (**2c**).



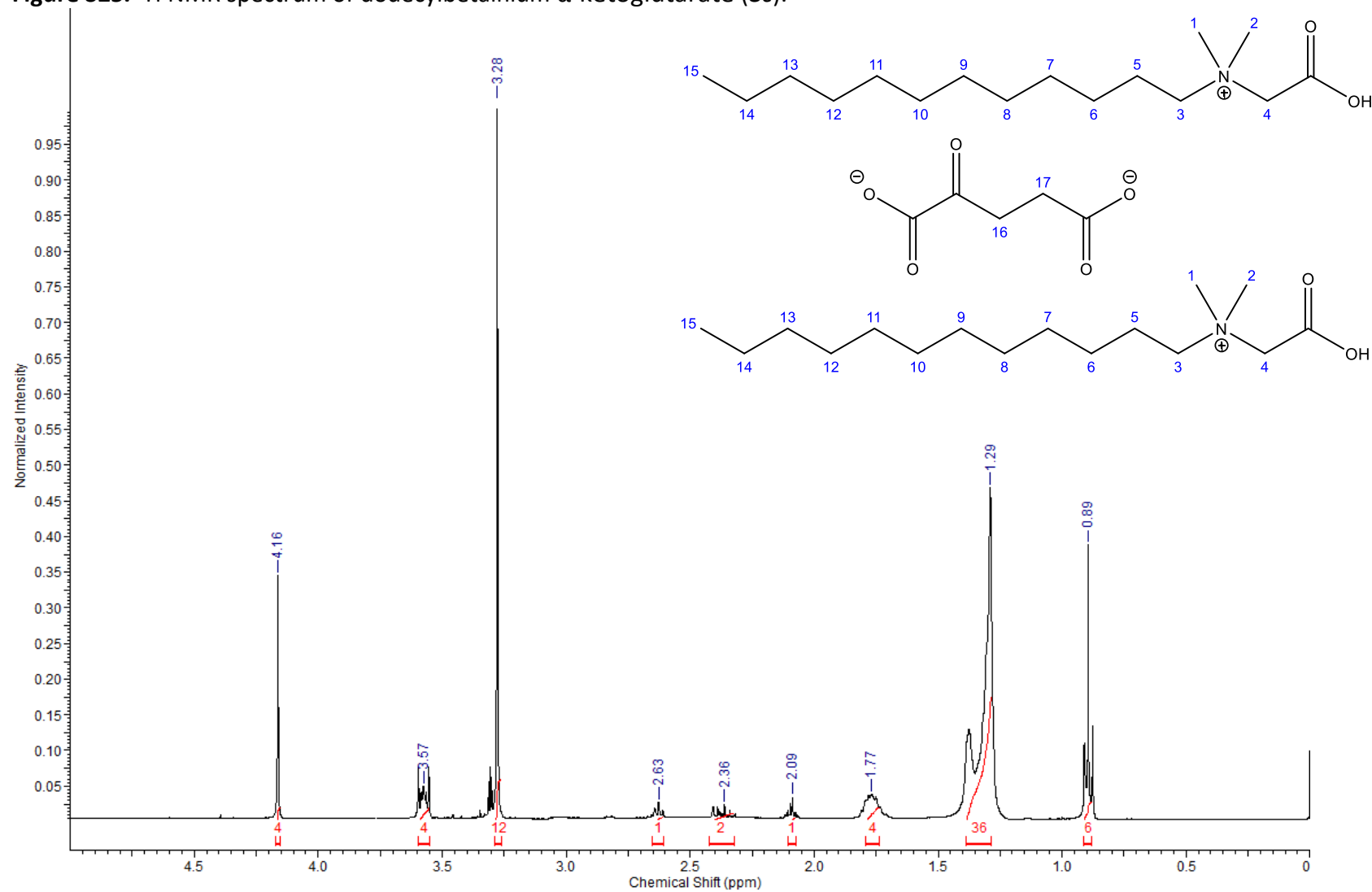
^{13}C NMR ($\text{CD}_3\text{OD}-d_4$, 298K, 100 MHz): δ_{C} [ppm] = 14.0 (2C), 20.7 (2C), 25.6 (2C), 29.4, 34.5, 52.0 (4C), 62.9 (2C), 66.0 (2C), 167.9 (3C), 173.7, 176.7.

Figure S24. IR spectrum of butylbetainium α -ketoglutarate (**2c**).



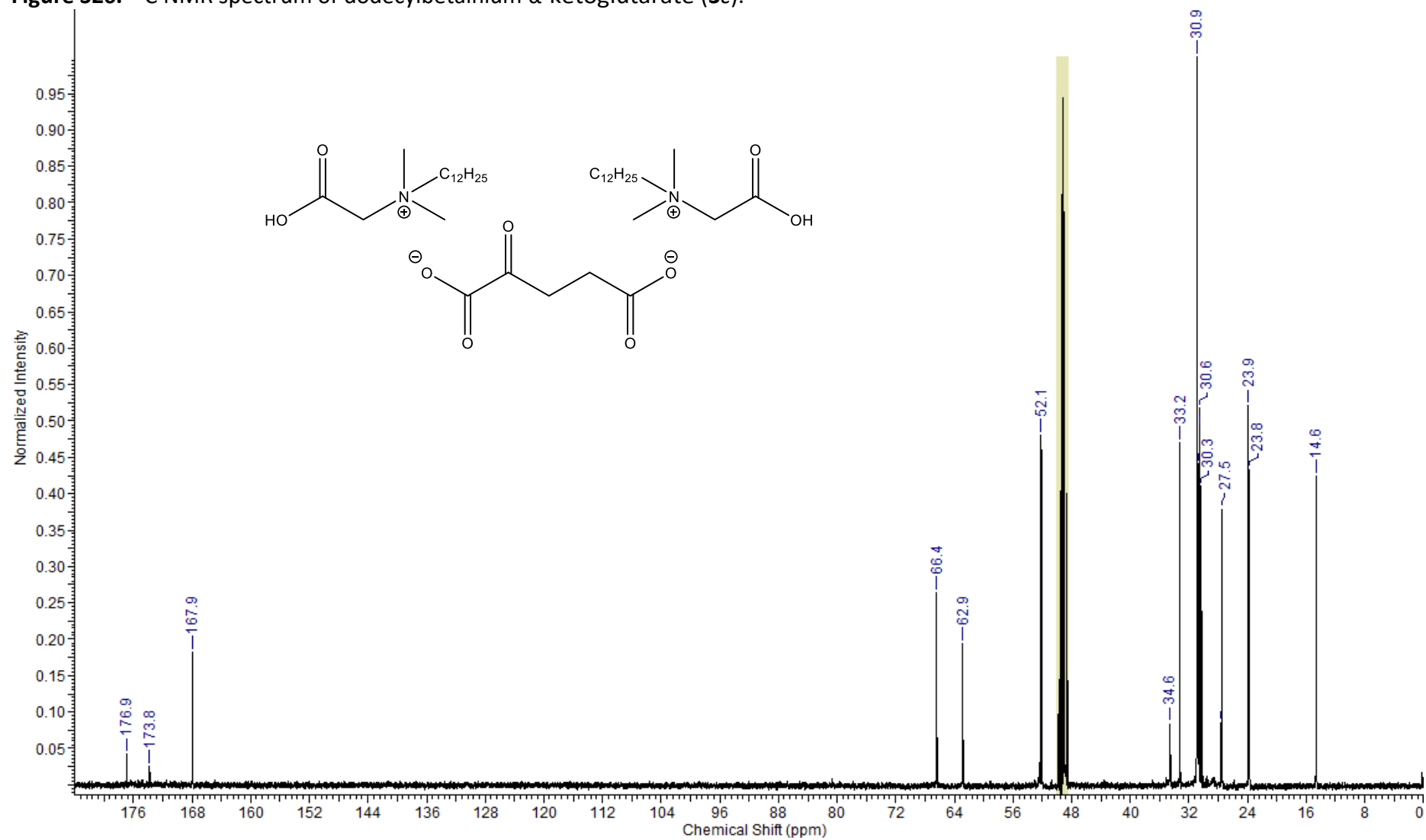
IR [cm^{-1}] = 688, 741, 784, 835, 901, 944, 1027, 1085, 1200, 1223, 1390, 1465, 1616, 1725, 2971.

Figure S25. ¹H NMR spectrum of dodecylbetainium α-ketoglutarate (**3c**).



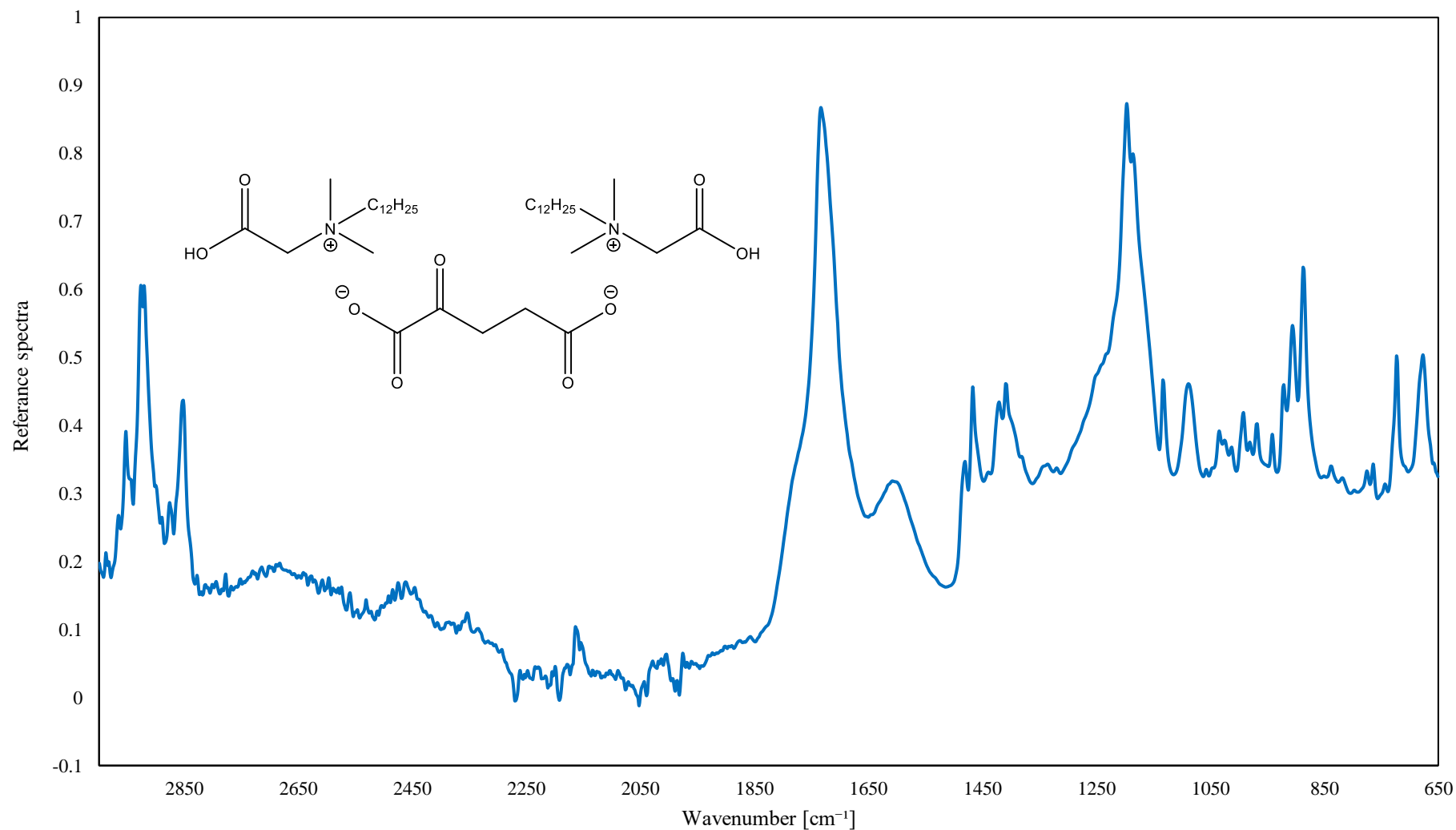
¹H NMR (CD₃OD-d₄, 298K, 400 MHz): δH [ppm] = 0.89 (t, 6H, *J* = 6.98 Hz; H-15); 1.29 (m, 36H; H-6–H-14); 1.77 (m, 4H; H-5); 2.09 (m, 1H; H-16); 2.36 (m, 2H; H-17); 2.63 (m, 1H; H-16); 3.28 (s, 12H; H-1, H-2); 3.57 (m, 4H; H-3); 4.16 (s, 4H, H-4).

Figure S26. ^{13}C NMR spectrum of dodecylbetainium α -ketoglutarate (**3c**).



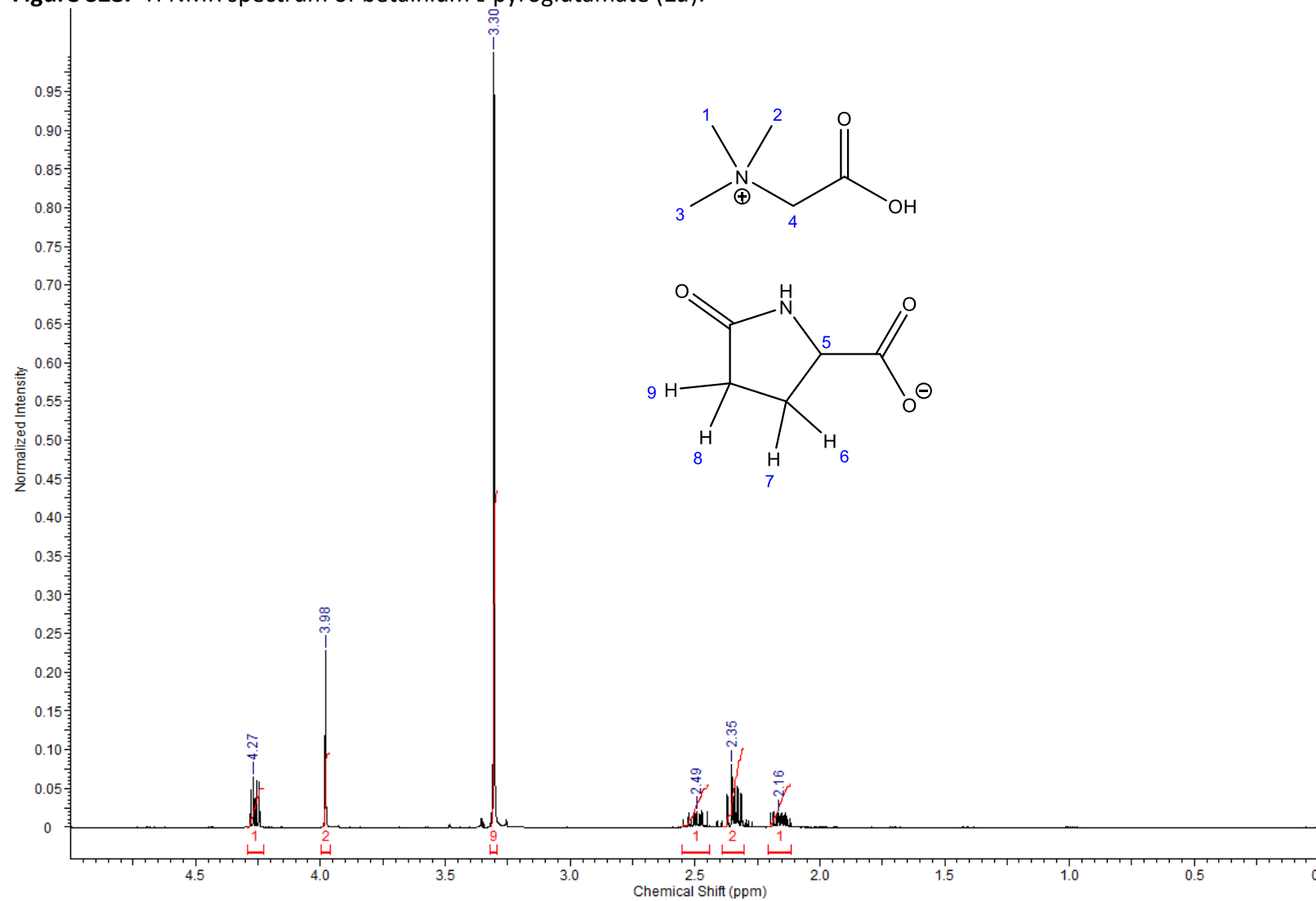
^{13}C NMR ($\text{CD}_3\text{OD}-d_4$, 298K, 100 MHz): δ_{c} [ppm] = 14.6(2C), 23.8(2C), 23.9(2C), 27.5(2C), 30.3(4C), 30.6(8C), 30.9, 33.2(2C), 34.6, 52.1(4C), 62.9(2C), 66.4(2C), 167.9(3C), 173.8, 176.9.

Figure S27. IR spectrum of dodecylbetainium α -ketoglutarate (**3c**).



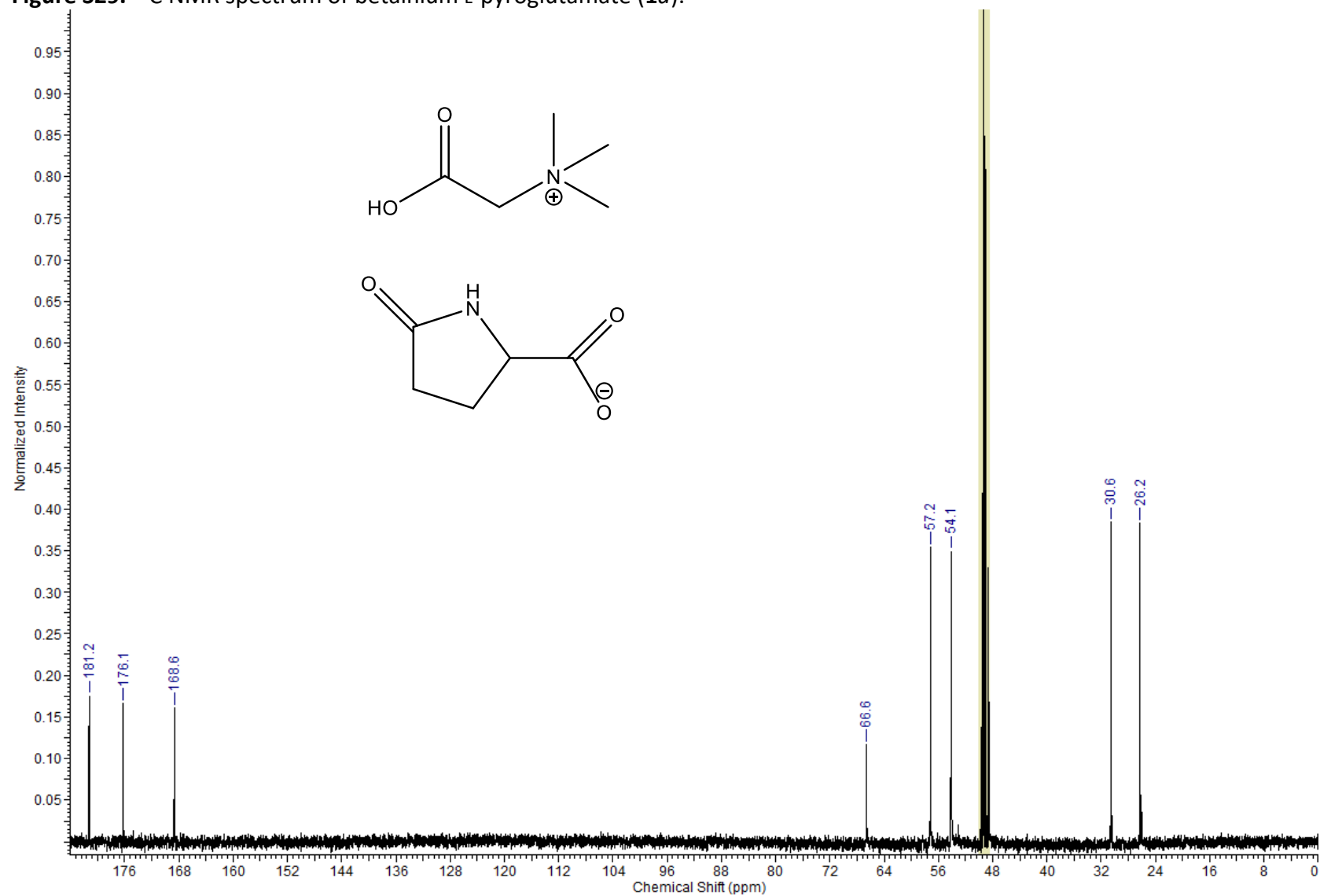
IR [cm^{-1}] = 677, 723, 764, 839, 887, 906, 941, 992, 1034, 1083, 1133, 1196, 1336, 1409, 1466, 1607, 1733, 2853, 2926, 2953.

Figure S28. ¹H NMR spectrum of betainium L-pyroglutamate (**1d**).



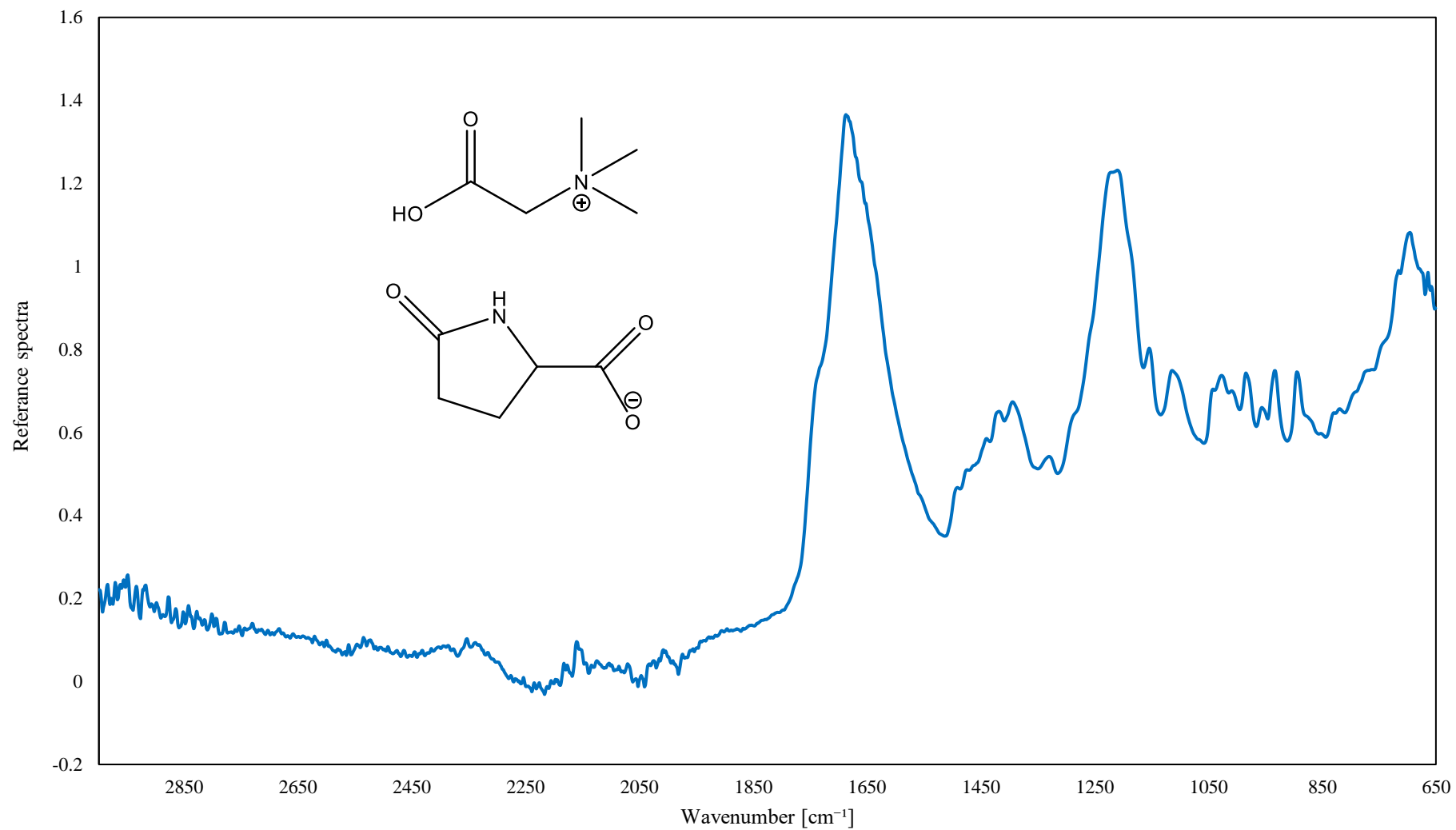
¹H NMR (CD₃OD-*d*₄, 298K, 400 MHz): δ_{H} [ppm] = 2.16 (m, 1H; H-8); 2.35 (m, 2H; H-6, H-7); 2.40 (m, 1H; H-9); 3.30 (s, 9H; H-1, H-2, H-3); 3.98 (s, 2H; H-4); 4.27 (m, 1H; H-5).

Figure S29. ¹³C NMR spectrum of betainium L-pyroglutamate (**1d**).



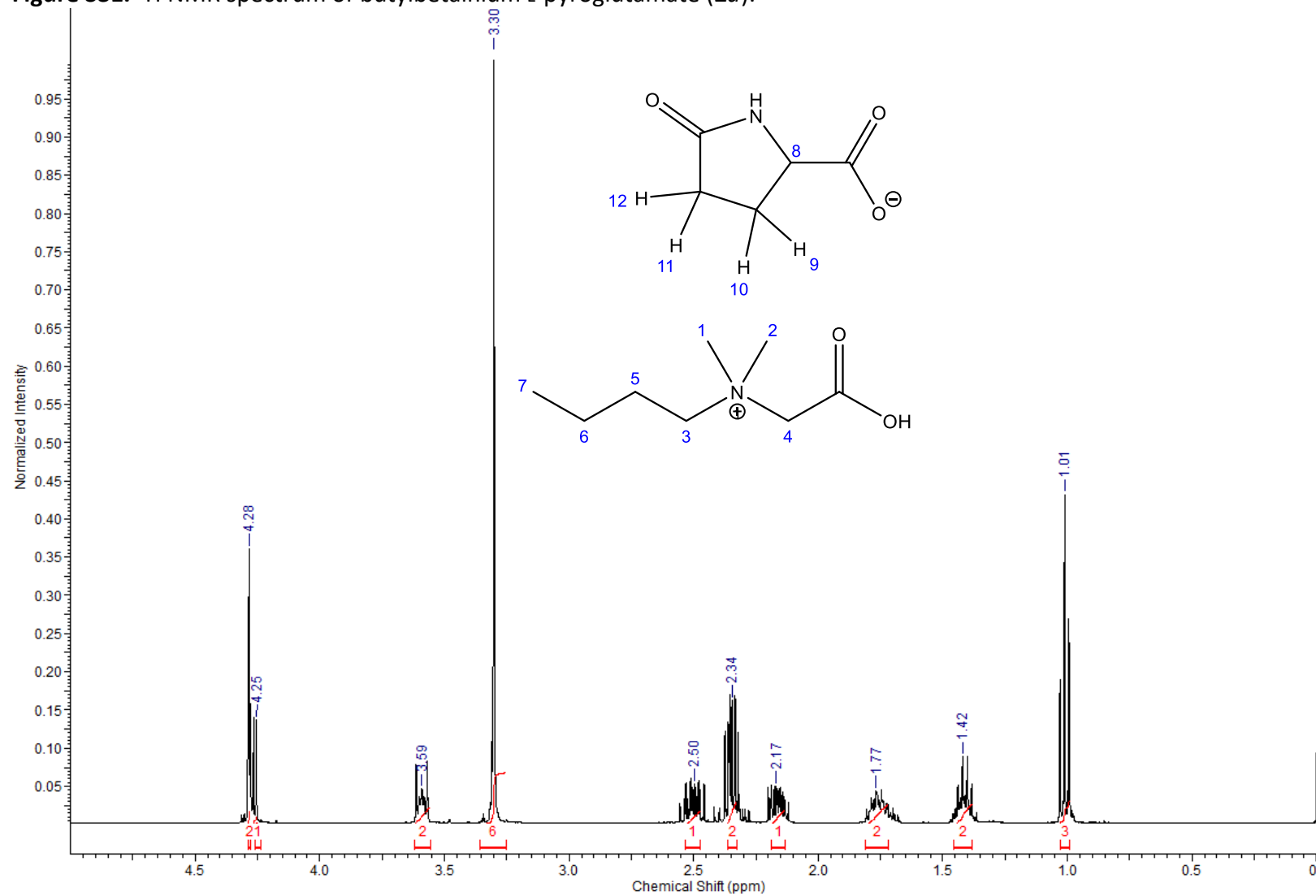
¹³C NMR (CD₃OD-*d*₄, 298K, 100 MHz): δ_c [ppm] = 26.2, 30.6, 54.1 (3C), 57.2, 66.6, 168.6, 176.1, 181.2.

Figure S30. IR spectrum of betainium L-pyroglutamate (**1d**).



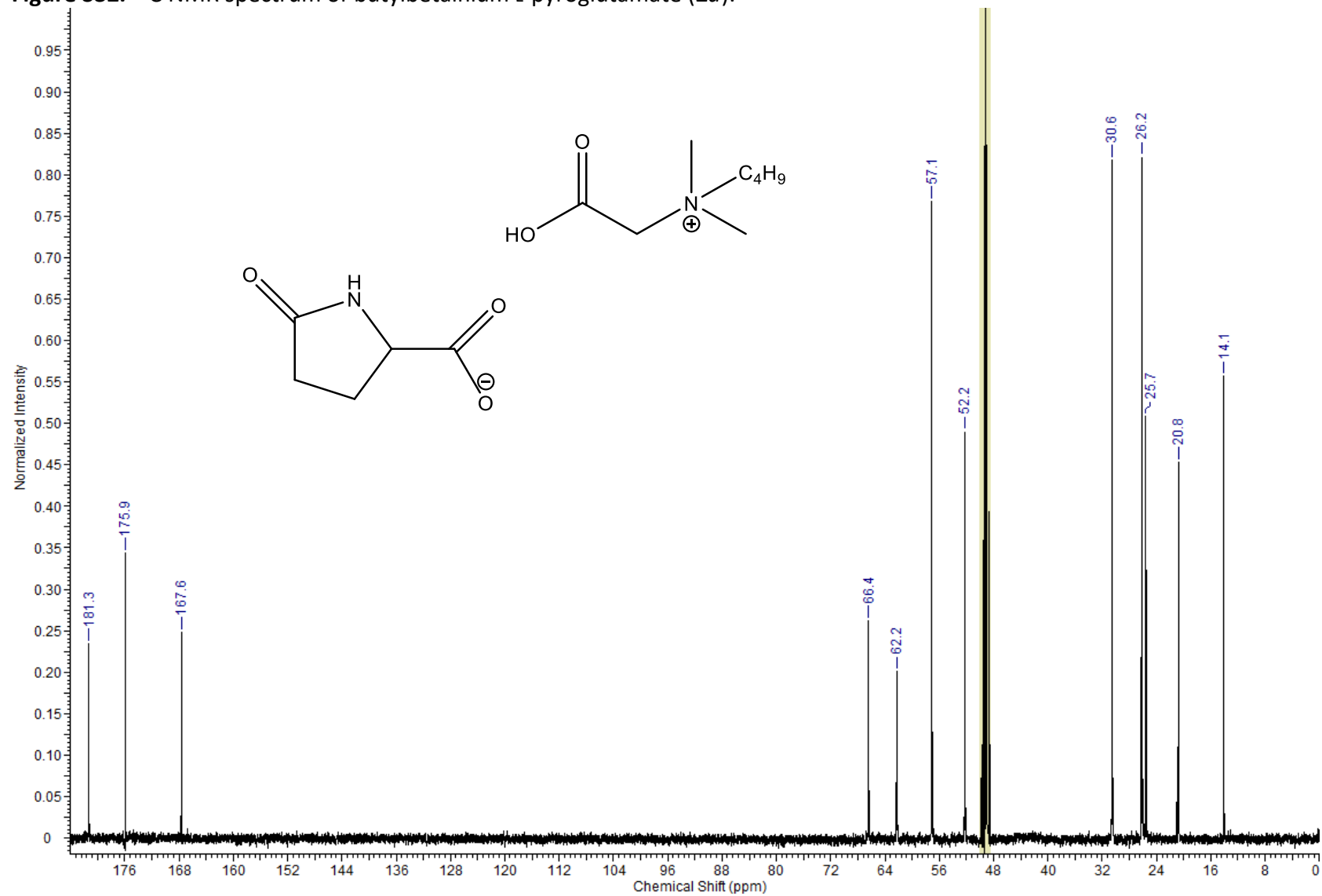
IR [cm⁻¹] = 695, 894, 933, 983, 1027, 1113, 1154, 1210, 1330, 1394, 1418, 1686.

Figure S31. ¹H NMR spectrum of butylbetainium L-pyrroglutamate (**2d**).



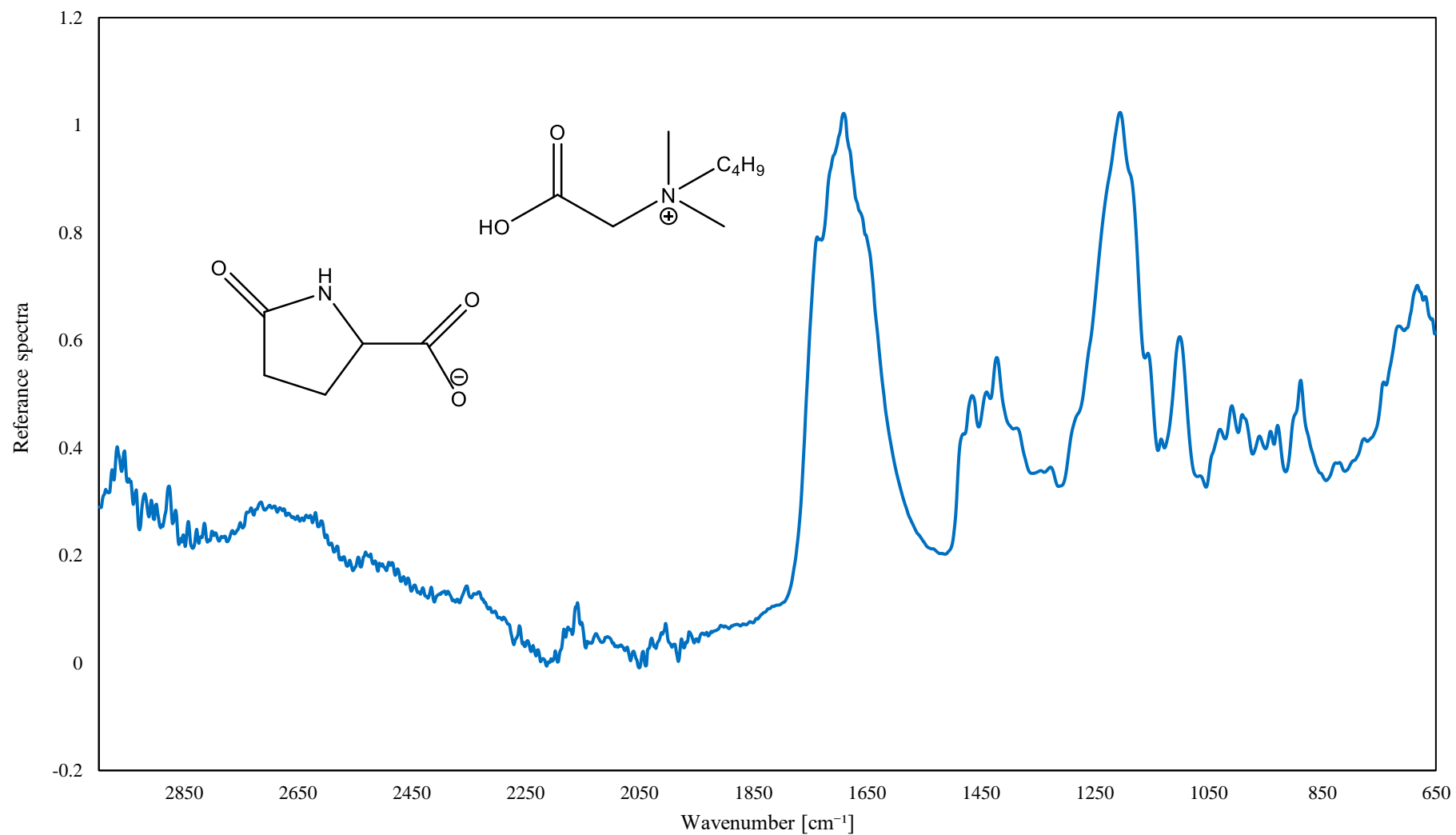
¹H NMR (CD₃OD-*d*₄, 298K, 400 MHz): δ_{H} [ppm] = 1.01 (t, 3H, $J = 7.36$ Hz; H-7); 1.42 (m, 2H; H-6); 1.77 (m, 2H; H-5); 2.17 (m, 1H; H-11); 2.34 (m, 2H; H-9, H-10); 2.50 (m, 1H; H-12); 3.30 (s, 6H; H-1, H-2); 3.59 (m, 2H; H-3); 4.25 (m, 1H; H-8); 4.28 (s, 2H; H-4).

Figure S32. ^{13}C NMR spectrum of butylbetainium L-pyroglutamate (**2d**).



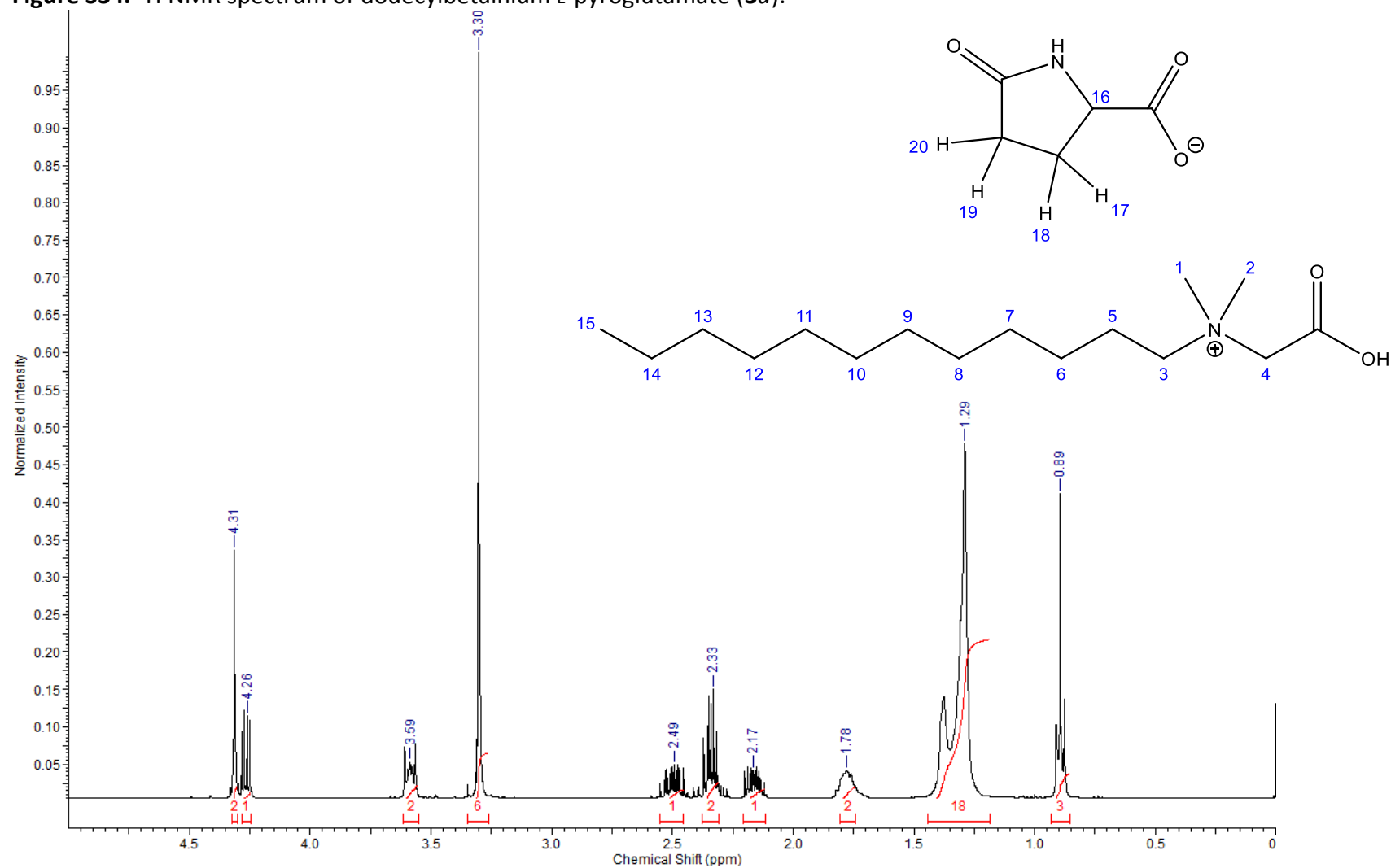
^{13}C NMR ($\text{CD}_3\text{OD}-d_4$, 298K, 100 MHz): δ_{C} [ppm] = 14.1, 20.8, 25.7, 26.2, 30.6, 52.2 (2C), 57.1, 62.2, 66.4, 167.6, 175.9, 181.3.

Figure S33. IR spectrum of butylbetainium L-pyroglutamate (**2d**).



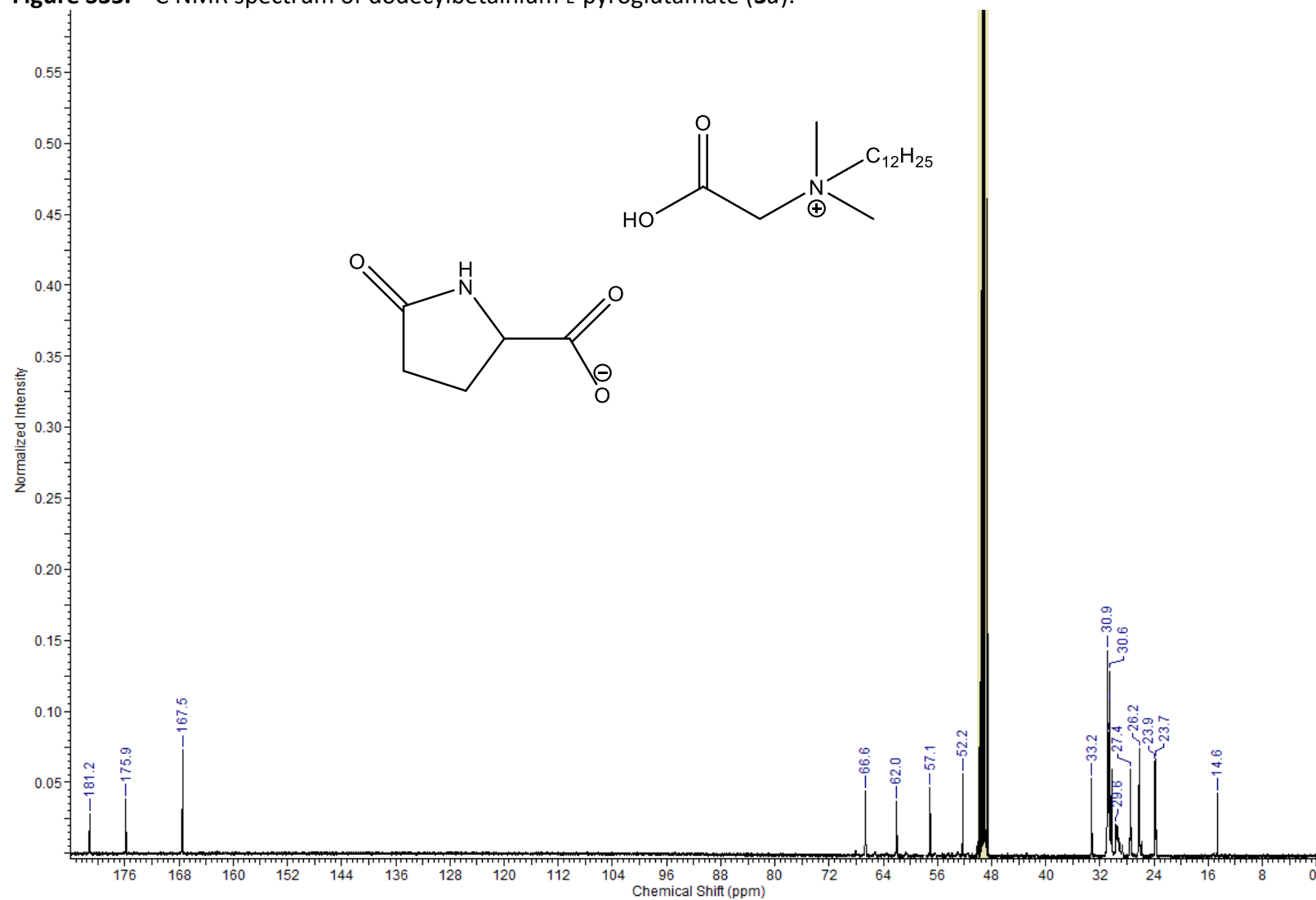
IR [cm⁻¹] = 683, 715, 888, 928, 960, 1009, 1100, 1205, 1328, 1394, 1422, 1691, 2967.

Figure S34. ¹H NMR spectrum of dodecylbetainium L-pyroglutamate (**3d**).



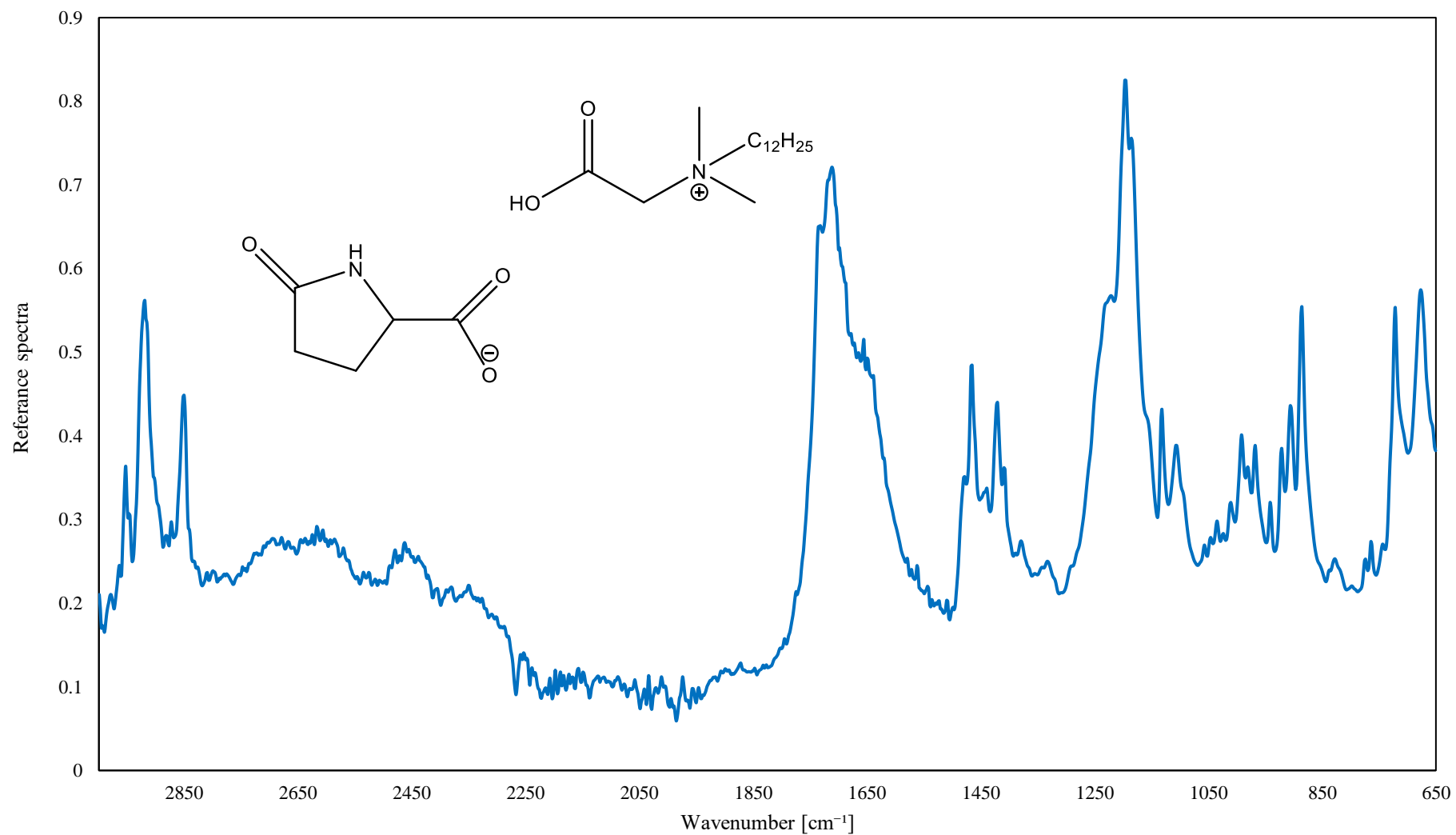
¹H NMR (CD₃OD-d₄, 298K, 400 MHz): δH [ppm] = 0.89 (t, 3H, *J* = 6.98 Hz; H-15); 1.29 (m, 18H; H-6–H-14); 1.78 (m, 2H; H-5); 2.17 (m, 1H; H-20); 2.33 (m, 2H; H-17, H-18); 2.49 (m, 1H; H-19); 3.30 (s, 6H; H-1, H-2); 3.59 (m, 2H; H-3); 4.26 (m, 1H, H-16); 4.31 (s, 2H, H-4).

Figure S35. ^{13}C NMR spectrum of dodecylbetainium L-pyrroglutamate (**3d**).



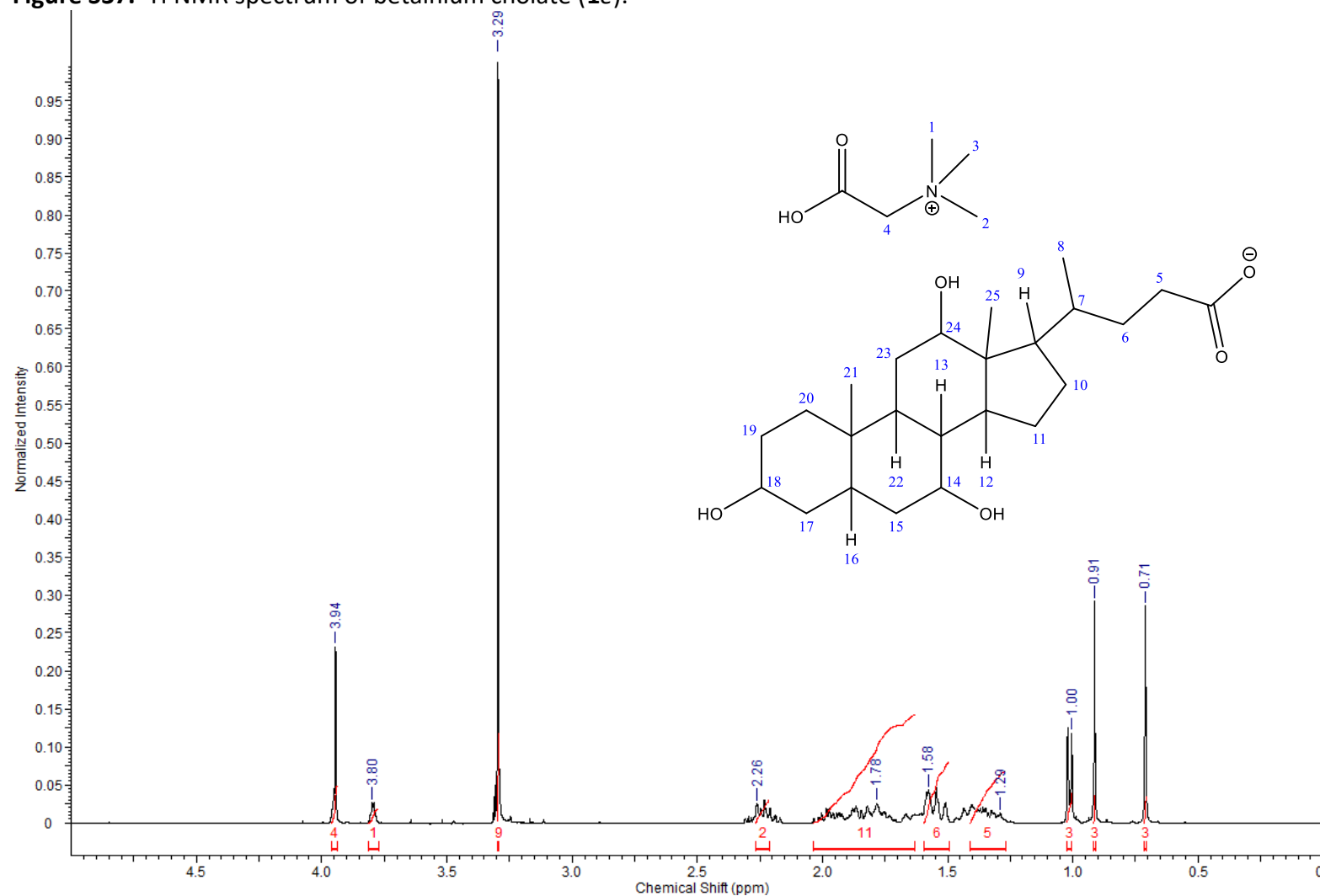
^{13}C NMR ($\text{CD}_3\text{OD}-d_4$, 298K, 100 MHz): δ_{C} [ppm] = 14.6, 23.7, 23.9, 26.2, 27.4, 29.6, 30.6 (2C), 30.8 (2C), 30.9 (2C), 33.2, 52.2 (2C), 57.1, 62.0, 66.6, 167.5, 175.9, 181.2.

Figure S36. IR spectrum of dodecylbetainium L-pyrroglutamate (**3d**).



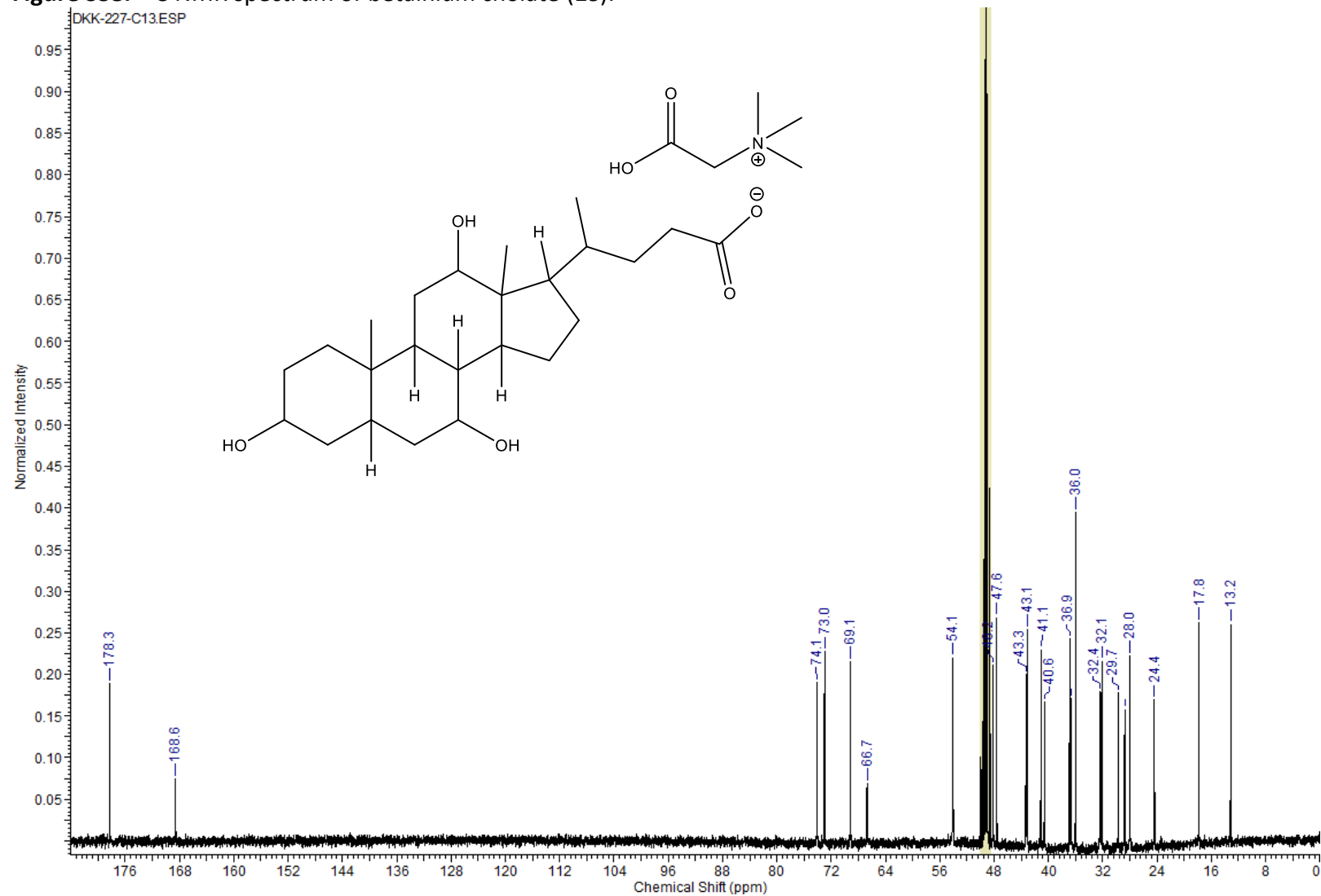
IR [cm⁻¹] = 677, 720, 886, 905, 968, 991, 1035, 1131, 1196, 1333, 1421, 1466, 1712, 2851, 2920, 2953.

Figure S37. ^1H NMR spectrum of betainium cholate (**1e**).



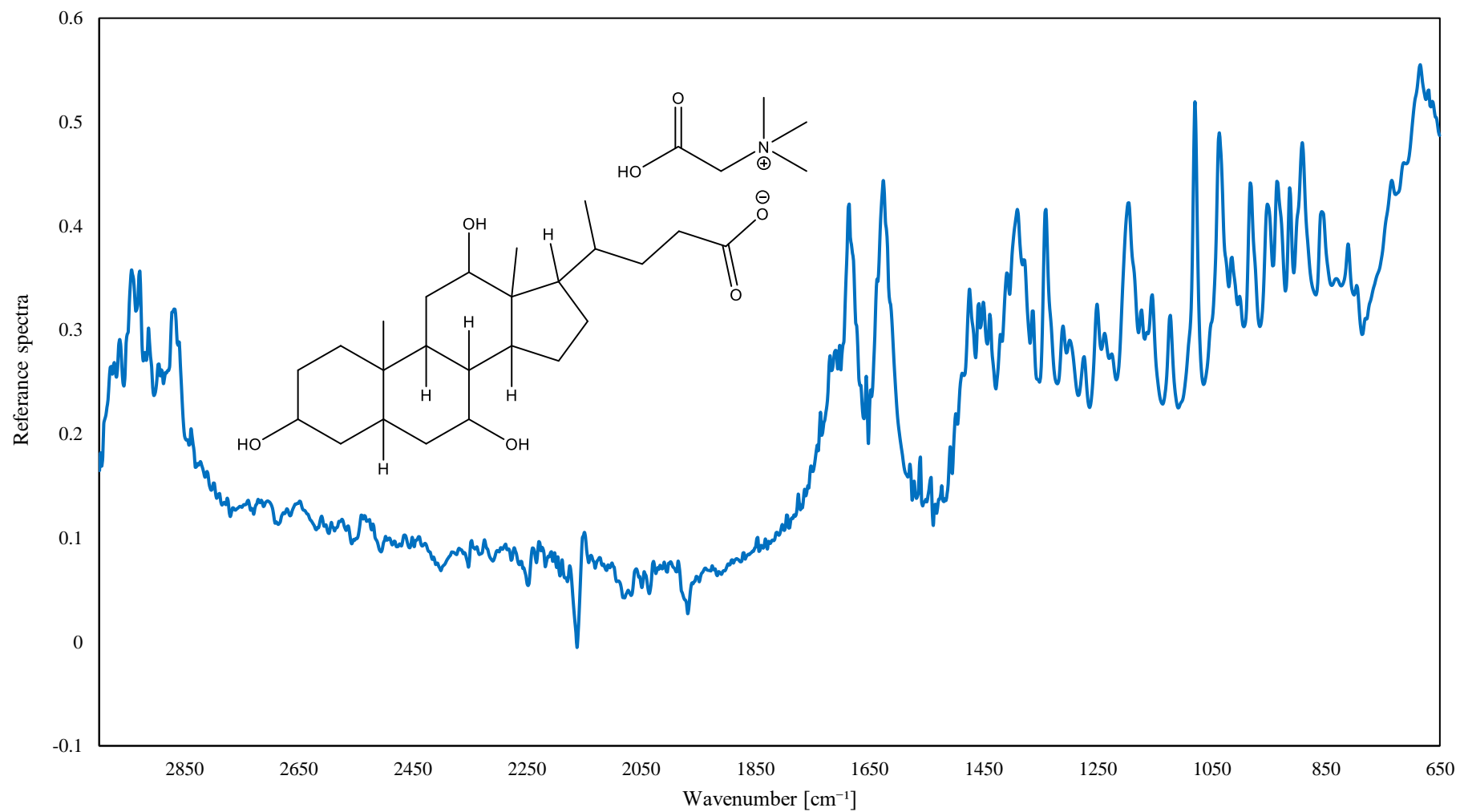
^1H NMR ($\text{CD}_3\text{OD}-d_4$, 298K, 400 MHz): δ_{H} [ppm] = 0.71 (s, 3H; H-21); 0.91 (s, 3H; H-8); 1.00 (d, 3H, $J = 6.41$; H-25); 1.29 (m, 5H, H-9, H-12, H-13, H-16, H-22); 1.58 (m, 6H; H-7, H-15, H-17, H-19, H-20, H-23); 1.78 (m, 11H; H-6, H-10, H-11, H-15, H-17, H-19, H-20, H-23); 2.26 (m, 2H; H-5); 3.29 (s, 9H; H-1, H-2); 3.80 (m, 1H; H-18); 3.94 (s, 4H; H-4, H-14, H-24).

Figure S38. ^{13}C NMR spectrum of betainium cholate (1e).



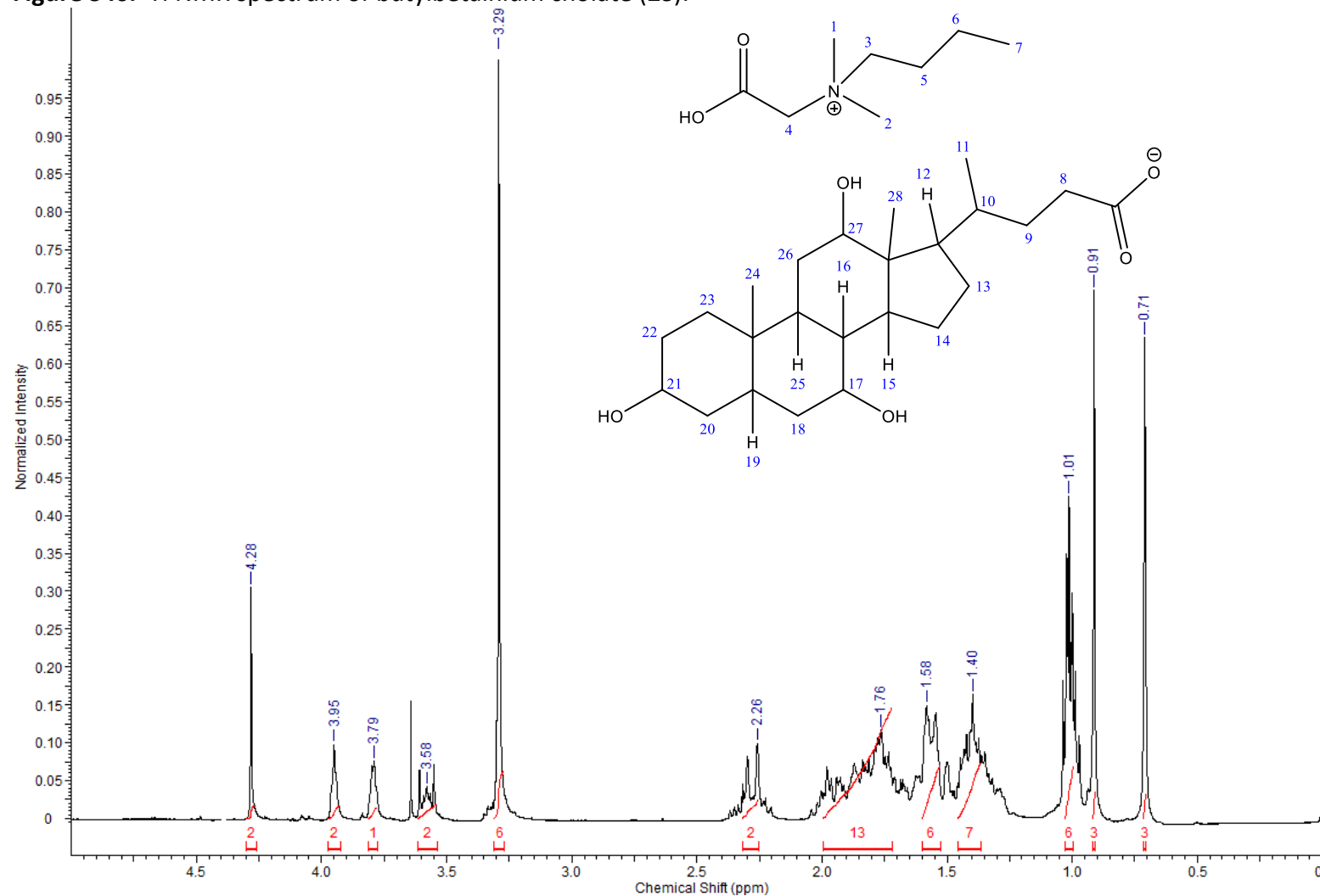
^{13}C NMR ($\text{CD}_3\text{OD}-d_4$, 298K, 100 MHz): δ_{C} [ppm] = 13.2 (2C), 17.8, 24.4, 28.0, 28.8, 29.7, 32.1, 32.4, 36.0 (3C), 36.6 (2C), 36.9, 40.6, 41.1, 43.1, 43.3, 47.6, 48.2, 54.1 (3C), 66.7, 69.1, 73.0, 74.1, 168.6, 178.3.

Figure S39. IR spectrum of betainium cholate (**1e**).



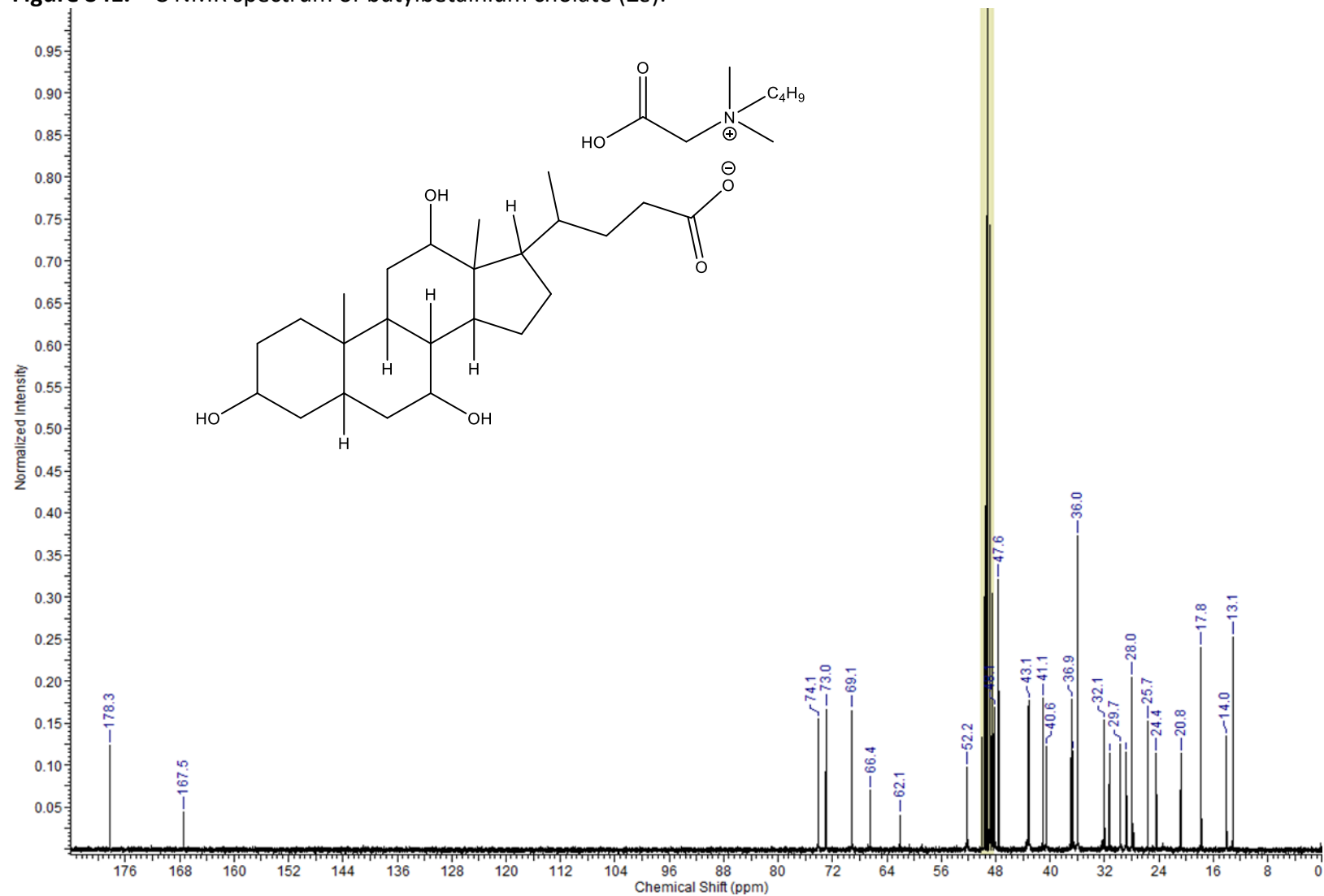
IR [cm^{-1}] = 685, 734, 856, 891, 913, 935, 951, 1036, 1079, 1123, 1155, 1196, 1251, 1274, 1310, 1341, 1391, 1450, 1474, 1626, 1685, 2870, 2942.

Figure S40. ¹H NMR spectrum of butylbetainium cholate (2e).



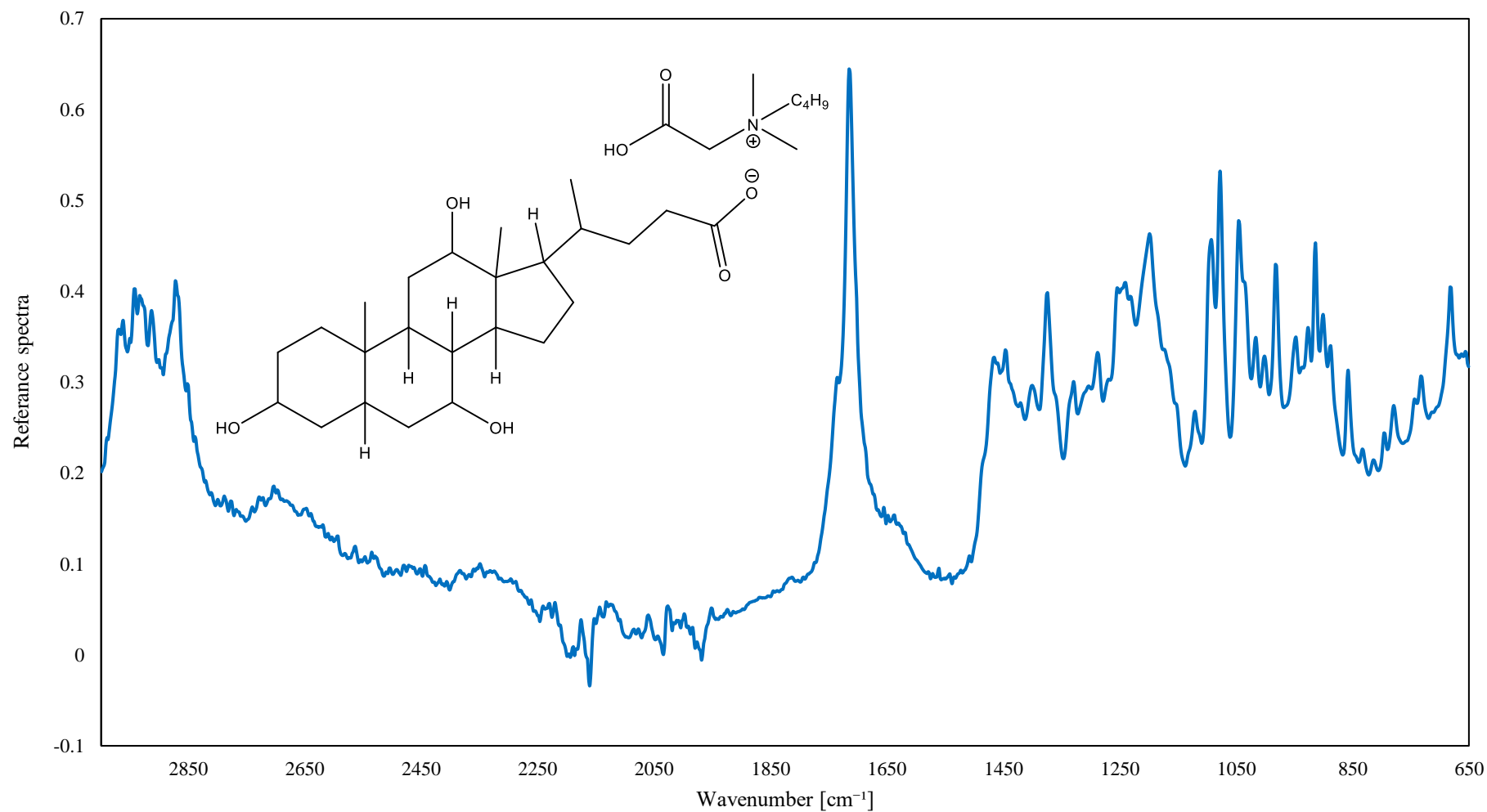
¹H NMR (CD₃OD-*d*₄, 298K, 300 MHz): δ_H [ppm] = 0.71 (s, 3H; H-24); 0.91 (s, 3H; H-11); 1.01 (m, 6H; H-7, H-28); 1.40 (m, 7H; H-6, H-12, H-15, H-16, H-19, H-25); 1.58 (m, 6H; H-10, H-18, H-20, H-22, H-23, H-26); 1.76 (m, 13H; H-5, H-9, H-13, H-14, H-18, H-20, H-22, H-23, H-26); 2.26 (m, 2H; H-8); 3.29 (s, 6H; H-1, H-2); 3.58 (m, 2H; H-3); 3.79 (m, 1H; H-21); 3.95 (m, 2H; H-17, H-27); 4.28 (s, 2H; H-4).

Figure S41. ^{13}C NMR spectrum of butylbetainium cholate (**2e**).



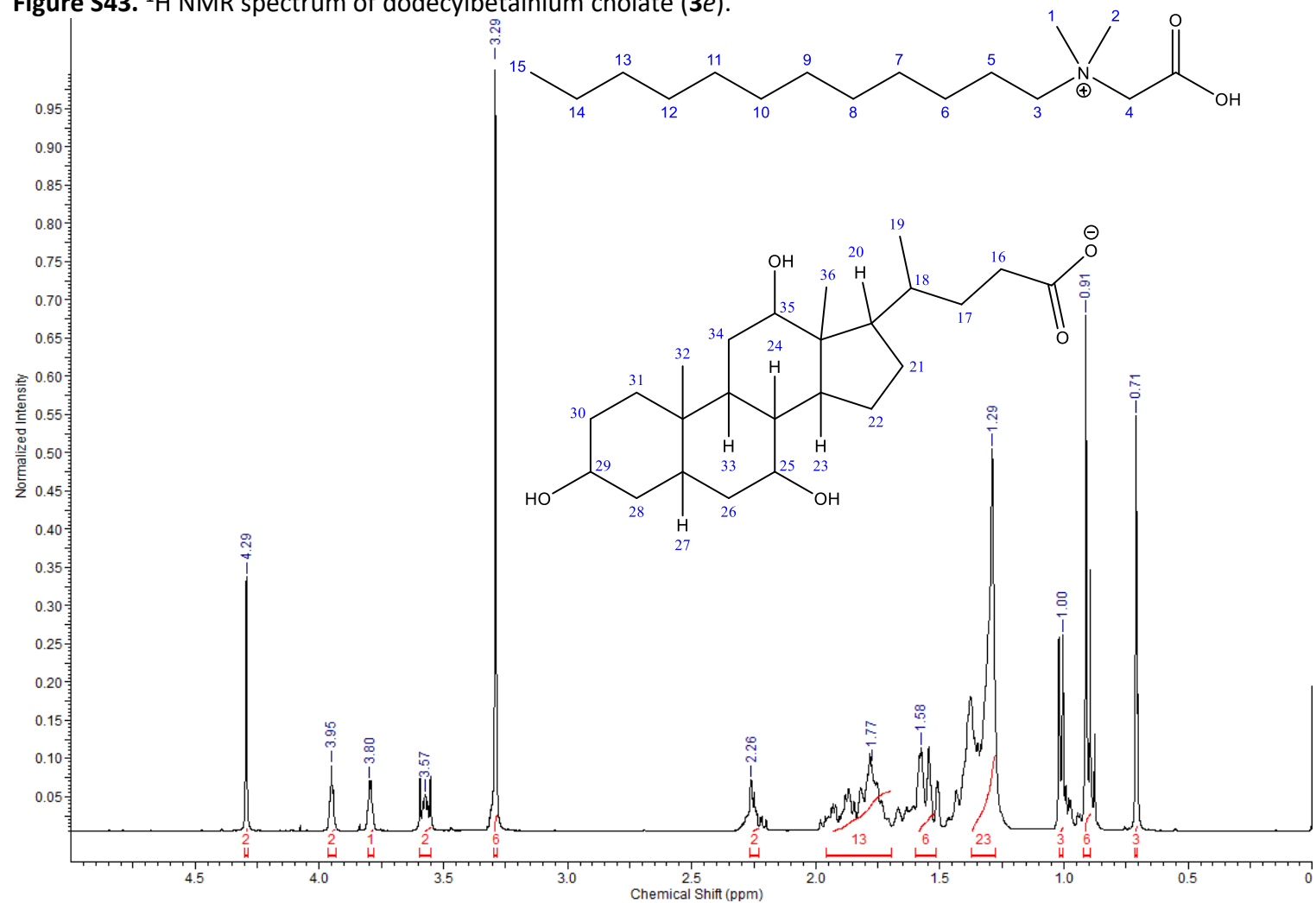
^{13}C NMR ($\text{CD}_3\text{OD}-d_4$, 298K, 75 MHz): δ_{C} [ppm] = 13.1 (2C), 14.0, 17.8, 20.8, 24.4, 28.0, 28.8, 29.7, 31.3, 32.1, 36.0 (3C), 36.6 (2C), 36.9, 40.6, 41.1, 43.1, 47.6, 48.1, 52.2 (2C), 62.1, 66.4 (2C), 69.1, 73.0, 74.1, 167.5, 178.3.

Figure S42. IR spectrum of butylbetainium cholate (**2e**).



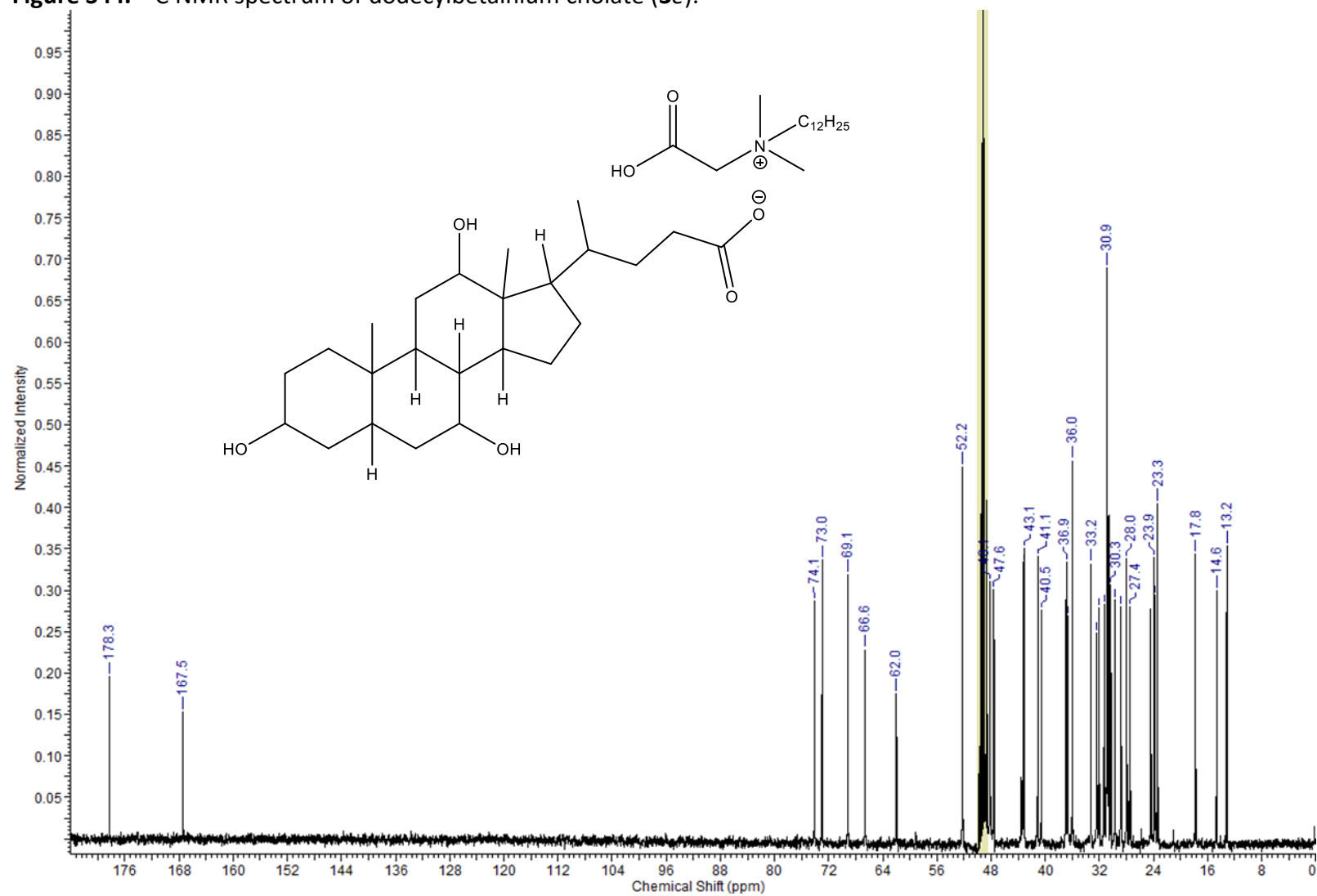
IR [cm⁻¹] = 681, 732, 779, 857, 914, 948, 962, 1045, 1078, 1121, 1199, 1241, 1288, 1310, 1330, 1374, 1400, 1464, 1465, 1675, 1714, 2872, 2942, 2963.

Figure S43. ^1H NMR spectrum of dodecylbetainium cholate (**3e**).



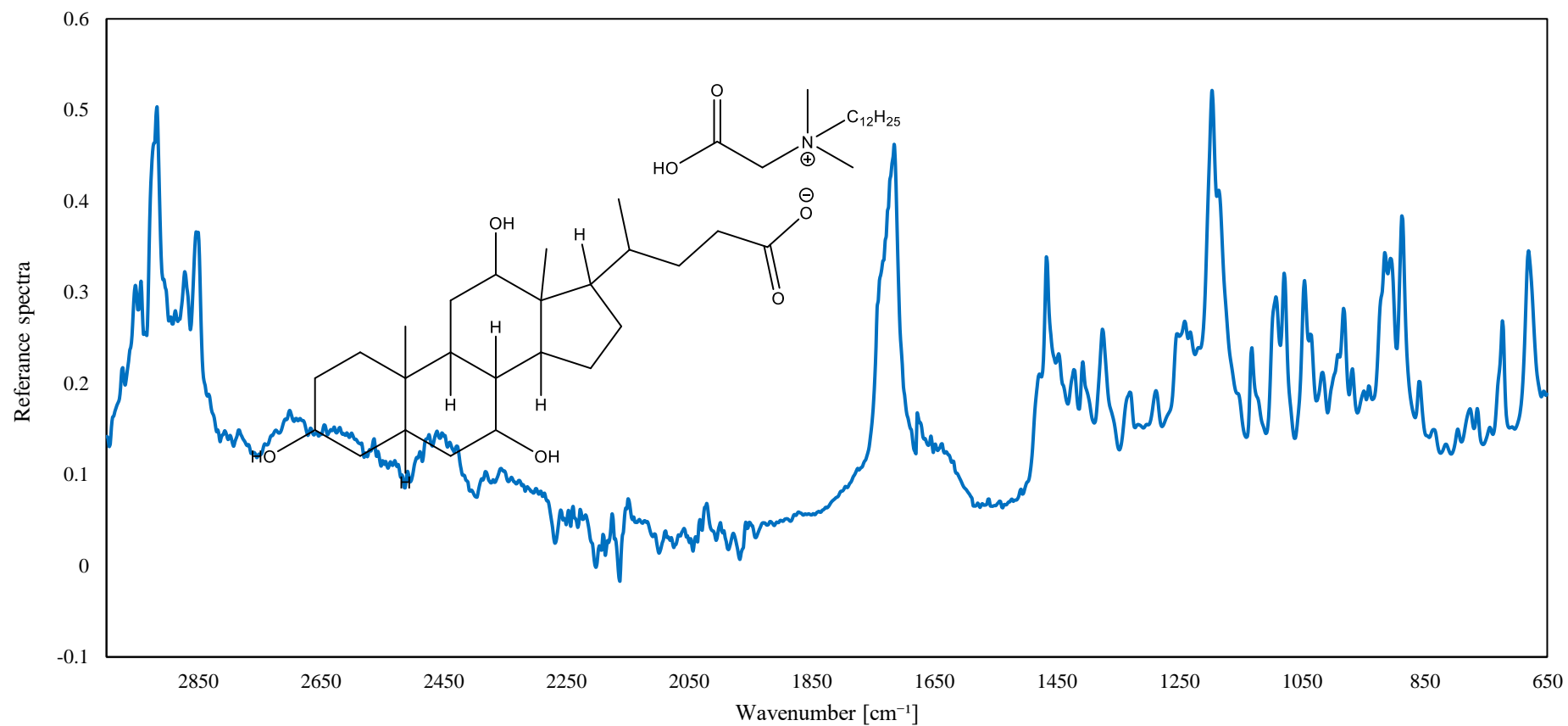
^1H NMR ($\text{CD}_3\text{OD}-d_4$, 298K, 300 MHz): δ_{H} [ppm] = 0.71 (s, 3H; H-32); 0.91 (m, 6H; H-15, H-19); 1.00 (d, 3H, $J = 6.40$ Hz; H-36); 1.29 (m, 23H; H-6–H-14, H-20, H-23, H-24, H-27, H-33); 1.58 (m, 6H; H-18, H-26, H-28, H-30, H-31, H-34); 1.77 (m, 13H; H-5, H-17, H-21, H-22, H-26, H-28, H-30, H-31, H-34); 2.26 (m, 2H; H-16); 3.29 (s, 6H; H-1, H-2); 3.57 (m, 2H; H-3); 3.80 (m, 1H; H-29); 3.95 (m, 2H; H-25, H-35); 4.29 (s, 2H; H-4).

Figure S44. ^{13}C NMR spectrum of dodecylbetainium cholate (**3e**).



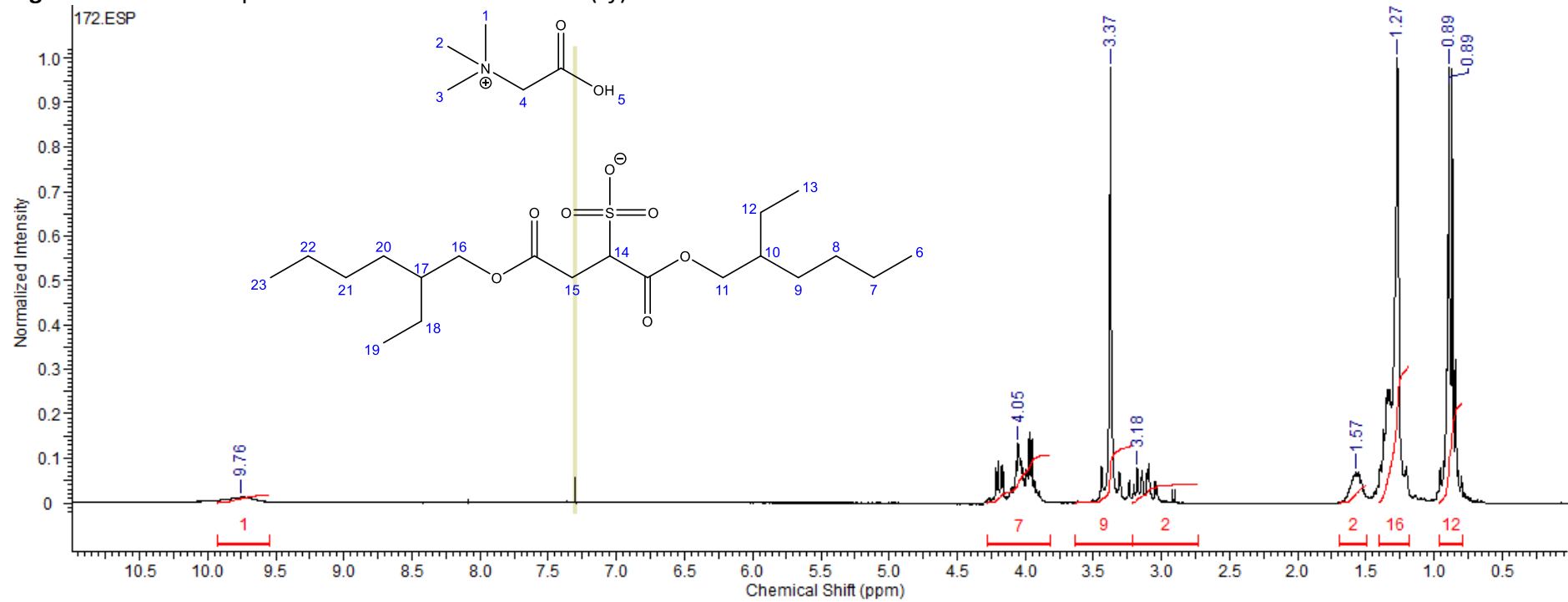
^{13}C NMR ($\text{CD}_3\text{OD}-d_4$, 298K, 75 MHz): δ_{C} [ppm] = 13.2 (2C), 14.6, 17.8, 23.3, 23.7, 23.9, 27.4, 28.0, 28.8, 29.5, 30.3 (2C), 30.9 (4C), 31.3, 32.1, 32.4, 33.2, 36.0 (3C), 36.6 (2C), 36.9, 40.5, 41.1, 43.1, 47.6, 48.1, 52.2 (2C), 62.0, 66.6, 69.1, 73.0, 74.1, 167.5, 178.3.

Figure S45. IR spectrum of dodecylbetainium cholate (**3e**).



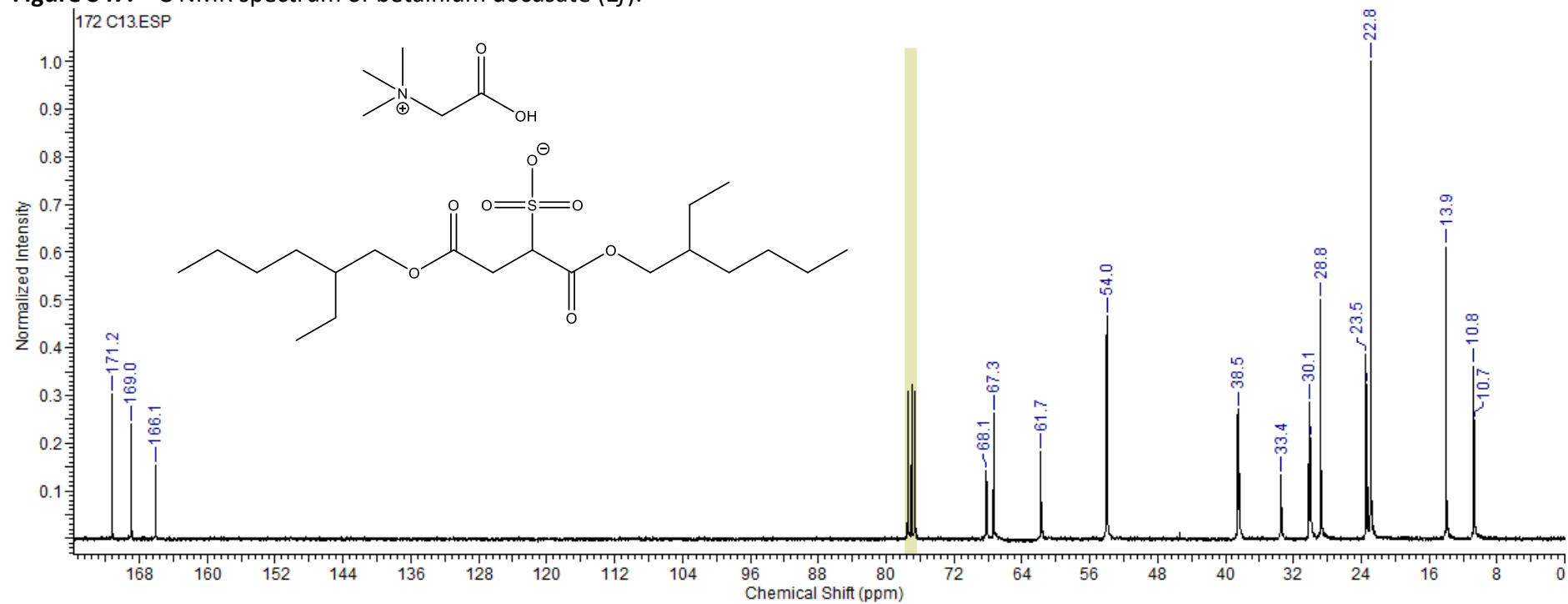
IR [cm^{-1}] = 680, 724, 764, 858, 887, 914, 982, 1017, 1046, 1079, 1131, 1197, 1242, 1288, 1332, 1375, 1406, 1466, 1675, 1715, 2852, 2872, 2918.

Figure S46. ¹H NMR spectrum of betainium docosate (**1f**).



¹H NMR (CD₃OD-*d*₄, 298K, 300 MHz): δ_{H} [ppm] = 0.89 (m, 12H; H-6, H-13, H-19, H-23); 1.27 (m, 16H; H-7, H-8, H-9, H-12, H-18, H-20, H-21, H-22); 1.57 (m, 2H; H-10, H-17); 3.18 (m, 2H; H-15); 3.37 (s, 9H; H-1, H-2, H-3); 4.05 (m, 7H; H-4, H-11, H-14, H-16); 9.76 (s, 1H; H-5).

Figure S47. ^{13}C NMR spectrum of betainium docosate (**1f**).



^{13}C NMR ($\text{CD}_3\text{OD}-d_4$, 298K, 75 MHz): δ_{C} [ppm] = 10.7, 10.8, 13.9(2), 22.8(2), 23.5(2), 28.8(2), 30.1(2), 33,4, 38.5(2), 54.0(3), 61.7, 67.3, 68.1(2), 166.1, 169.0, 171.2.

Figure S48. IR spectrum of betainium docusate (**1f**).

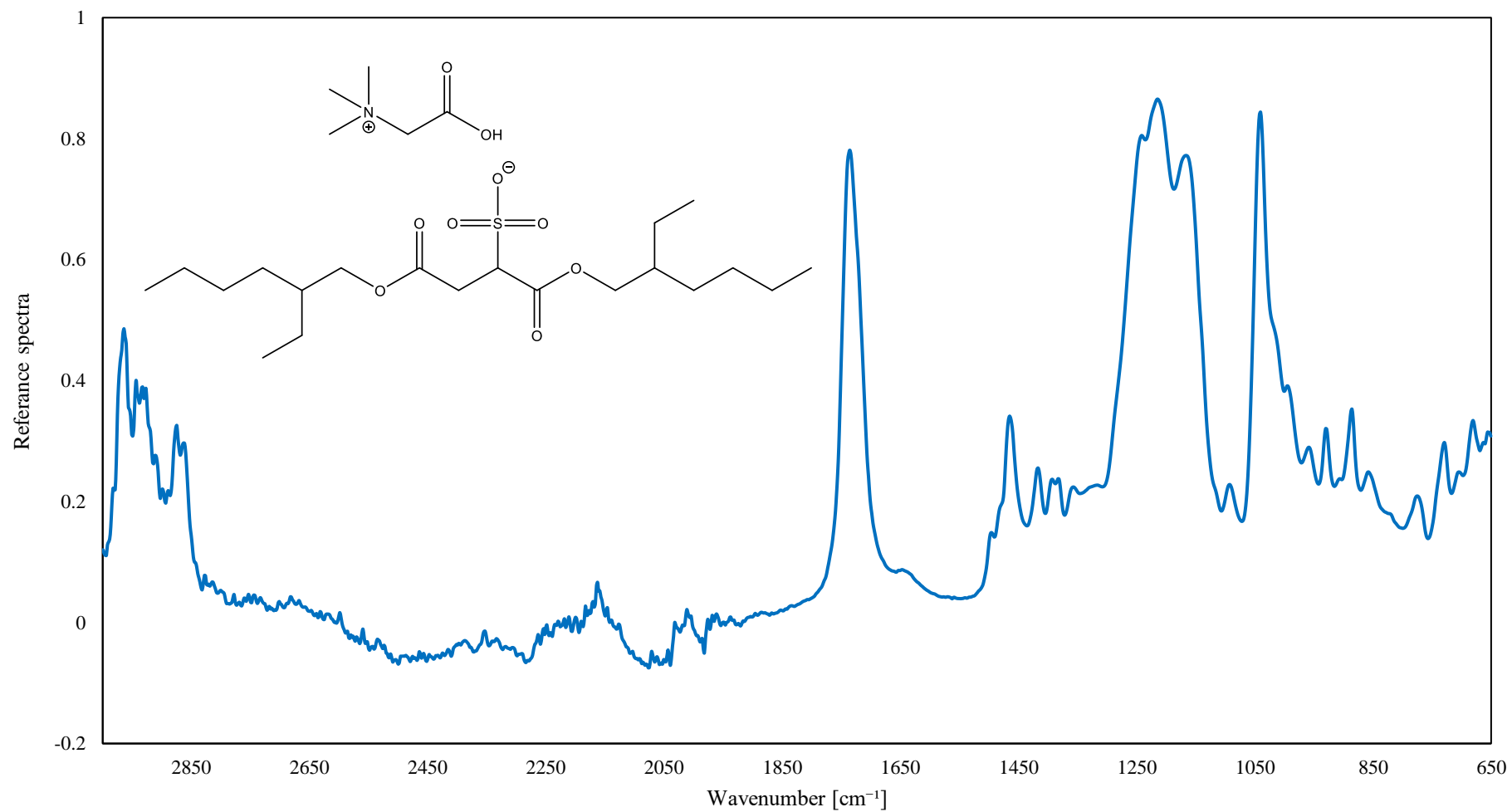
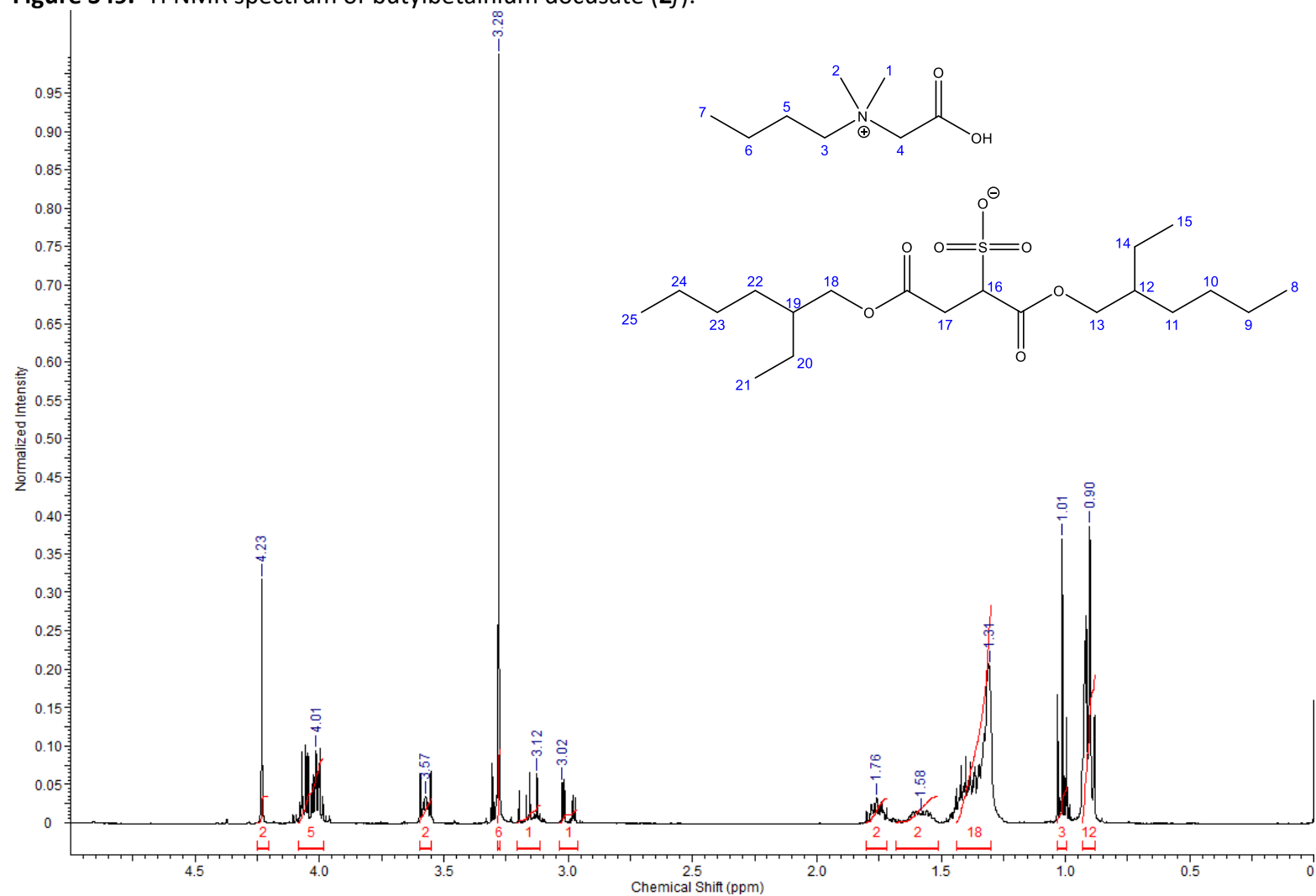
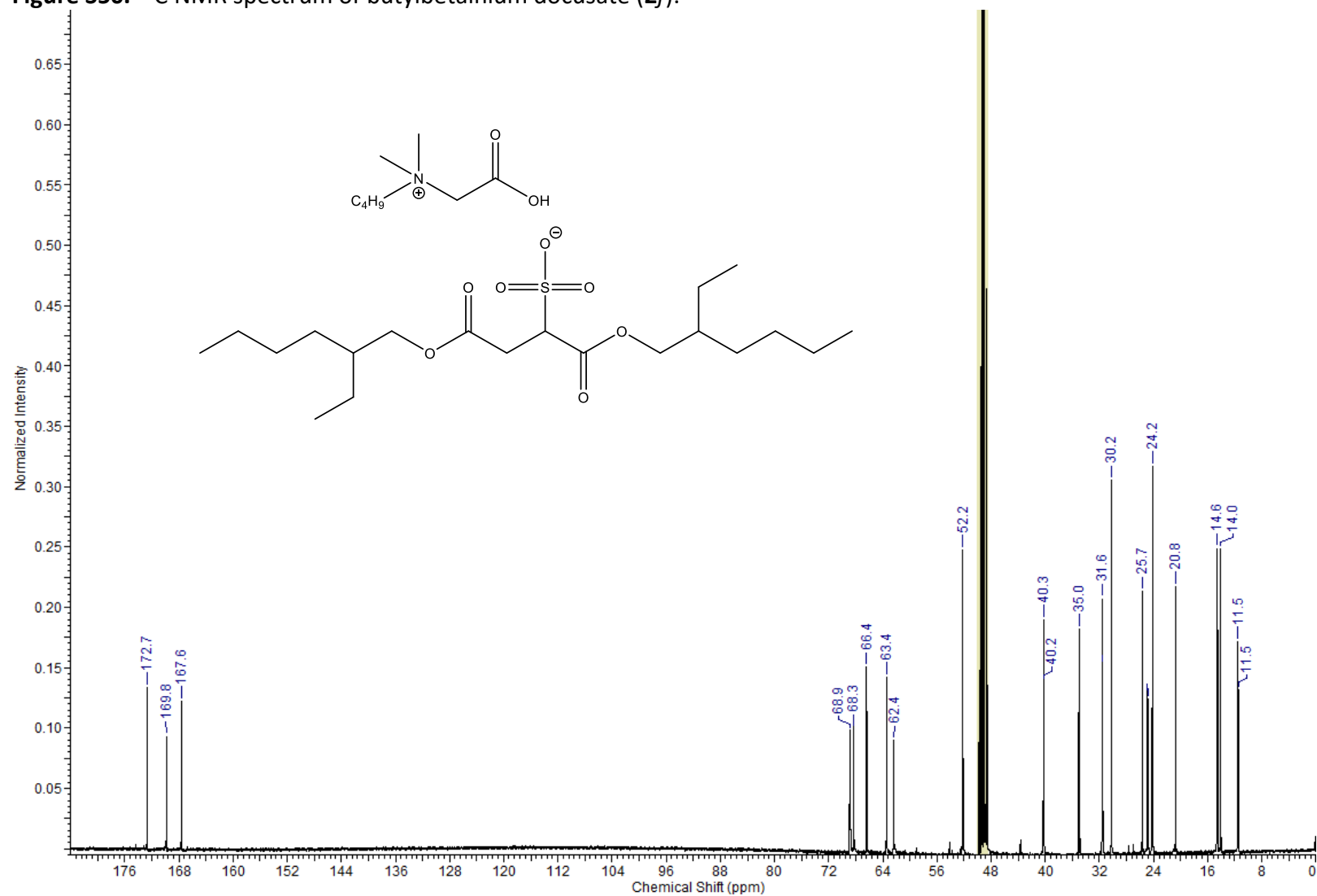


Figure S49. ¹H NMR spectrum of butylbetainium docusate (2f).



¹H NMR (CD₃OD-*d*₄, 298K, 400 MHz): δ_{H} [ppm] = 0.90 (m, 12H; H-8, H-15, H-21, H-25); 1.01 (t, 3H, *J* = 7.43 Hz; H-7); 1.31 (m, 18H; H-6, H-9-H-11, H-14, H-20, H-22-H-24); 1.58 (m, 2H; H-12, H-19); 1.76 (m, 2H; H-5); 3.02 (m, 1H; H-17); 3.12 (m, 1H; H-17); 3.28 (s, 6H; H-1, H-2); 3.57 (m, 2H; H-3); 4.01 (m, 5H; H-13, H-16, H-18); 4.23 (s, 2H; H-4).

Figure S50. ^{13}C NMR spectrum of butylbetainium docusate (**2f**).



^{13}C NMR ($\text{CD}_3\text{OD}-d_4$, 298K, 100 MHz): δ_{C} [ppm] = 11.5 (2C), 14.0, 14.6 (2C), 20.8, 24.1, 24.2, 24.9, 25.0, 25.7, 30.2 (2C), 31.5, 31.6, 35.0, 40.2, 40.3, 52.2 (2C), 62.4, 63.4, 66.4, 68.3, 68.9, 167.6, 169.8, 172.7.

Figure S51. IR spectrum of butylbetainium docusate (**2f**).

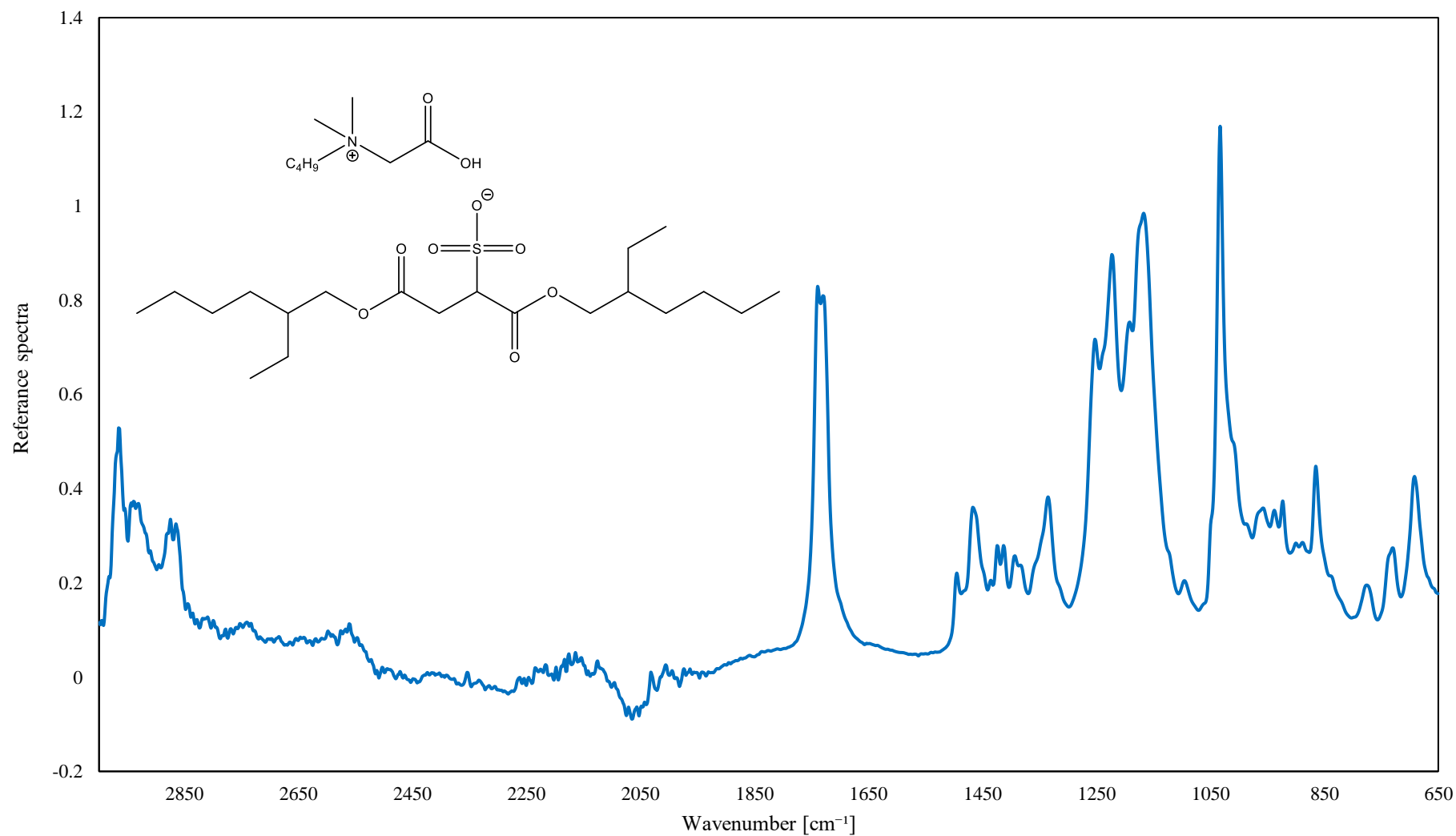
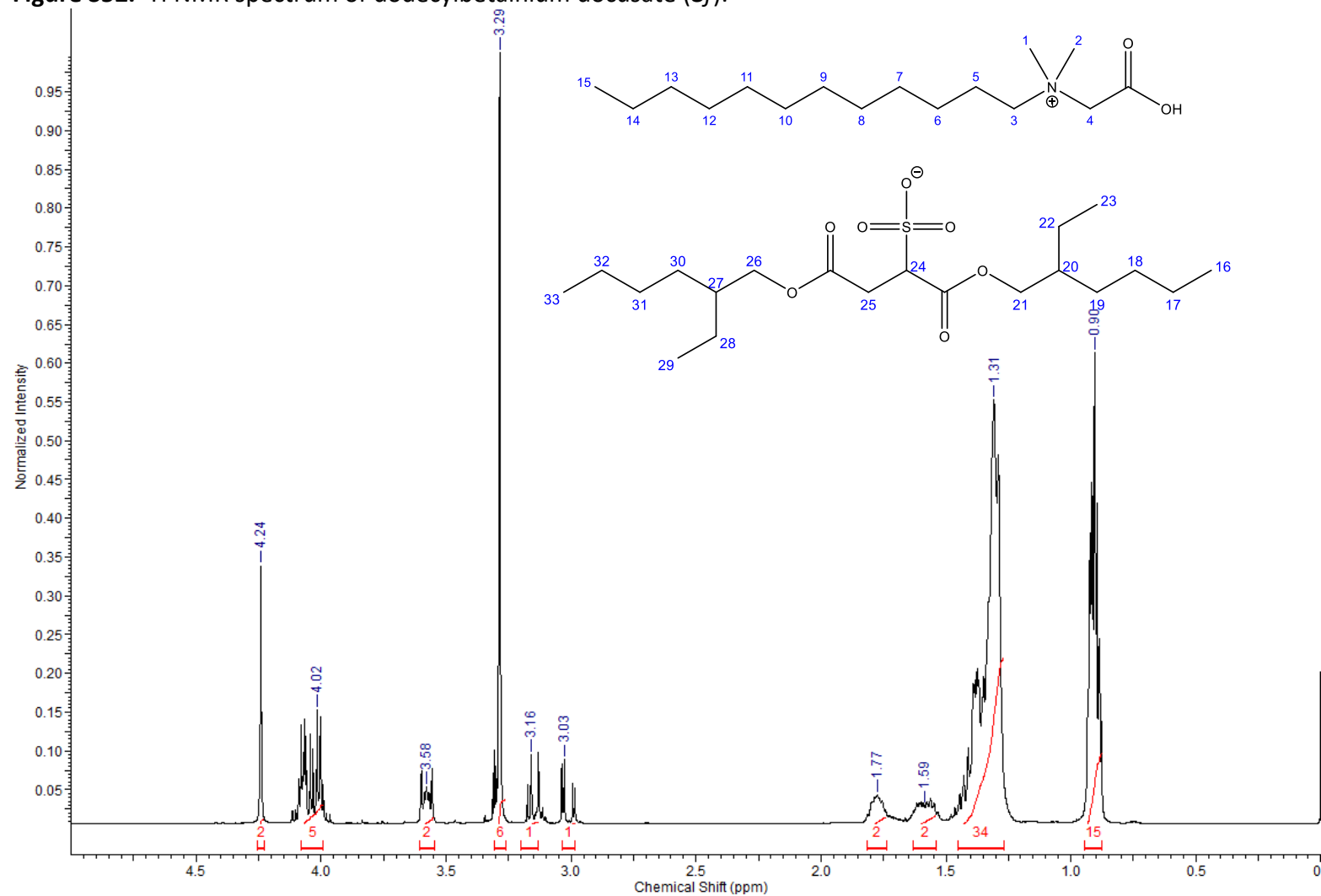
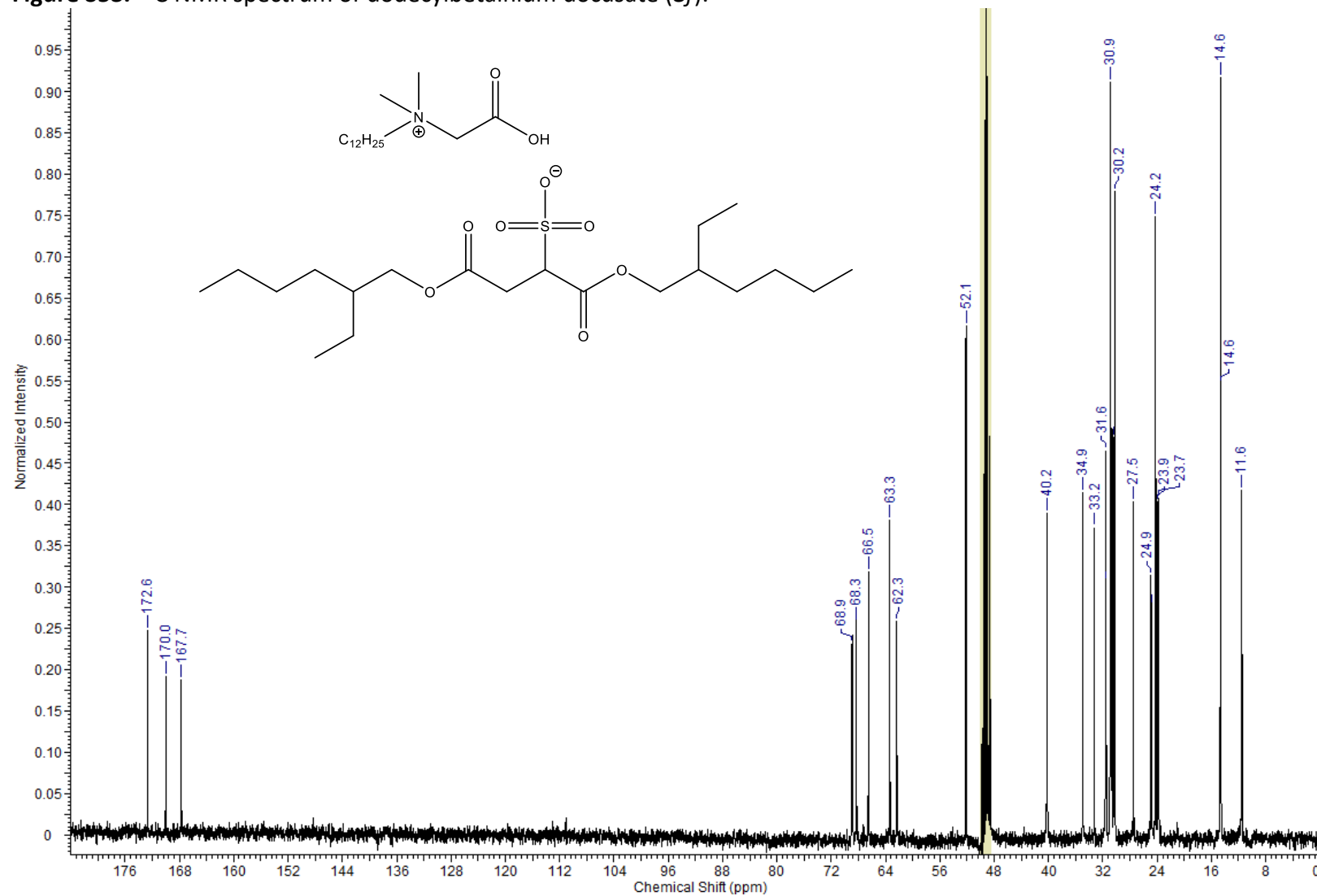


Figure S52. ¹H NMR spectrum of dodecylbetainium docosate (**3f**).



¹H NMR (CD₃OD-*d*₄, 298K, 400 MHz): δ_{H} [ppm] = 0.90 (m, 15H; H-15, H-16, H-23, H-29, H-33); 1.31 (m, 34H; H-6 – H-14); 1.59 (m, 2H; H-21, H-27); 1.77 (m, 2H; H-5); 3.03 (m, 1H; H-25); 3.16 (m, 1H; H-25); 3.29 (s, 6H; H-1, H-2); 3.58 (m, 2H; H-3); 4.02 (s, 5H; H-20, H-24, H-26); 4.24 (s, 2H; H-4).

Figure S53. ^{13}C NMR spectrum of dodecylbetainium docusate (**3f**).



^{13}C NMR ($\text{CD}_3\text{OD}-d_4$, 298K, 100 MHz): δ_{C} [ppm] = 11.6 (2C), 14.6 (3C), 23.7, 23.9, 24.2 (2C), 24.8, 24.9, 27.5, 30.2 (4C), 30.9 (4C) 31.5, 31.6, 33.2, 34.9, 40.2 (2C), 52.1 (2C), 62.3, 63.3, 66.5, 68.3, 68.9, 167.7, 170.0, 172.6.

Figure S54. IR spectrum of dodecylbetainium docusate (**3f**).

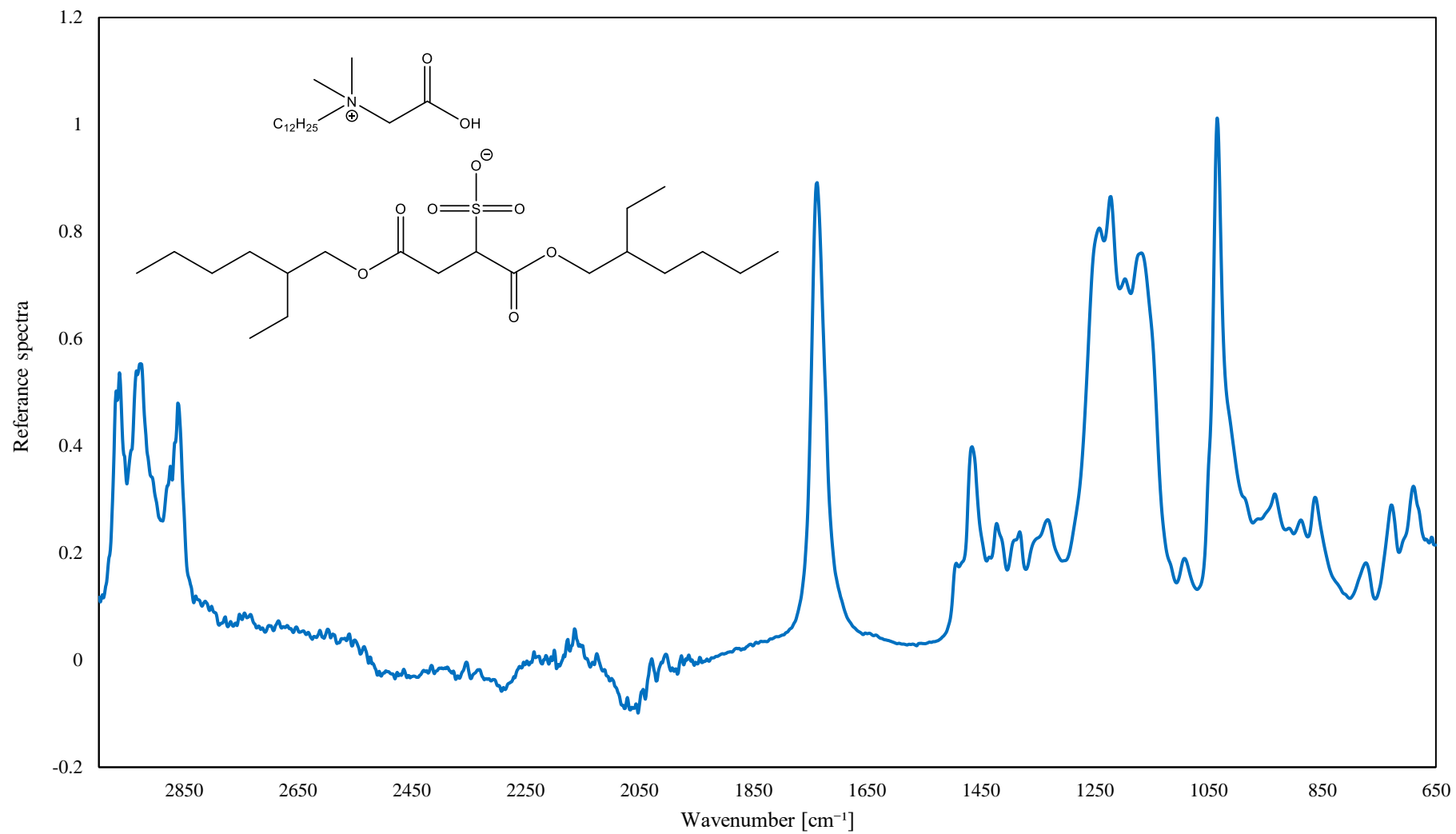
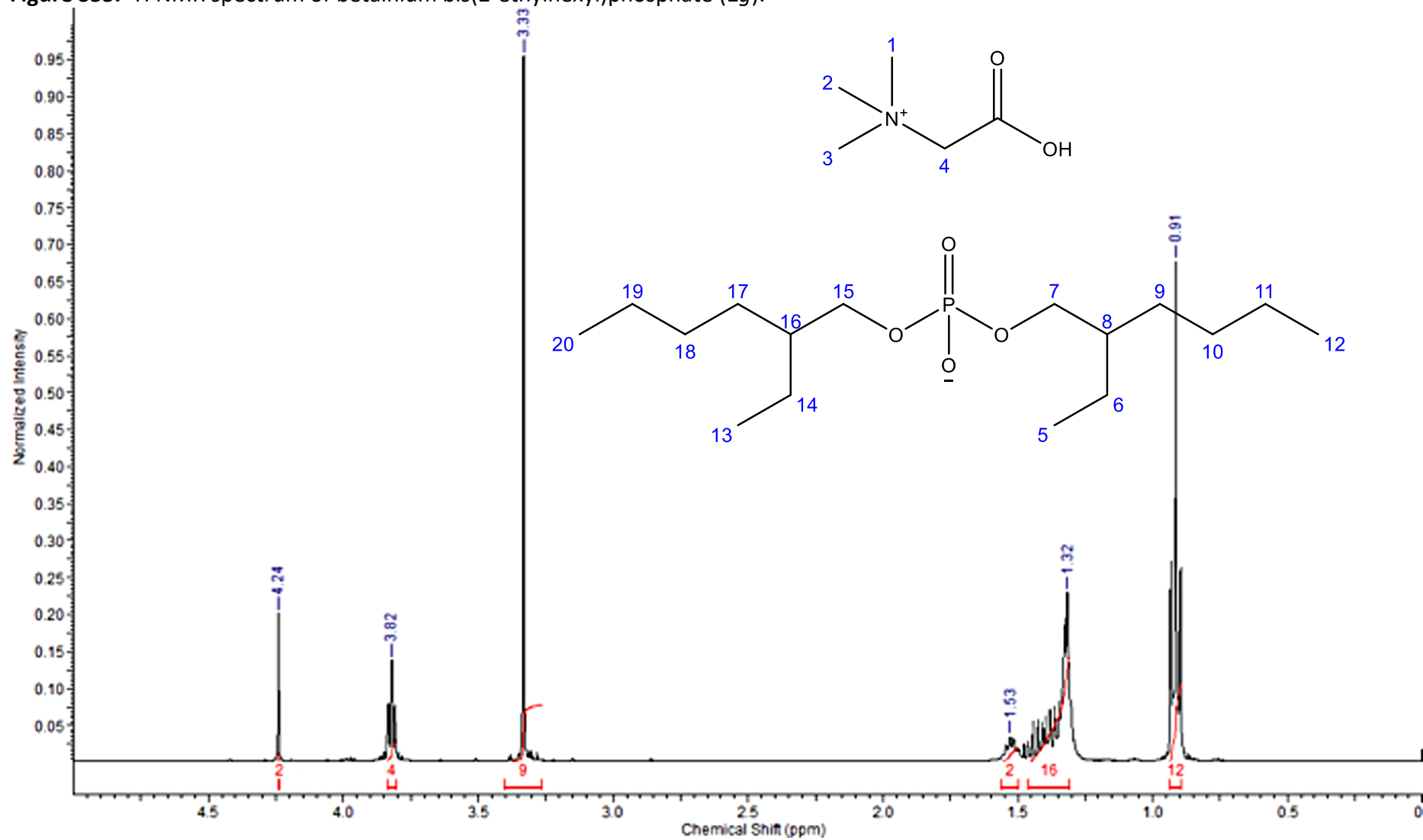
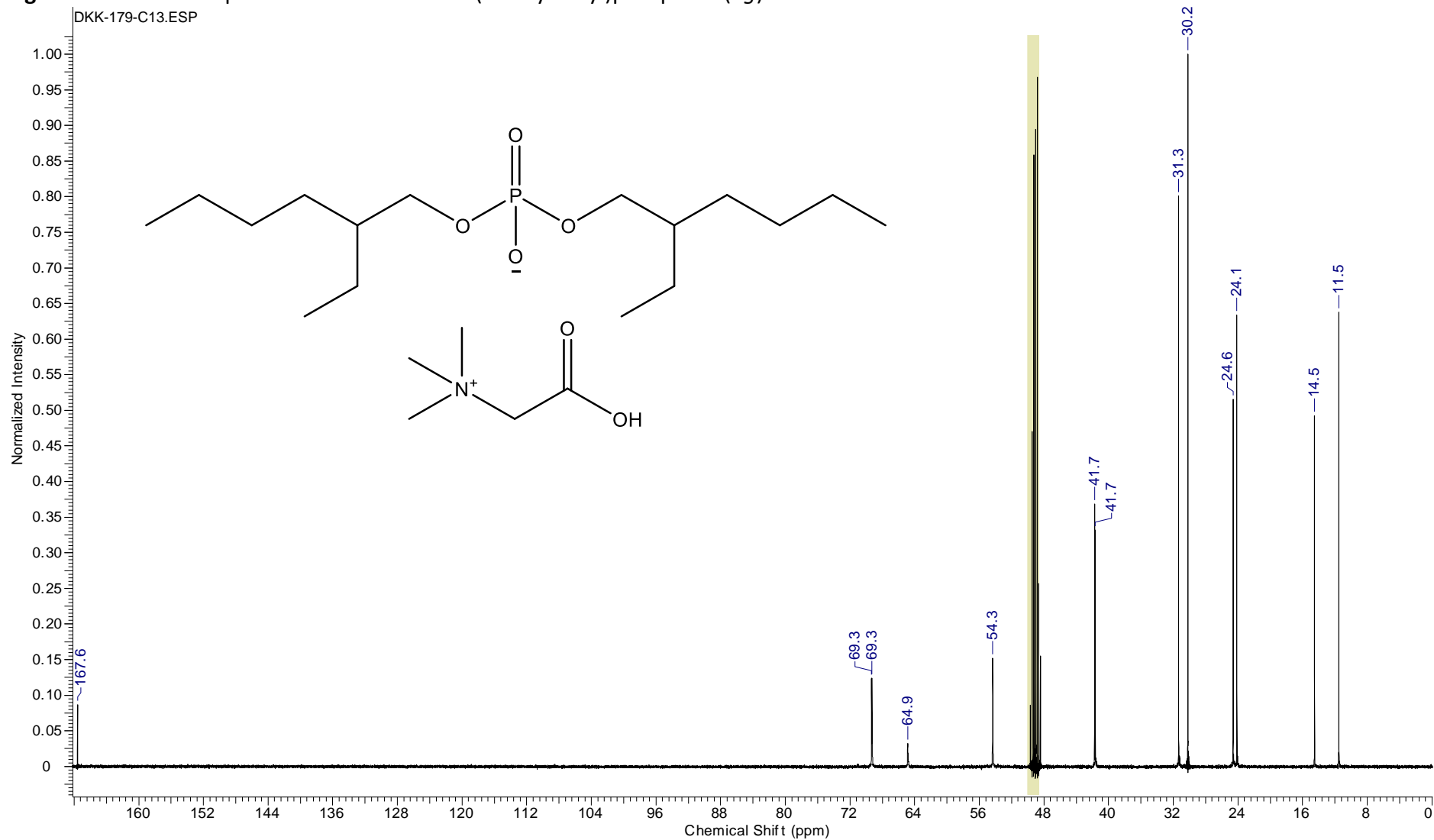


Figure S55. ^1H NMR spectrum of betainium bis(2-ethylhexyl)phosphate (**1g**).



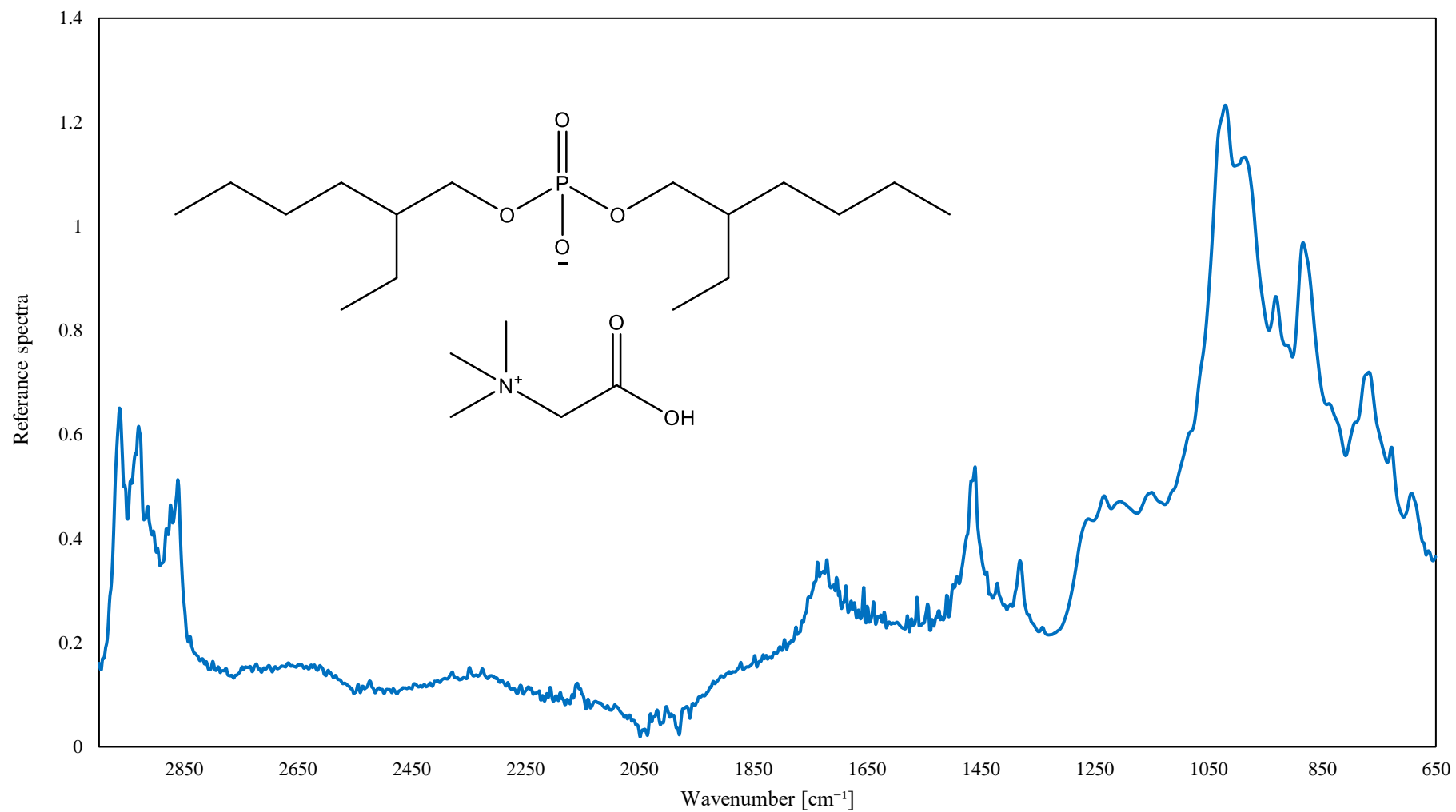
^1H NMR ($\text{CD}_3\text{OD}-d_4$, 298K, 400 MHz): δ_{H} [ppm] = 0.91 (t, $J = 7,38$ Hz, 12H; H-5, H-12, H-13, H-20); 1.32 (m, 16H; H-6, H-9, H-10, H-11, H-14, H-17, H-18, H-19); 1.53 (m, 2H; H-8, H-16); 3.33 (s, 9H; H-1, H-2, H-3); 3.82 (td, $J_{1,2} = 1.26$ Hz, $J_{1,3} = 5,34$ Hz, 4H; H-7, H-15); 4.24 (s, 2H; H-4).

Figure S56. ^{13}C NMR spectrum of betainium bis(2-ethylhexyl)phosphate (**1g**).



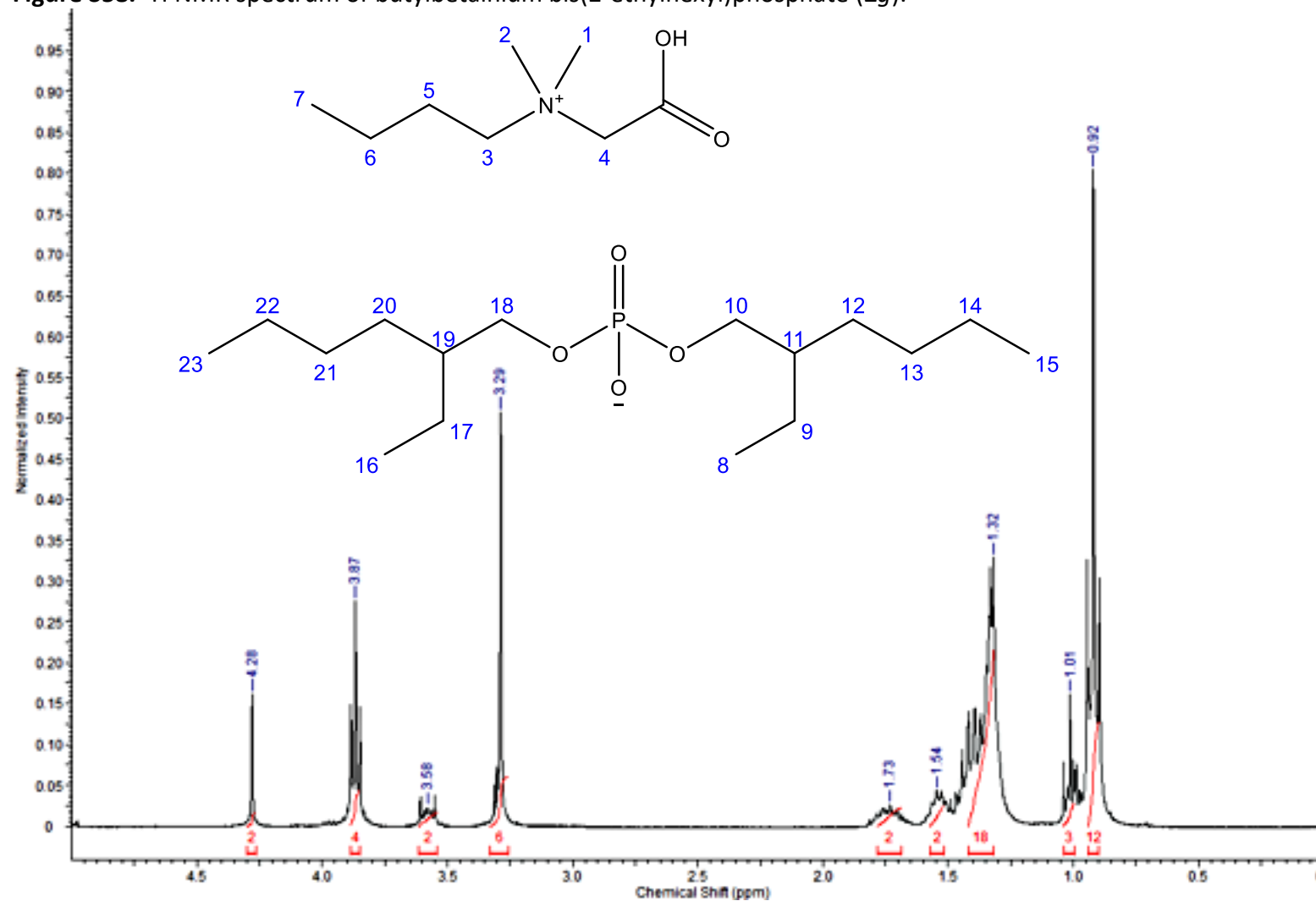
^{13}C NMR ($\text{CD}_3\text{OD}-d_4$, 298K, 100 MHz): δ_{C} [ppm] = 11.5(2), 14.5(2), 24.1(2), 24.6(2), 30.2(2), 31.3(2), 41.7(2), 54.3(3), 64.9, 69.3(2), 167.6.

Figure S57. IR spectrum of betainium bis(2-ethylhexyl)phosphate (**1g**).



IR [cm^{-1}] = 693, 724, 768, 883, 931, 987, 1020, 1150, 1205, 1233, 1380, 1421, 1461, 1737, 2862, 2930, 2964.

Figure S58. ^1H NMR spectrum of butylbetainium bis(2-ethylhexyl)phosphate (**2g**).



^1H NMR ($\text{CD}_3\text{OD}-d_4$, 298K, 400 MHz): δ_{H} [ppm] = 0.92 (t, 12H, $J = 7.37$ Hz; H-8, H-15, H-16, H-23); 1.01 (t, 3H, $J = 7.22$ Hz; H-7); 1.32 (m, 18H; H-6, H-9, H-12, H-13, H-14, H-17, H-20, H-21, H-22); 1.54 (m, 2H; H-11, H-19); 1.73 (m, 2H; H-5); 3.29 (s, 6H; H-1, H-2); 3.58 (m, 2H; H-3); 3.87 (td, $J_{1,2} = 0.45$ Hz, $J_{1,3} = 5.41$ Hz, 4H; H-10, H-18); 4.28 (s, 2H; H-4).

Figure S59. ^{13}C NMR spectrum of butylbetainium bis(2-ethylhexyl)phosphate (**2g**).

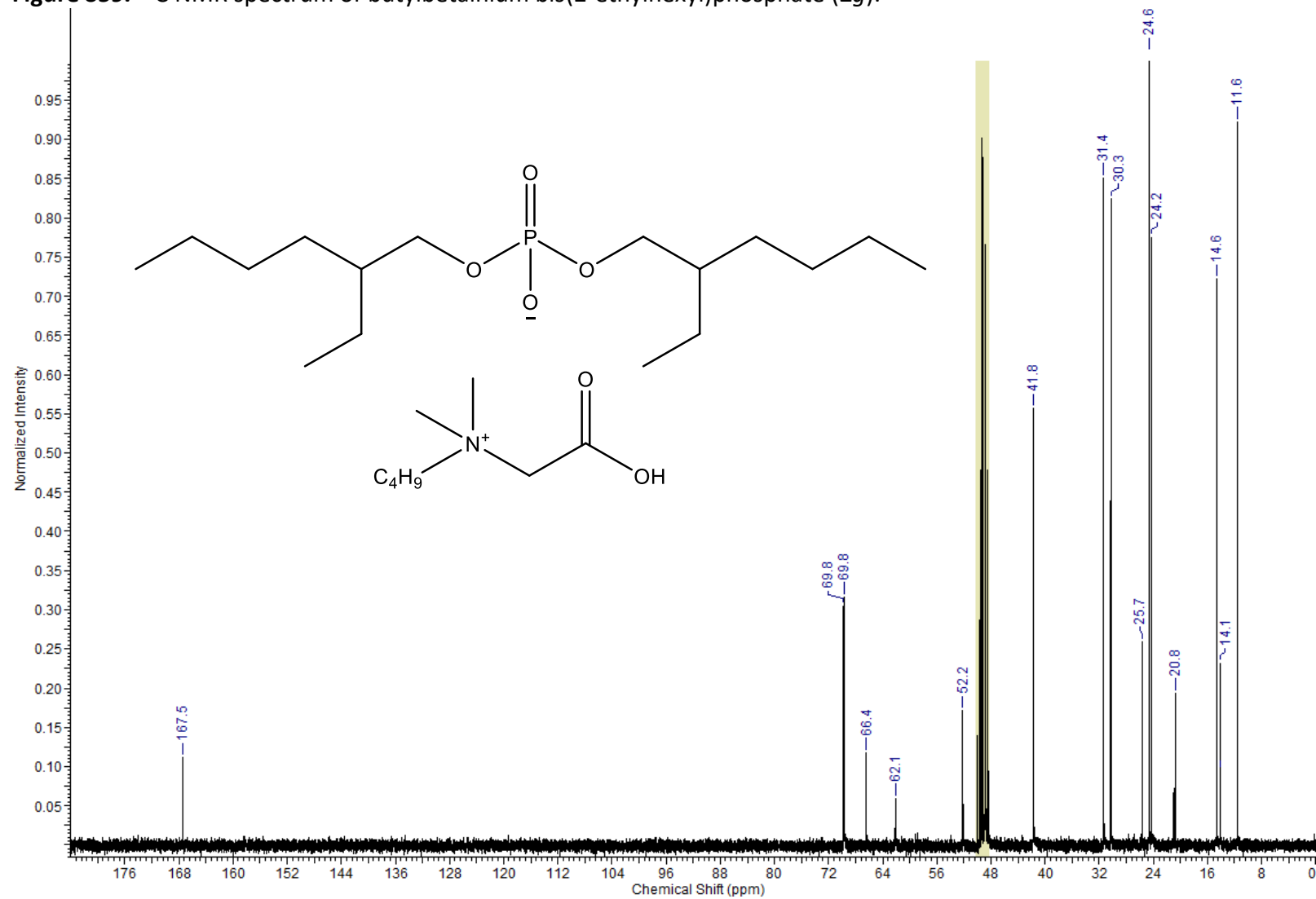
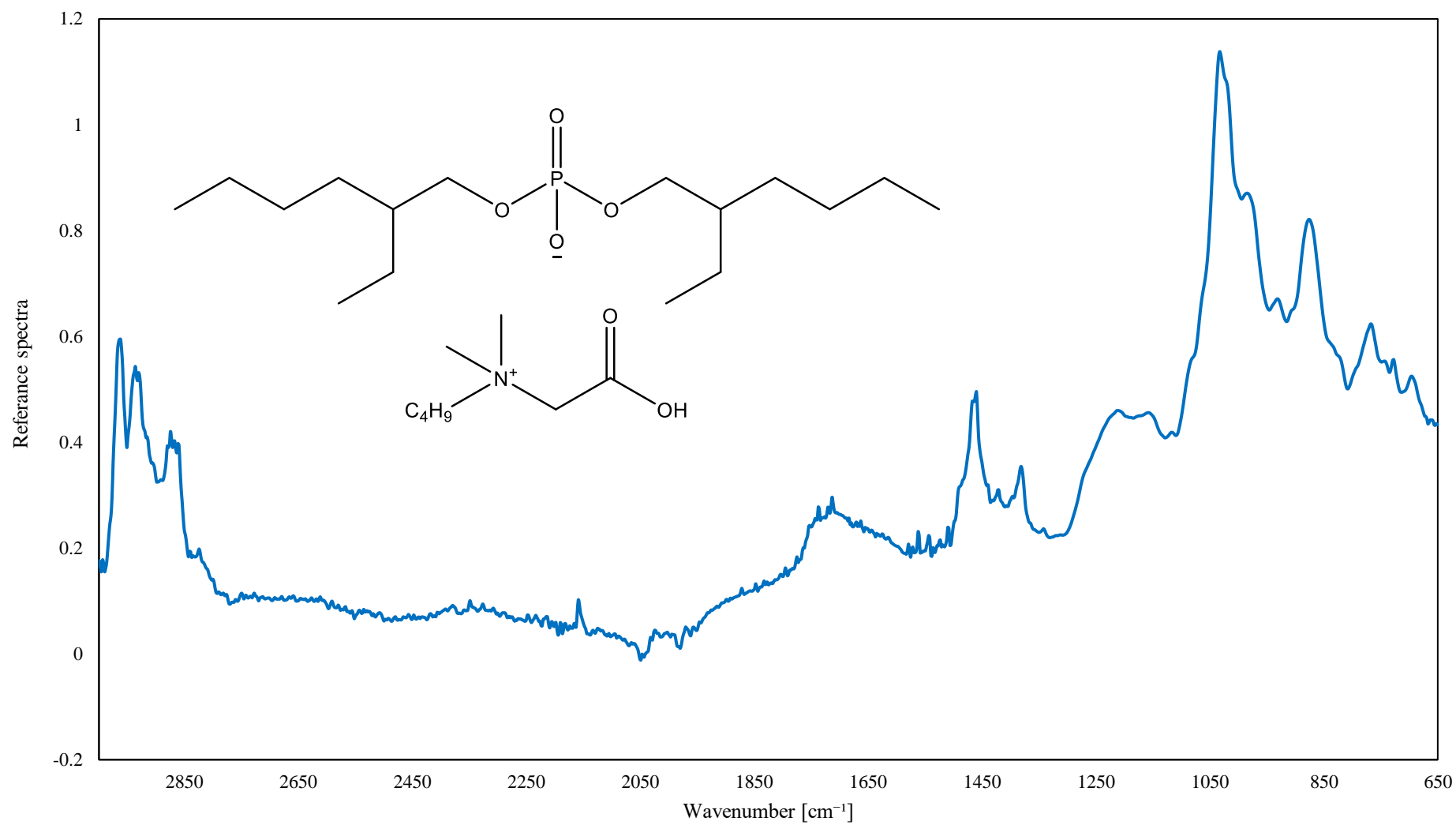
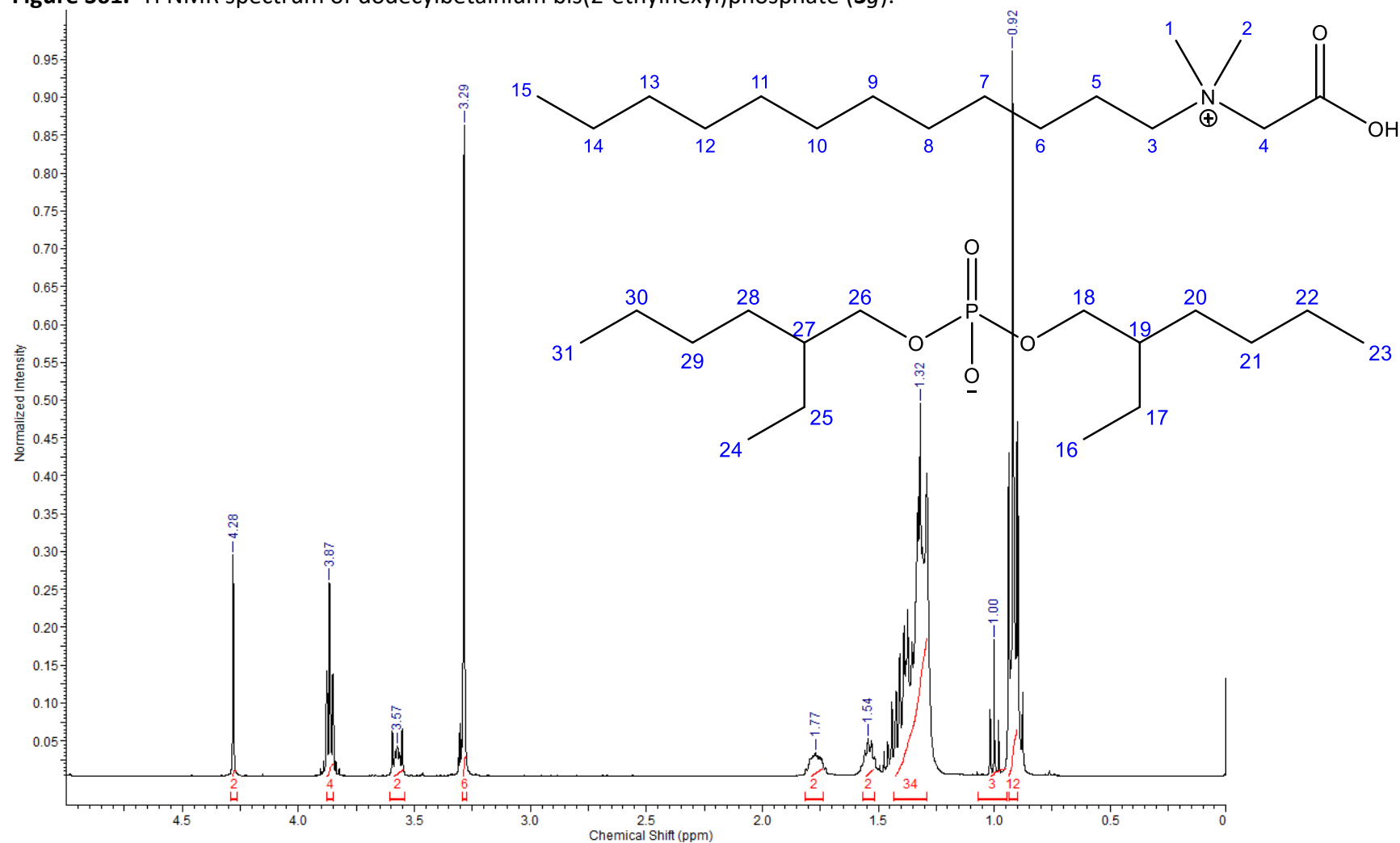


Figure S60. IR spectrum of butylbetainium bis(2-ethylhexyl)phosphate (**2g**).



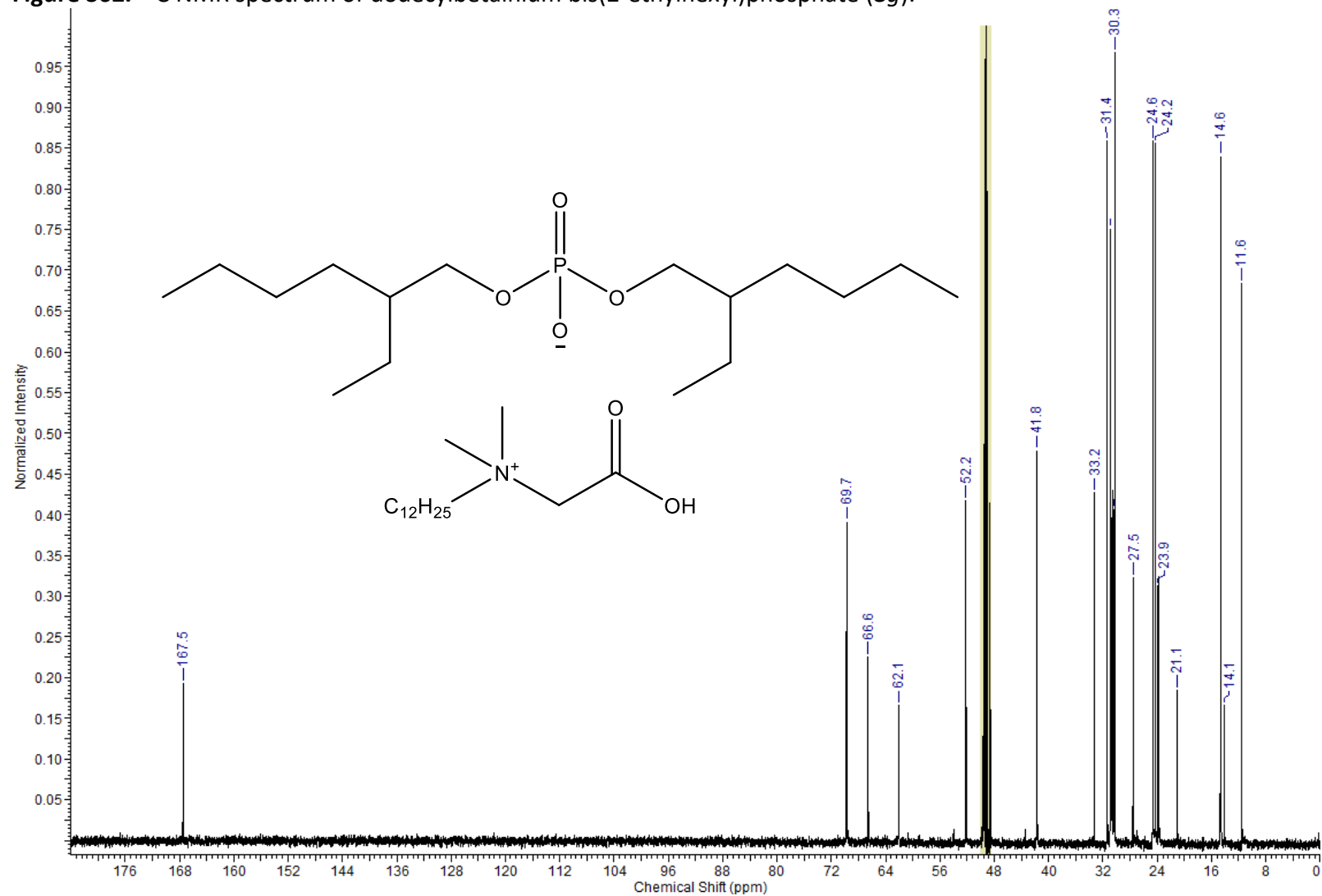
IR [cm⁻¹] = 696, 728, 767, 876, 932, 987, 1032, 1158, 1211, 1381, 1421, 1461, 1737, 2874, 2937, 2964.

Figure S61. ^1H NMR spectrum of dodecylbetainium bis(2-ethylhexyl)phosphate (**3g**).



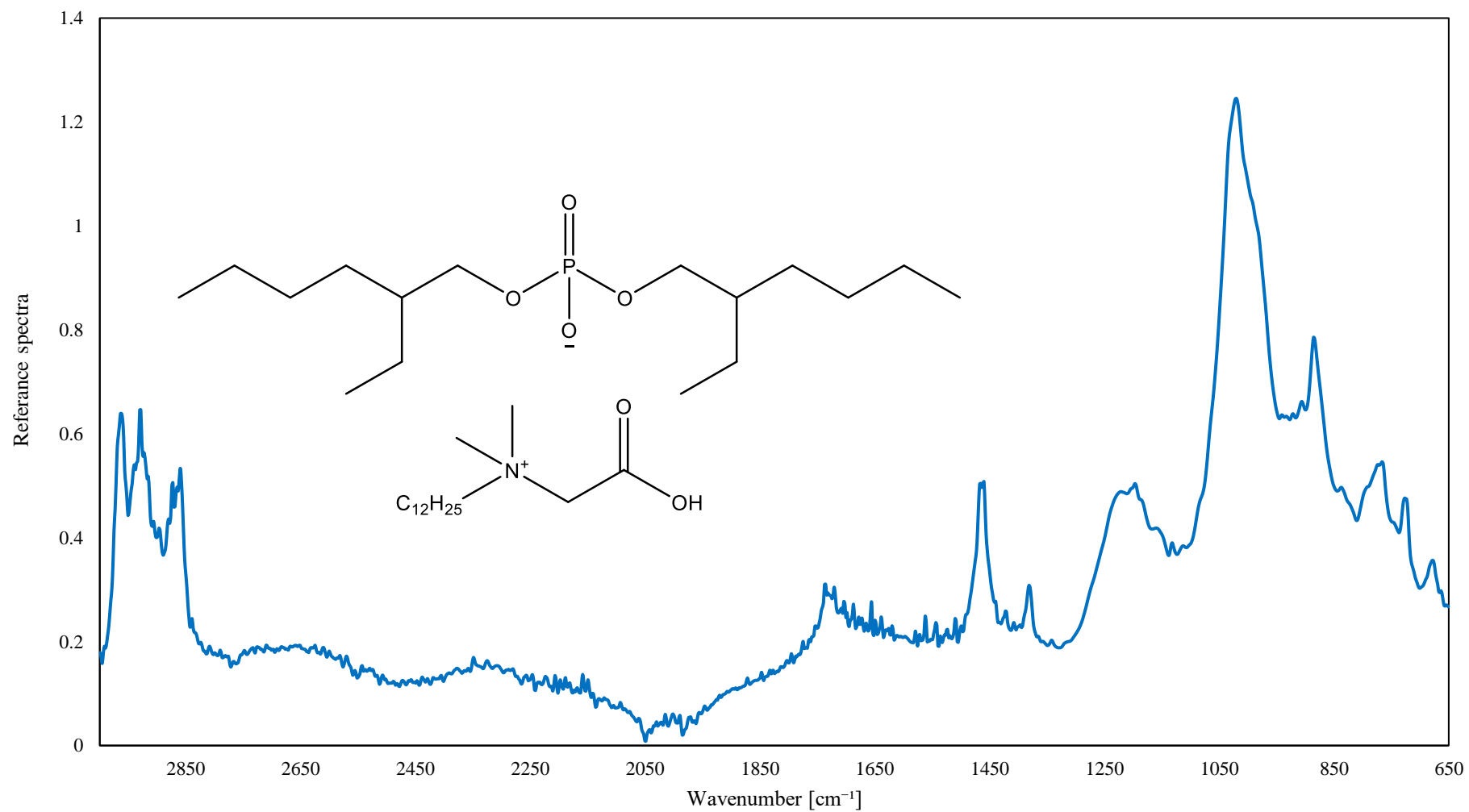
^1H NMR ($\text{CD}_3\text{OD}-d_4$, 298K, 400 MHz): δ_{H} [ppm] = 0.92 (t, $J = 7.48$ Hz, 12H; H-16, H-23, H-24, H-31); 1.00 (t, 3H, $J = 7.48$ Hz; H-15); 1.32 (m, 34H; H-6–H-14, H-17, H-20, H-21, H-22, H-25, H-28, H-29, H-30); 1.54 (m, 2H; H-19, H-27); 1.77 (m, 2H; H-5); 3.29 (s, 6H; H-1, H-2); 3.57 (m, 2H; H-3); 3.87 (td, $J_{1,2} = 1.12$ Hz, $J_{1,3} = 5.36$ Hz, 4H; H-18, H-26); 4.28 (s, 2H; H-4).

Figure S62. ^{13}C NMR spectrum of dodecylbetainium bis(2-ethylhexyl)phosphate (**3g**).



^{13}C NMR ($\text{CD}_3\text{OD}-d_4$, 298K, 100 MHz): δ_{C} [ppm] = 11.6(2), 14.1, 14.6(2), 21.1, 23.9, 24.2(2), 24.6(2), 27.5, 30.3(4), 30.9(4), 31.4(2), 33.2, 41.8(2), 52.2(2), 62.1, 66.6, 69.7(2C), 167.5

Figure S63. IR spectrum of dodecylbetainium bis(2-ethylhexyl)phosphate (**3g**).



IR [cm⁻¹] = 680, 725, 766, 885, 933, 1021, 1197, 12131, 1380, 1422, 1461, 1735, 2860, 2929, 2963.

Figure S64. Surface tension of the aqueous solutions of the obtained salts with the betainium cation.

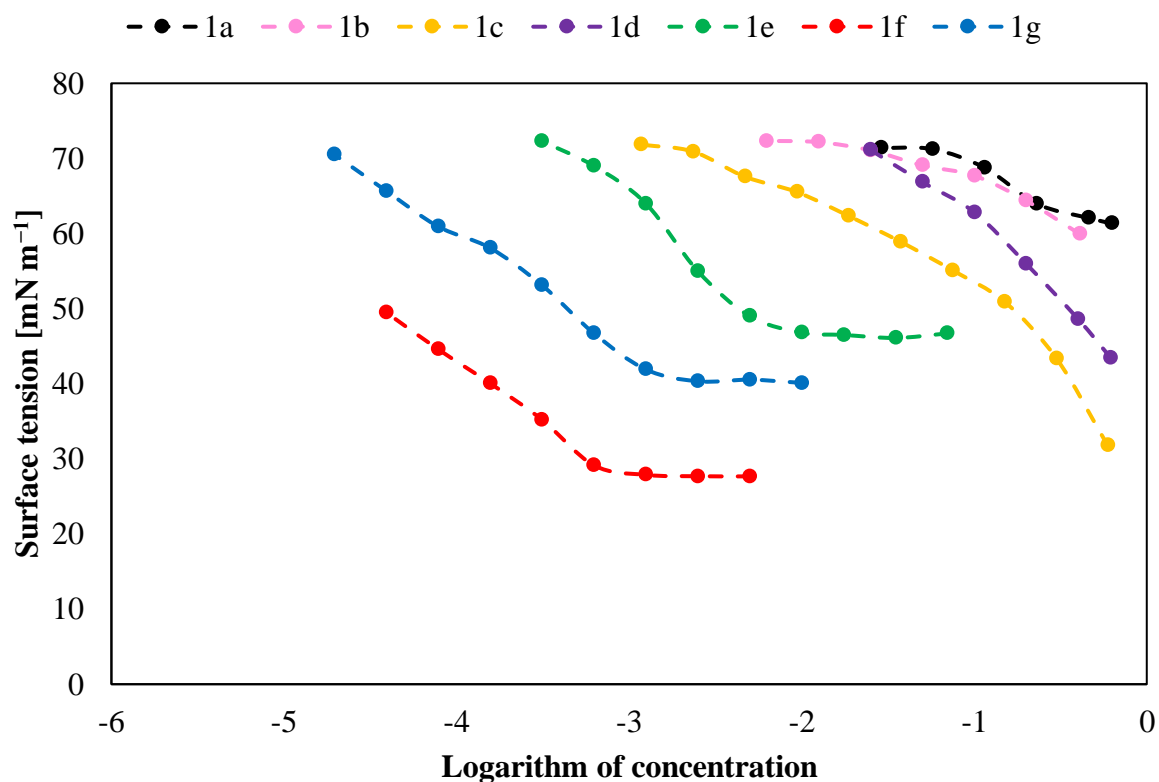


Figure S65. Surface tension of the aqueous solutions of the obtained salts with the butylbetainium cation.

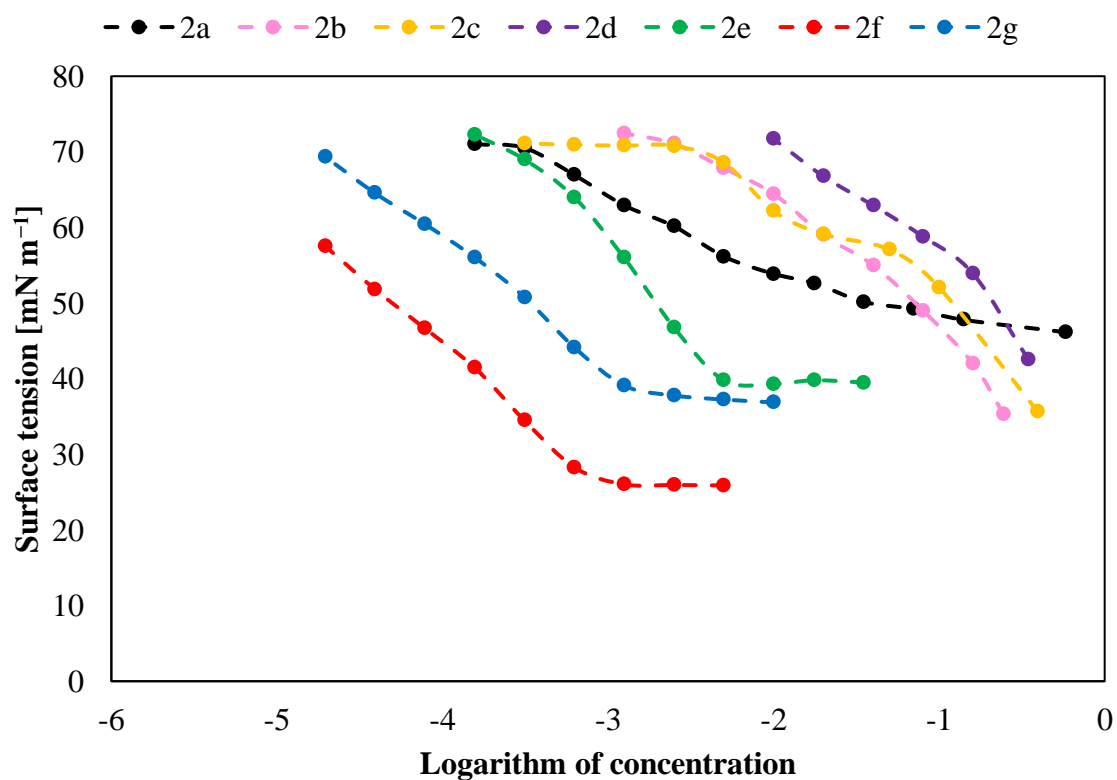


Figure S66. Surface tension of the aqueous solutions of the obtained salts with the dodecylbetainium cation.

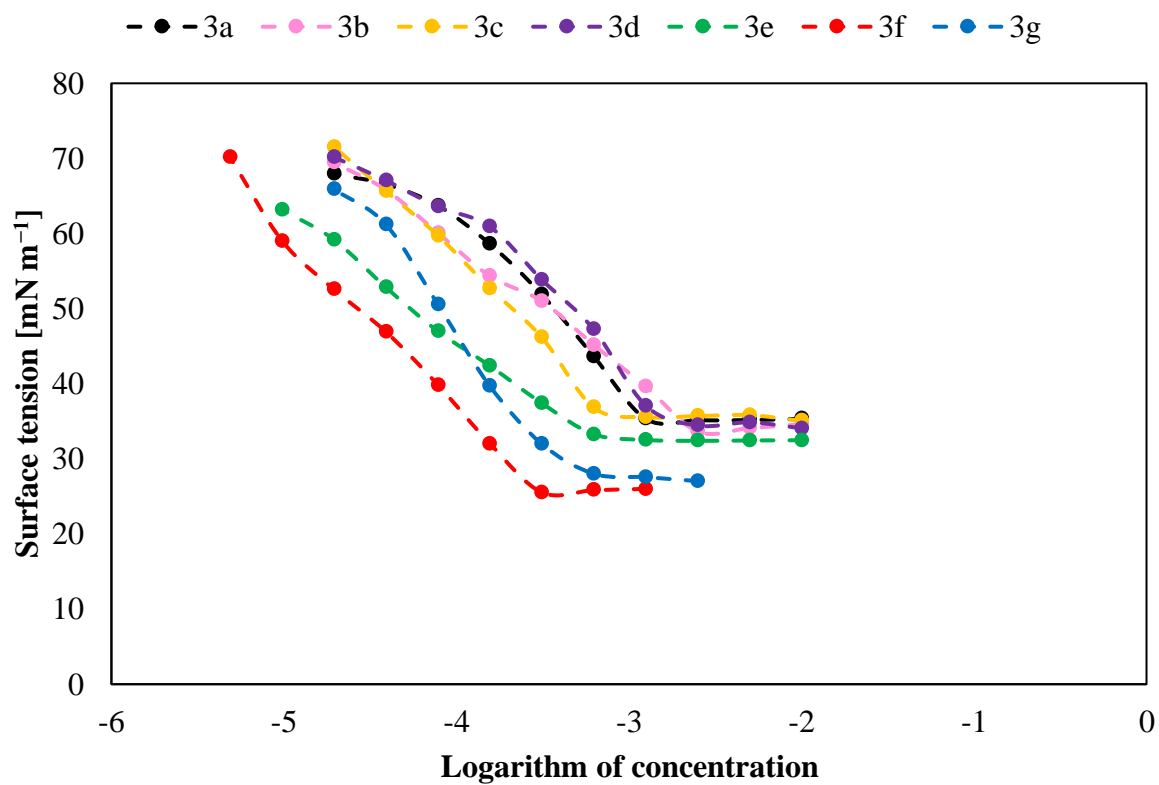


Table S2. Deterrent activity of salts towards adults of granary weevils and larvae of khapra beetles.

No.	Granary weevil (<i>Sitophilus granarius</i>)						Khapra beetle (<i>Trogoderma granarium</i>)					
	Adults						Larvae					
	R		A		T		R		A		T	
1a	59	AB	54	AB	113	BCD	76	ABCD	46	BC	122	D
2a	92	A	59	AB	151	AB	93	AB	35	CDEF	128	D
3a	92	A	9	EFG	101	CDE	94	AB	44	BCD	138	CD
1b	0	CD	9	EFG	9	I	0	G	10	GH	10	F
2b	73	AB	12	DEFG	86	DEF	88	ABC	27	CDEFGH	115	D
3b	99	A	-19	HI	80	DEF	44	EF	20	EFGH	65	E
1c	-7	CD	30	CD	24	HI	3	G	18	EFGH	20	F
2c	75	AB	39	BC	114	BCD	93	AB	31	CDEFG	124	D
3c	100	A	-3	FGH	97	DE	63	CDEF	15	FGH	78	E
1d	-25	D	31	CD	6	I	-3	G	16	EFGH	13	F
2d	62	AB	28	CDE	90	DE	84	ABC	34	CDEF	119	D
3d	100	A	-29	I	71	EFG	48	DEF	22	DEFGH	70	E
1e	20	C	31	CD	49	FGH	-10	G	14	FGH	4	F
2e	75	AB	14	DEF	90	DE	85	ABC	34	CDEF	119	D
3e	100	A	-14	HI	86	DEF	69	BCDE	4	H	74	E
1f	3	CD	29	CDE	32	GHI	0	G	13	FGH	13	F
2f	78	AB	28	CDE	106	CDE	83	ABC	39	CDE	121	D
3f	100	A	-8	GH	92	DE	36	F	22	DEFGH	58	E
1g	78	AB	63	A	141	ABC	81	ABC	89	A	171	AB
2g	100	A	72	A	172	A	100	A	98	A	198	A
3g	100	A	16	DEF	116	BCD	96	AB	66	B	162	BC
LSD _{0.05}	31,2		20,9		38,8		29,1		23,2		30,2	
azadiraktyna ^b	99,0		91,3		190,3		100,0		94,2		194,2	

^bB. Łozowicka, P. Kaczyński, J. Nawrot, J. Wysocka .2007. Aktywność deterrentna nowych pochodnych alfa-asaronu, Progress in Plant Protection, 47, 303-309

Table S3. Effect of the obtained salts at 0.1% concentration on mustard shoot and root length and mass.

No.	Root length on 5th day		Shoos length on 5th day		Shoot mass on 5th day	
	[cm]	± St. Dev.	[cm]	± St. Dev.	[mg]	± St. Dev.
1a	3.3	0.55	7.14	0.46	59.6	4.6
2a	5.68	0.50	8.75	0.54	77.4	4.3
3a	8.78	0.39	9.07	0.56	81.2	5.5
1b	2.91	0.52	7.00	0.55	65.5	4.9
2b	3.79	0.49	8.94	0.46	66.1	4.5
3b	8.34	0.44	9.73	0.52	72.1	5.1
1c	1.82	0.56	6.39	0.45	58.8	5.9
2c	3.40	0.60	8.30	0.41	60.3	4.6
3c	6.42	0.44	10.71	0.69	106.0	6.2
1d	2.98	0.59	8.10	0.53	80.0	5.6
2d	2.58	0.35	8.34	0.64	67.2	4.5
3d	2.66	0.48	6.80	0.62	55.4	4.8
1e	4.94	0.62	6.58	0.60	65.7	4.9
2e	3.08	0.60	5.93	0.43	67.6	4.8
3e	3.38	0.69	4.93	0.39	54.8	5.9
1f	6.12	0.61	9.59	0.58	53.6	3.3
2f	5.43	1.23	7.97	0.66	69.1	5.7
3f	3.28	0.53	8.17	0.57	67.3	5.3
1g	1.73	0.63	6.90	0.61	59.7	4.6
2g	1.25	0.24	5.13	0.18	39.4	5.9
3g	0.85	0.11	5.44	0.61	39.4	5.6
Control	3.17	0.48	6.71	0.43	53.7	3.9
Biopower	6.90	0.59	8.15	0.56	64.0	5.2

Table S4. Influence of the obtained salts at a concentration of 0.1% on mustard seed germination capacity.

No.	I day		II day		III day		IV day		V day	
	[%]	± St. Dev.	[%]	± St. Dev.	[%]	± St. Dev.	[%]	± St. Dev.	[%]	± St. Dev.
1a	60.00	1.00	96.67	0.58	100.00	0.00	100.00	0.00	100.00	0.00
2a	40.00	1.00	100.00	0.00	100.00	0.00	100.00	0.00	100.00	0.00
3a	86.67	0.58	100.00	0.00	100.00	0.00	100.00	0.00	100.00	0.00
1b	80.00	0.00	90.00	0.00	93.33	0.58	93.33	0.58	93.33	0.58
2b	96.67	0.58	96.67	0.58	100.00	0.00	100.00	0.00	100.00	0.00
3b	66.67	1.53	96.67	0.58	100.00	0.00	100.00	0.00	100.00	0.00
1c	83.33	1.53	93.33	0.58	100.00	0.00	100.00	0.00	100.00	0.00
2c	40.00	2.00	100.00	0.00	100.00	0.00	100.00	0.00	100.00	0.00
3c	96.67	0.58	93.33	1.15	100.00	0.00	100.00	0.00	100.00	0.00
1d	76.67	1.15	90.00	1.00	100.00	0.00	100.00	0.00	100.00	0.00
2d	100.00	0.00	90.00	1.00	100.00	0.00	100.00	0.00	100.00	0.00
3d	76.67	2.31	86.67	0.58	100.00	0.00	100.00	0.00	100.00	0.00
1e	43.30	0.58	100.00	0.00	100.00	0.00	100.00	0.00	100.00	0.00
2e	63.33	0.58	93.33	1.15	100.00	0.00	100.00	0.00	100.00	0.00
3e	70.00	1.00	93.33	0.58	100.00	0.00	100.00	0.00	100.00	0.00
1f	63.33	2.08	80.00	1.00	90.00	1.00	96.67	0.58	96.67	0.58
2f	60.00	3.00	90.00	1.73	100.00	0.00	100.00	0.00	100.00	0.00
3f	43.33	0.58	90.00	1.00	100.00	0.00	100.00	0.00	100.00	0.00
1g	56.67	2.08	70.00	1.00	90.00	0.00	96.67	0.58	96.67	0.58
2g	40.00	1.00	83.33	2.08	100.00	0.00	100.00	0.00	100.00	0.00
3g	50.00	0.00	90.00	0.00	93.33	0.58	93.33	0.58	93.33	0.58
Control	36.67	0.58	66.67	0.58	80.00	1.00	93.33	0.58	100.00	0.00
Biopower	53.33	0.58	83.33	2.08	100.00	0.00	100.00	0.00	100.00	0.00

Table S5. MIC ($\mu\text{g mL}^{-1}$) and MBC or MFC ($\mu\text{g mL}^{-1}$) values recorded for ILs with betainium cations.

Microbe	MIC/ MBC/ MFC	2a	2b	2c	2d	2e	2f	2g	[DDA][Cl]	[Ba][Cl]
Gram-positive bacteria										
<i>Staphylococcus aureus</i> ATCC 33862	MIC	> 1000	> 1000	> 1000	> 1000	> 1000	> 1000	> 1000	< 0.5	< 0.5
	MBC	> 1000	> 1000	> 1000	> 1000	> 1000	> 1000	> 1000	0.5	1
<i>Staphylococcus epidermidis</i> ATCC 12228	MIC	> 1000	> 1000	> 1000	> 1000	1000	62	> 1000	< 0.5	< 0.5
	MBC	> 1000	> 1000	> 1000	> 1000	1000	125	> 1000	< 0.5	< 0.5
<i>Bacillus subtilis</i> ATCC 11774	MIC	> 1000	> 1000	> 1000	> 1000	1000	62	> 1000	0.5	0.5
	MBC	> 1000	> 1000	> 1000	> 1000	1000	62	> 1000	1	1
<i>Enterococcus faecalis</i> ATCC 19433	MIC	> 1000	> 1000	> 1000	> 1000	> 1000	125	> 1000	< 0.5	0.5
	MBC	> 1000	> 1000	> 1000	> 1000	> 1000	125	> 1000	< 0.5	1
<i>Micrococcus luteus</i> ATCC 4698	MIC	1000	1000	1000	1000	> 1000	62	> 1000	< 0.5	< 0.5
	MBC	1000	> 1000	1000	1000	> 1000	125	> 1000	< 0.5	< 0.5
Gram-negative bacteria										
<i>Pseudomonas aeruginosa</i> ATCC 9027	MIC	> 1000	> 1000	> 1000	> 1000	> 1000	> 1000	> 1000	8	16
	MBC	> 1000	> 1000	> 1000	> 1000	> 1000	> 1000	> 1000	8	31
<i>Serratia marcescens</i> ATCC 8100	MIC	> 1000	> 1000	> 1000	> 1000	> 1000	1000	> 1000	4	4
	MBC	> 1000	> 1000	> 1000	> 1000	> 1000	> 1000	> 1000	8	8
<i>Proteus vulgaris</i> ATCC 49132	MIC	1000	> 1000	1000	> 1000	> 1000	> 1000	> 1000	4	8
	MBC	1000	> 1000	> 1000	> 1000	> 1000	> 1000	> 1000	4	16
<i>Moraxella catarrhalis</i> ATCC 25238	MIC	> 1000	> 1000	> 1000	> 1000	> 1000	1000	> 1000	< 0.5	0.5
	MBC	> 1000	> 1000	> 1000	> 1000	> 1000	> 1000	> 1000	< 0.5	1
<i>Escherichia coli</i> ATCC 8739	MIC	> 1000	> 1000	> 1000	> 1000	> 1000	> 1000	> 1000	1	4
	MBC	> 1000	> 1000	> 1000	> 1000	> 1000	> 1000	> 1000	1	8
Yeasts										
<i>Rhodotorula rubra</i>	MIC	> 1000	> 1000	> 1000	> 1000	250	62	> 1000	1	4
	MFC	> 1000	> 1000	> 1000	> 1000	250	62	> 1000	2	8
<i>Candida albicans</i> ATCC	MIC	500	500	500	500	250	16	500	2	4
	MFC	1000	1000	1000	1000	250	16	500	2	4

Table S6. MIC ($\mu\text{g mL}^{-1}$) and MBC or MFC ($\mu\text{g mL}^{-1}$) values recorded for ILs with butylbetainium cations.

Microbe	MIC/ MBC/ MFC	2a	2b	2c	2d	2e	2f	2g	[DDA][Cl]	[Ba][Cl]
Gram-positive bacteria										
<i>Staphylococcus aureus</i> ATCC 33862	MIC	> 1000	> 1000	1000	> 1000	> 1000	62	> 1000	< 0.5	< 0.5
	MBC	> 1000	> 1000	1000	> 1000	> 1000	125	> 1000	0.5	1
<i>Staphylococcus epidermidis</i> ATCC 12228	MIC	> 1000	> 1000	1000	> 1000	1000	62	> 1000	< 0.5	< 0.5
	MBC	> 1000	> 1000	1000	> 1000	1000	125	> 1000	< 0.5	< 0.5
<i>Bacillus subtilis</i> ATCC 11774	MIC	> 1000	> 1000	1000	> 1000	> 1000	62	> 1000	0.5	0.5
	MBC	> 1000	> 1000	1000	> 1000	> 1000	125	> 1000	1	1
<i>Enterococcus faecalis</i> ATCC 19433	MIC	> 1000	> 1000	> 1000	> 1000	1000	> 1000	> 1000	< 0.5	0.5
	MBC	> 1000	> 1000	> 1000	> 1000	1000	> 1000	> 1000	< 0.5	1
<i>Micrococcus luteus</i> ATCC 4698	MIC	1000	> 1000	1000	1000	> 1000	125	> 1000	< 0.5	< 0.5
	MBC	1000	> 1000	1000	1000	> 1000	125	> 1000	< 0.5	< 0.5
Gram-negative bacteria										
<i>Pseudomonas aeruginosa</i> ATCC 9027	MIC	> 1000	> 1000	1000	> 1000	> 1000	> 1000	> 1000	8	16
	MBC	> 1000	> 1000	1000	> 1000	> 1000	> 1000	> 1000	8	31
<i>Serratia marcescens</i> ATCC 8100	MIC	> 1000	> 1000	> 1000	> 1000	1000	> 1000	> 1000	4	4
	MBC	> 1000	> 1000	> 1000	> 1000	1000	> 1000	> 1000	8	8
<i>Proteus vulgaris</i> ATCC 49132	MIC	1000	> 1000	1000	> 1000	> 1000	> 1000	> 1000	4	8
	MBC	> 1000	> 1000	> 1000	> 1000	> 1000	> 1000	> 1000	4	16
<i>Moraxella catarrhalis</i> ATCC 25238	MIC	> 1000	> 1000	> 1000	> 1000	1000	> 1000	> 1000	< 0.5	0.5
	MBC	> 1000	> 1000	> 1000	> 1000	1000	> 1000	> 1000	< 0.5	1
<i>Escherichia coli</i> ATCC 8739	MIC	> 1000	> 1000	> 1000	> 1000	> 1000	> 1000	> 1000	1	4
	MBC	> 1000	> 1000	> 1000	> 1000	> 1000	> 1000	> 1000	1	8
Yeasts										
<i>Rhodotorula rubra</i>	MIC	> 1000	> 1000	> 1000	> 1000	> 1000	62	> 1000	1	4
	MFC	> 1000	> 1000	> 1000	> 1000	> 1000	62	> 1000	2	8
<i>Candida albicans</i> ATCC	MIC	125	1000	500	1000	1000	16	125	2	4
	MFC	250	1000	500	1000	1000	16	250	2	4

Table S7. MIC ($\mu\text{g mL}^{-1}$) and MBC or MFC ($\mu\text{g mL}^{-1}$) values recorded for ILs with dodecylbetainium cations.

Microbe	MIC/ MBC/ MFC	3a	3b	3c	3d	3e	3f	3g	[DDA][Cl]	[Ba][Cl]
Gram-positive bacteria										
<i>Staphylococcus aureus</i> ATCC 33862	MIC	62	125	125	62	125	125	250	< 0.5	< 0.5
	MBC	62	125	125	125	125	> 1000	250	0.5	1
<i>Staphylococcus epidermidis</i> ATCC 12228	MIC	62	125	125	125	125	125	125	< 0.5	< 0.5
	MBC	62	125	125	125	125	> 1000	125	< 0.5	< 0.5
<i>Bacillus subtilis</i> ATCC 11774	MIC	31	125	62	62	125	125	125	0.5	0.5
	MBC	62	250	125	62	250	> 1000	250	1	1
<i>Enterococcus faecalis</i> ATCC 19433	MIC	62	125	125	125	62	1000	125	< 0.5	0.5
	MBC	125	250	125	125	125	> 1000	250	< 0.5	1
<i>Micrococcus luteus</i> ATCC 4698	MIC	31	62	62	62	62	> 1000	125	< 0.5	< 0.5
	MBC	62	62	62	62	125	> 1000	250	< 0.5	< 0.5
Gram-negative bacteria										
<i>Pseudomonas aeruginosa</i> ATCC 9027	MIC	500	1000	500	1000	1000	1000	> 1000	8	16
	MBC	1000	1000	1000	1000	> 1000	> 1000	> 1000	8	31
<i>Serratia marcescens</i> ATCC 8100	MIC	125	250	125	250	500	> 1000	> 1000	4	4
	MBC	125	250	125	250	500	> 1000	> 1000	8	8
<i>Proteus vulgaris</i> ATCC 49132	MIC	250	500	250	500	> 1000	> 1000	> 1000	4	8
	MBC	250	500	250	500	>1000	> 1000	> 1000	4	16
<i>Moraxella catarrhalis</i> ATCC 25238	MIC	62	125	62	125	62	> 1000	500	< 0.5	0.5
	MBC	62	125	62	125	62	> 1000	500	< 0.5	1
<i>Escherichia coli</i> ATCC 8739	MIC	250	500	250	250	500	> 1000	> 1000	1	4
	MBC	250	500	250	500	500	> 1000	> 1000	1	8
Yeasts										
<i>Rhodotorula rubra</i>	MIC	125	250	125	125	250	62	250	1	4
	MFC	125	250	125	250	250	> 1000	500	2	8
<i>Candida albicans</i> ATCC	MIC	62	125	62	62	62	16	125	2	4
	MFC	62	250	125	62	125	16	250	2	4

References

- 1 A. R. Tehrani-Bagha, K. Holmberg, C. G. van Ginkel and M. Kean, *J. Colloid Interface Sci.*, 2015, **449**, 72-79.
- 2 K. Czerniak, A. Biedziak, K. Krawczyk and J. Pernak, *Tetrahedron*, 2016, **72**, 7409-7416.
- 3 D. K. Kaczmarek, K. Czerniak and T. Klejdysz, *Chem. Pap.*, 2018, **72**, 2457-2466.
- 4 A. I. Vogel, B. S. Furniss, *Vogel's Textbook of Practical Organic Chemistry*, 4th ed. Wiley, John & Sons, Inc. 1984.
- 5 D. K. Kaczmarek, T. Rzemieniecki, K. Marcinkowska and J. Pernak, *J. Ind. Eng. Chem.*, 2019, **78**, 440-447.